Electrochemical multi-sensors for biomedical applications

Islam Bogachan Tahirbegi

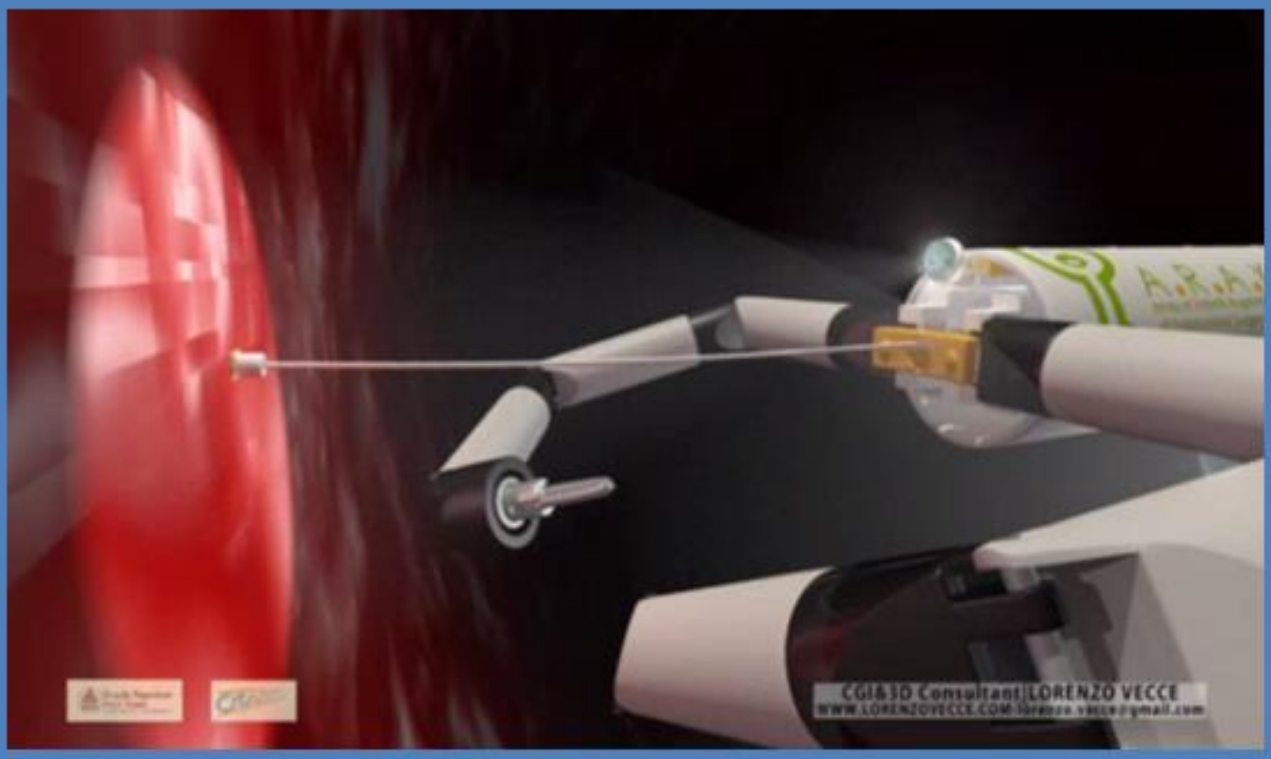

Electrochemical multi-sensors for biomedical applications

Islam Bogachan Tahirbegi

University of Barcelona
Nanobioengineering, IBEC
Barcelona, Spain

Electrochemical multi-sensors for biomedical applications

written by

Islam Bogachan Tahirbegi

PhD dissertation submitted to the
University of Barcelona
Faculty of Physics
Department of Electronics

Doctorate Program
Nano-science

in partial fulfillment of the requirements for the degree of
Doctor of Philosophy

Thesis Director
Dr. Mònica Mir Llorente

Thesis Tutor
Prof. Josep Samitier Martí

Barcelona, 2013

To my family

“I don't know anything,
but I do know that everything is interesting
if you go into it deeply enough."
Richard Feynman

Acknowledgments

First of all, the author would like to thank to his thesis supervisors, Dr. Monica Mir and Prof. Josep Samitier Marti for the great opportunity, confidence and support. In addition, the strong help during in-vivo experiments from his partner in ARAKNES project, Prof. Marc Schur, is gratefully acknowledged. Moreover, Dr. Sebastian Schostek has provided useful guidance in the experimental in-vivo stage of research and furthermore, I want to thank to Dr. Margarita Alvira for taking the photos during in-vivo experiments and for the fruitful discussions in the laboratory. Also, this author wishes to express his gratitude to the SIC-BIO Department of the University of Barcelona for lending their impedance device and to Xavier Giralt and Luis Ernesto Amigo Vásquez from robotics group at IBEC for their help during pressure sensor experiments. The author wants to express his deepest gratitude for the funding of this study during his stay in Spain by Fundacio Bosch i Gimpera and IBEC. Furthermore, I want to thank to all my friends Billur Cakirer, Ahmet Utku Yazgan, Ilker Demiroglu, Ilker Demirkol, Emre Manzak, Ahmet Karal, Fatih Ertinaz, Mark Fields, Ernest Moles and Caglar Karakurum, who accompanied me and offered their help in different ways on the road. Last but foremost the author wholeheartedly wishes to thank his parents, Leyla Kilicoglu and Subutay Tahirbegi, his grandmother Turkan Azak and his family Turker-Oya Karamizrak for their years of help and support.

LIST OF PUBLICATIONS

Journal articles:

Electrochemical array for in vivo monitoring of gastric ischemia Islam Bogachan Tahirbegi, Mònica Mir, Sebastian Schostek, Marc Schurr, Josep Samitier (Manuscript preparation)

Real-time monitoring of ischemia inside stomach, Tahirbegi IB, Mir M, Samitier J. Biosensors and Bioelectronics Volume 40, Issue 1, pp. 323–328 (2013)

In vitro study of magnetite-amyloid β complex formation. Mir M, Tahirbegi IB, Valle-Delgado JJ, Fernàndez-Busquets X, Samitier J. Nanomedicine: Nanotechnology, Biology and Medicine Volume 8, Issue 06, pp. 974–980 (2012)

Abbreviations

A	Area,
AC	Alternating current
Ag/AgCl	Silver/silver chloride
Ag_2SO_4	Silversulfate
ARAKNES	Array of Robots Augmenting the KiNematics of Endoluminal Surgery
α	Protonated ionophore
BBPA	Bis(1-butylpentyl) adipate
BER	Basic electrical rhythm
C	Capacitance
CE	Counter electrode
C_i,	Ions concentration
CN	Chloronaphthalene
COO^-	Carboxyl groups
CO_2	Carbon dioxide
CP	Conductive polymers
CV	Cyclic voltammetry
CWE	Coated wire electrodes
D	Diffusion coefficient of the redox species
DBBP	Dibutyl butylphosphonate
DC	Direct current
DOP,	Dioctylpthalate
d_t	Delay time

E_{ac}	Anodic peak value
ECW	Extracellular water
E_D	Potential inside the membrane or film
E_M	Electric potential
E_{PB}	Boundary potential
E_{pc}	Cathodic peak value
ESI	Electrospray ionization
f	Frequency
F	Faraday constant,
FDA	Food and Drug administration
FET	Field effect transistor
FFM	Fat-free mass
HCO_3^-	Bicarbonate
HPLC	High Performance Liquid Chromatography
i	Ion of interest,
I	Current
ICT	Information, communication technology
ICW	Intracellular water
I_{pa}	Anodic current
I_{pc}	Cathodic current
ISE	Ion selective electrodes
ISFET	Ion sensitive field effect transistors
j	Interfering ions
k_{ij}	Selectivity coefficient.
KTpClPB	Potassium tetrakis (4-chlorophenyl) borate
K_2PtCl_4	Potassium tetrachloroplatinate(II)
L	Uracil

LOD	Limit of detection
MilliQ	Double deionized water
NH_3^+	Charged amino groups
NO_x	Oxides of nitrogen
NOTES	Natural orifice translumenal endoscopic surgery
NPOE	Nitrophenyloctylether
O	Probability of occurrence
pCO_2	CO_2 pressure
PDMS	Polydimethylsiloxane
PEI	Polyethyleneimine-1800
pK	Acidity constant
PMMA	Poly(methyl methacrylate)
PVC	Polyvinyl chloride
R	Resistance
RE	Reference electrode
RP	Risk point
S	Severity
SQUID	Superconducting quantum interference device
T	Temperature
t	Time.
TBP	Tri-n-butylphosphate
TBW	Total body water
THF	Tetrahydrofurane
ToF-SIMS	Time-of-Flight Secondary Ion Mass Spectrometry
TPBNa	Sodium tetraphenylborate
u_i	Ion mobility

USTAN	University of St. Andrews
V	Voltage
X	Reactance
w	Radial frequency
WE	Working electrode
WS	Working sensing electrode
Z	Impedance
Z_i	Ionic valence

CONTENTS

CHAPTER 1

General introduction

1.1. Sensors

1.1.1. Importance of sensors in biotechnology

The developments in electronics opened a new horizon in the biomedical research area. Micro-nanotechnological tools made easier to characterize complicated biological systems. The combination of electronics devices with micro-nano and biotechnology hastened the development in this area. Currently, there are techniques allowing the miniaturization and production of advanced sensors for monitoring and diagnosis in situ the evolution of the patient. These electronics based medical sensors can convert different forms of stimuli into electrical signals for analysis, so that they increase the intelligence of medical equipment providing bedside and remote monitoring of vital signs and other health factors. These developments are also supported by companies to satisfy the need of advanced new medical equipment used inside or outside the body for wide different applications. Thus, real-time, reliable, and accurate diagnostic results should be collected and provided by devices that may be monitored remotely, no matter the patients are in a hospital, clinic, or at home. For that purpose, the field of electrochemical sensors based on microelectronic devices has increased its important role in the last decade (Grieshaber *et al.*, 2008). These electrochemical sensors can sense gases, electrolytes and metabolites in vivo and in vitro for different kind of applications. The changes in these parameters are directly related with disease occurrence such as; cancer (Keller *et al.,* 2011), diabetes (Lin *et al.,* 2011), neurological disorders (Mattson, 2004) and ischemia (Oesch et al., 1986), among others. Monitoring of these diseases was promoted by the World Health Organization as their overall strategy for prevention and control diseases (Martinez *et al.,* 2003). 21st century will be

revolutionary in the biotechnology and biomedical field to cure pandemic diseases such as brain disorders, heart diseases, cancer and diabetes by advanced monitoring, diagnosis technologies.

Moreover, the usage of these technologies is not only limited to biomedical field, being also used for agriculture, environment, food industry and aquaculture. In the field of agriculture it is very important to control nitrate, chloride, potassium, ammonium, calcium and cyanide concentrations in soil and fertilizers. Also, determinations of nitrates and nitrites in vegetables and meat, calcium fluoride in milk, or heavy metal ions in seafood are critical for a healthy consume. In aquaculture applications; the dissolved oxygen and pH in fish tanks need to be controlled continuously. Furthermore, the water quality of our rivers, aquifers and see, as well as the waste water should be controlled by sensing pH, calcium, chloride and other ions, to assure a sustainable environment (Meyers, 2000).

1.1.2. Working principle of biosensors

According to the IUPAC definition (Theavenoti et al, 1999); "A chemical sensor is a device that transforms chemical information, ranging from the concentration of a specific sample component to total composition analysis, into an analytically useful signal. Chemical sensors usually contain two basic components connected in series: a chemical (molecular) recognition system (receptor) and a physicochemical transducer. Biosensors are chemical sensors in which the recognition system utilises a biochemical mechanism." (figure 1).

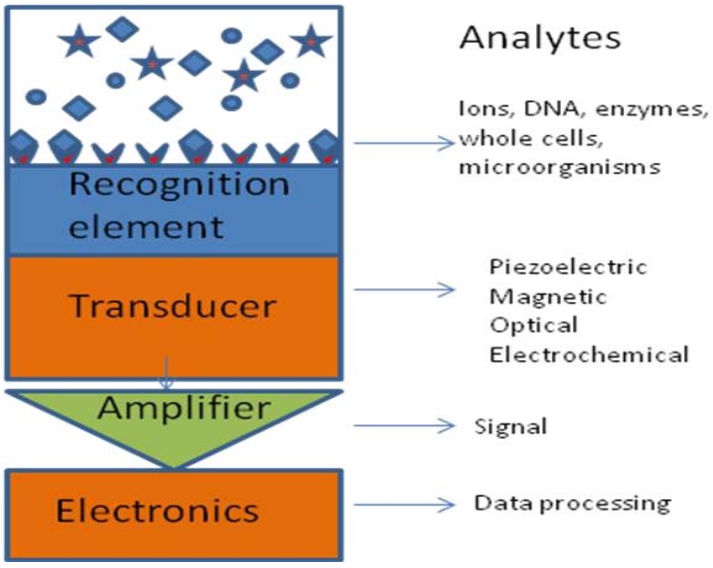

Figure 1. The biosensor parts

The sensors and biosensors may be classified depending on the type of receptor; could be found DNA, enzymatic, ionic, cell or inmuno-sensors, and also could be classified by their transducer; being reported as mass, magnetic, optical or electrochemical sensors.

Mass transducers transform mass change on the surface due to the analyte presence, by means of piezoelectric materials, which have high sensitivity to mass changes. The magnetic measurement in sensors is based on the changes that occur in the paramagnetic properties of the material after interacting with analytes. Optical transducers are the most widely commercialized. Different kinds of optical methods are used in sensor application, probably the most widespread are the ones based on fluorescence or colorimetric detection. In both cases, it is required a label attached to the analyte or to a secondary receptor. The transduction system is based on using a light source and an optical receiver, being different the intensity of light depending on the analyte concentration. But also, optical label free methods have been developed based on the excitation of the plasma on the sensing area, such as surface plasmon resonance or optical wavelight spectroscopy. All these described sensors have in common; high complexity and cost of fabrication in addition to difficulties for miniaturization.

On the other hand, electrochemical sensors do not require a transduction from a physical property to electronics, since this kind of sensors detect directly the electron transfer between the analyte and the electrode, which creates an electrical response proportional to the analyte concentration. This direct transduction permits simple devices, with low cost and easy to miniaturize.

The system required for an electrochemical readout is three electrodes in contact by an electrolyte solution. The electrodes required are working, reference and counter electrodes. The working electrode (WE) is the designation for the electrode under study, where the receptor is immobilized and all the interaction with the analyte happens. The counter electrode (CE) completes the current path in the electrochemical cell. And the reference electrode (RE) provides the experimental reference points for the measurements. Thus, RE should have a constant potential during testing. This can be provided by having very little or no current flow and if there is a current flow (no CE into the electrochemical cell), it should not affect the potential. There are many commercially available RE such as silver/silver chloride (Ag/AgCl), saturated calomel, mercury/mercury oxide, mercury/mercury sulfate, copper/copper sulfate and normal hydrogen electrode.

Electrochemical sensors are classified by the type technique used for the measurement. Conductiometric sensors measures the changes on the solution conductivity, amperometric sensors the detection of current at a fixed voltage, and voltammetric sensors monitors the changes of current scanning at different voltages. Potentiometric sensors measure potential change between WE and RE. Potentiometric and impedance sensors will be explained in detail in chapters 2 and 3 respectively.

1.2. Ionic sensors

Ionic sensors integrate chemical receptors that specifically recognize different type of ions, which are mainly based on potentiometry detection. Ionic sensors have demonstrated their applicability in the early 20th century due to its simplicity and low cost. Currently, potentiometric sensors have been successfully introduced into fields such as diagnosis, clinical process monitoring, chemical and food industry and environmental analysis. Ion selective electrodes (ISE) are the most popular potentiometric sensor due to its high sensitivity and selectivity.

At the end of the 19th century, the first trial to measure electrochemically the solution ion activity was done by Walter Nernst, measuring the acidity of a solution by potentiometry with hydrogen electrodes (Nernst, 1897). In following years, it was observed that a potential difference can be created between two sides of glass separating two sodium chloride solutions at different concentrations (Cremer, 1906). The experiments proved that the potential difference can be varied by changing the concentration of the solutions (Haber *et al.,* 1909). In following years, a glass electrode with perfect electrical properties was developed for wide pH range detection, which was the predecessor of the widely used pH sensors (McInnes *et al.,* 1930). These findings were supported by the fabrication of a stable and sensitive electron tube potentiometer (Stadie, 1929), which makes the glass electrode method easy for ordinary potentiometric detection. The glass electrodes contain a glass bulb membrane carried by an electrically insulating tubular body. This body integrates the internal solution and a Ag/AgCl electrode, which is separated by the glass from the studied solution (Figure 2).

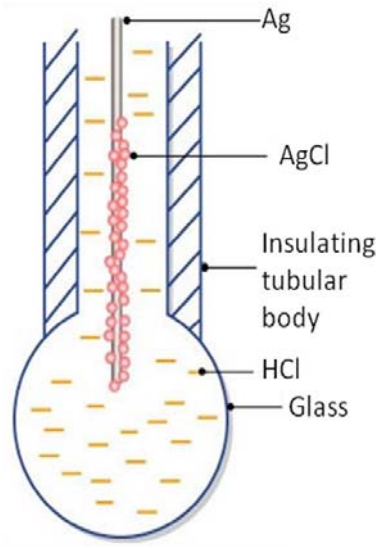

Figure 2. Scheme of a glass electrode

The glass electrodes measure the potential difference across the glass membrane, in respect to the inner reference solution. Normally, the inner reference electrode is integrated in the glass electrode (combined electrodes), although separated electrodes have shown an identical behavior (Vanysek, 2004) (Figure 3). This opened the way to study reference and glass electrodes separately.

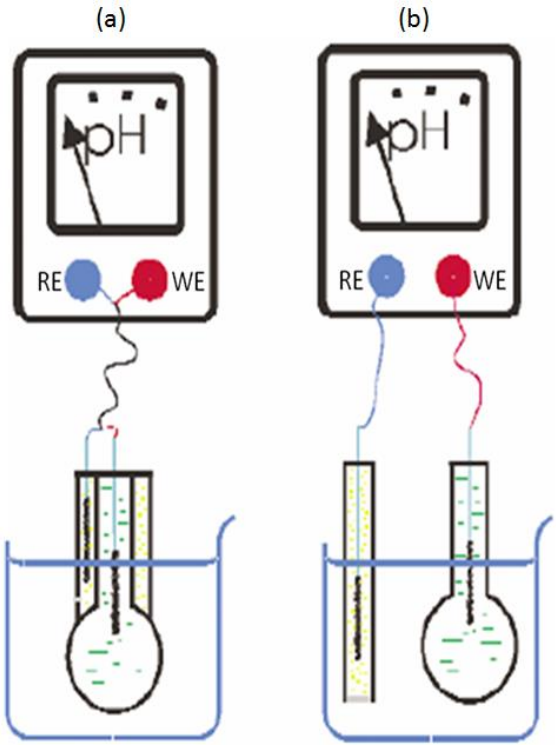

Figure 3. Measurement with combined electrodes (a) and separated glass and reference electrode (b).

Although, there were a lot of developments as mentioned above, in 1920´s the efforts were focused in the improvement of the irreproducibility instrumentation and definition of the pH units. Irreproducibility problems were solved by the invention of vacuum glass electrodes (Elder *et al.* 1928). The glass pH electrodes were evoluted to the conventional ISE, in which the ion-selective membrane is in electrical contact with the inner reference electrode through the inner reference solution. In this kind of systems, ionic conductivity was transferred through the membrane and reference solution to the inner RE. So, ionic conductivity is transduced to electronic signal by reversible electrode reaction of the inner RE (Figure 4). This provides an ISE with stable and reproducible standard potential.

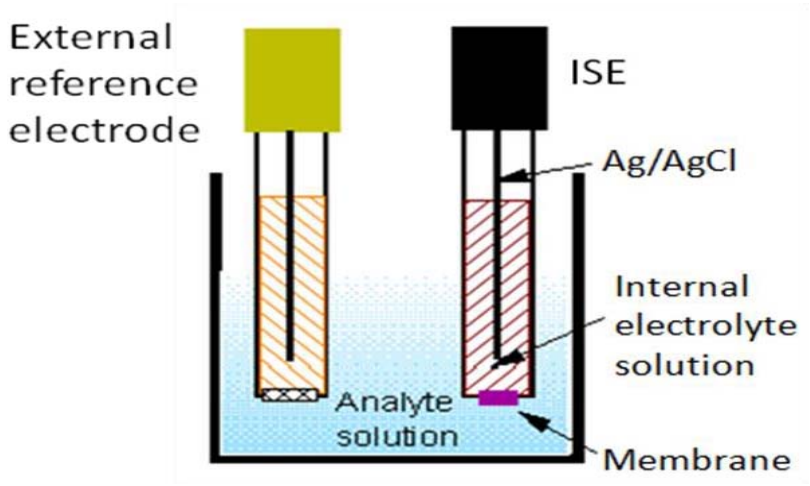

Figure 4. Conventional ISE electrodes with external RE.

These experimental improvements were supported by the theoretical works of Nikolski and Eisenman. This theory was named as the ion exchange theory for glass electrodes. Thus, the equation of Nikolski-Eisenman formed the basis of the modern theory of the potentiometric ISE sensors (Bobacka *et al.,* 2008). According to this theory, measured potential difference can be calculated by adding different potential creators to the equation. The electric potential (E_M) of an ion sensor is represented by the sum of a boundary potential (E_{PB}) at the sample ion-sensitive membrane boundary and by the diffusion potential inside the membrane or film (E_D).

$$E_{M=} E_{PB} + E_D + E_{internal} \quad (1.1)$$

$E_{internal}$ is a constant value, which was assumed as zero for simplifying the equation, so that, the equation turns to:

$$E_M = E_{PB} + E_D \quad (1.2)$$

$$E_{\mathrm{M}} = E_{\mathrm{PB}} + E_{\mathrm{D}} = \mathrm{const} + \frac{RT}{z_i F} \ln\left(c_i + \frac{\bar{u}_j}{\bar{u}_i} K_{i,j} c_j\right) \quad \text{(Bobacka et al., 2008) (1.3)}$$

According to the equation (1.3); the measured potential is a function of the absolute temperature (T), the ionic valence (z_i) and the ions concentration (C_i,C_j). In these equations, i symbolizes the ion of interest, j the interfering ions and k_{ij} the selectivity coefficient. The smaller the selectivity coefficient less is the interference by j. The

equation can be simplified considering that the ion mobility u_i and u_j are equal and so, the equation turns to:

$$E_{\mathrm{M}} = \text{const} + \frac{RT}{z_i F} \ln(c_i + K_{i,j} c_j) \qquad (1.4)$$

Where R is the gas constant, 8.314 JK^{-1} mol^{-1} and F is the Faraday constant, 9.6487* 10^4 C mol^{-1}

Based on this equation, potentiometric works by electric potential difference generated between the sensor, WE, and the RE, which is proportional to the variation of species activity in solution during recognition in zero current conditions. In an ideal case, the equation above turns to nernstian equation (1.5), where there is no ion interference and ionic valiance of ion of interest Z_i is equal to one.

$E_M = const + 59,16\ log_{10}(C_i)$ (Oesch et al., 1986) (1.5)

According to the equation (1.5) at room temperature, the response slope of the sensor should be 59, 16 mV for ions with ionic valence of 1. Most of ISE electrodes respond according to the Nernst equation, but often the slope of the response is slightly different from the expected theoretical value, with the validity of this equation limited to a certain range. In the presence of interfering ions, there are significant changes from Nernst equation. When the interfering ions are cations, it is affected by the primary ion activity, so that the detection limit was decreased according to the Nikolski-Eisenman equation (Figure 5a). Furthermore, if an ion is interfering, the sensing properties were totally lost at high concentrations (Figure 5 b) and the slope of the sensor was less than the nernstian slope.

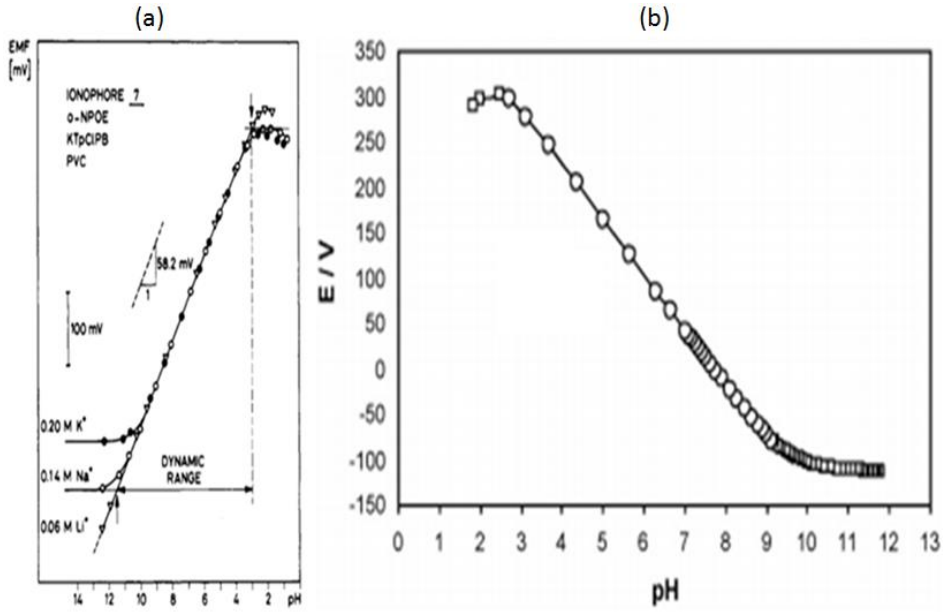

Figure 5. Smaller detection limit under the interference of cations (Oesch et al., 1986) (a). Anion interference at low pH (Anastova-Ivanova et al., 2010) (b)

Conventional ISE electrodes have worldwide usage in agriculture, food, chemical and biomedical industries (Simonian *et al.,* 2010; Harsanyi, 2000). In the biomedical field, the real time analysis of body fluids such as blood, plasma, serum or urine can be performed with this kind of sensors. Body fluids contain many different metabolites and analytes, which give direct information about the occurrence of diseases (Oesch *et al.,* 1986).

1.2.1. All-solid-state ISE sensors

Although conventional ISE electrodes have wide usage as listed above, these electrodes are very fragile and hard to miniaturize specially because of requirement of internal solution (Figure 4). A new breakthrough in the ISE field was started with the construction of all-solid-state ISE sensors, which eliminate the internal solution, improving its robustness and making easier its miniaturization. These kinds of sensors use highly selective molecules, called ionophores, chemically synthetized with and appropriate structure and functional groups for a selective interaction with the ion of interest (Stefanac *et al.,* 1967). One of the most famous ionophore is the valinomycin, a macrocyclic molecule that is a potassium holder for its specific detection, over other ions such as ammonium and alkali metal ions (Hauser *et al.,* 1995). This ionophore is entrapped inside a polymer based membranes, mainly fabricated with polyvinyl chloride (PVC), which simplified ISE membrane construction. This plasticized polymer acted as a liquid viscous, so that the properties of the electrodes are similar to those of liquid membrane without the difficulties of the inner solution.

Initially, all-solid-state sensors were PVC-based selective membrane coated platinum wires (Cattral *et al.,* 1971). These coated wire electrodes (CWE) had two main disadvantages; first the potential instability caused by blockage of the charge transfer process in the interface formed between the conductive electrode and the ISE membrane (PVC) and second; the poor adhesion of the membrane on the electrode surface (Esson *et al.,* 1997). Because of these reasons, CWEs had shorter lifetimes and low reproducibility compared to conventional ISE electrodes. Blockage of the charge transfer problem was solved by using an intermediate layer of interface material between conductive electrode and PVC membrane; AgCl, AgCl-Hydrogel or conductive polymers (CP) were used for this purpose (Alegret *et al,* 1989, Cosofret *et al,* 1995). There are a lot of scientific works focused in solving the adhesion problem, mainly modifying the plasticizer chemically or physically. One chemical modification used for this purpose was done by Harrison et al., oxidizing PVC for its reaction with an oxide surface (Harrison et al., 1988), or by modifying its structure with carboxylic acid groups (PVC–COOH) (Cosofret *et al,* 1995), and photocuring techniques by UV light (Abramova *et al.,* 2009). Also a mechanical attachment of the membrane by suspended polymer mesh was attempted (Blackburn et al., 1982).

Apart from the difficulties encountered in the WE, where the ISE membrane is deposited, there are also drawbacks for the development of all-solid state RE. The commercial glass REs were kept in saturated KCl solutions to minimize liquid-junction potential for having constant potential against time. Also with the aim of avoiding the glass coverage for a higher robustness and size reduction, some approaches have been undertaken to fabricate such miniaturized REs with inner electrolyte in a micro-channel liquid-junction (Hassel *et al.,* 1999), liquid-junction with thin-film techniques (Suzuki *et al,* 1999) and liquid-junction-free RE (Cranny *et al.,* 1998, Lee *et al.,* 1998), in which KCl is immobilized in a carrier material.

1.2.1.1. Characteristics of the ion selective membrane

The key to develop ISEs is the selective membrane that acts as a perm selective barrier. The most important part of the membrane is the ionophore, which should interact with the primary ion of interest in a fast, reversible sensitive and selective way. The ionophore is a compound designed to interact specifically with certain analytes having a cavity of suitable size and shape to coordinate with the primary ion, so that it defines the membrane selectivity. In the case of pH detection, the dynamic ranges of the corresponding membrane electrodes are dependent on the acidity constant (pK) of the employed ionophore (Oesch *et al.,* 1986). pK can be tuned by changing the basicity of the nitrogen atom of the ionophore e.g. by the elongation of the alkyl chain (Figure 6). The range of detection shifts to higher pH values as the pK of the ionophore is increased.

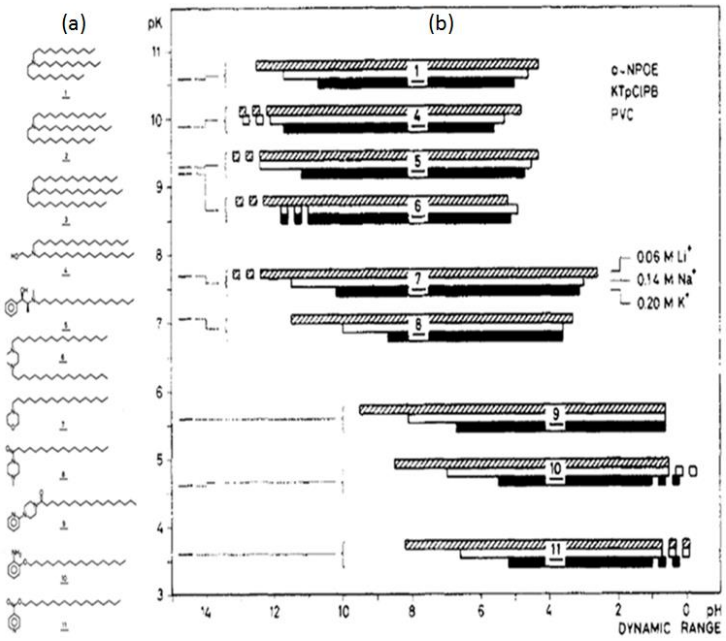

Figure 6. Different hydrogen ionophores with different alkylchains (a) determine working range of sensor depending their acidity constant (pK) under the interference of lithium (Li^+), sodium (Na^+), potassium (K^+) (b) (Oesch et al., 1986)

However, the increase of the ionophore basicity leads to an increase in the degree of the protonation of the ionophore (Figure 7), so that anion interference starts to occur at low pH values (Figure 6) decreasing the range of selective pH detection.

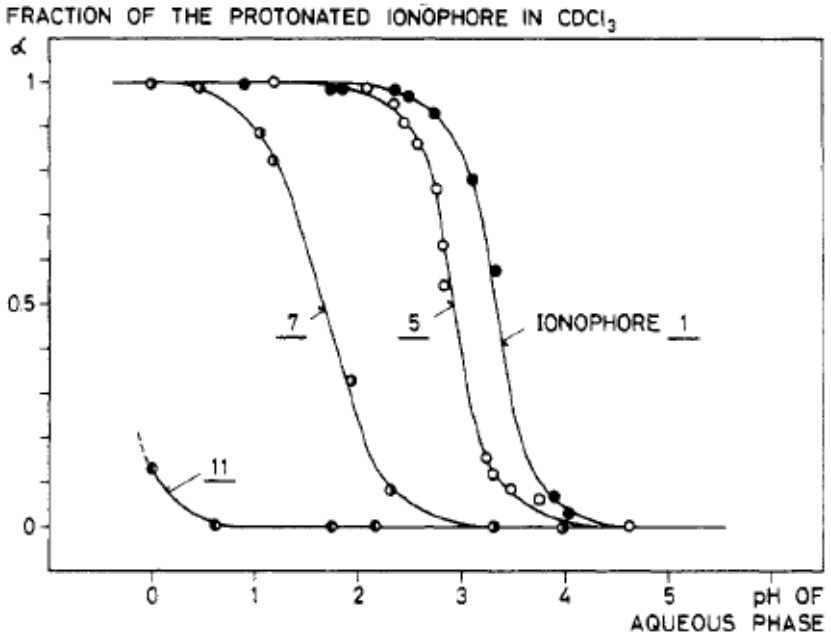

Figure 7. Fraction of the protonated ionophore (α) in $CDCl_3$ for different ionophores *vs* pH (Oesch et al., 1986)

In the case of valinomycin, it is used to sense potassium ions over other ions such as ammonium and alkali metal ions (Figure 8). In this kind of crown structures, the electron donor atoms present in the receiving cavity influence the interaction with the ion to be determined.

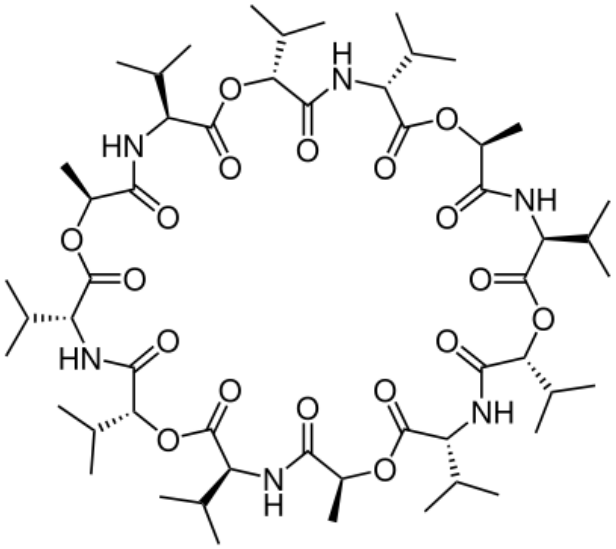

Figure 8. Structure of valinomycin

There are also synthetic ionophores based on crownethers that are able to form stable complexes with ions of alkali metals or alkaline earth metals. However, oxygen atoms can weakly coordinate to the heavy and noble metals. In this regard, oxygen atoms were substituted by sulfur atoms to sense heavy and noble metals, since the sulfur atoms are mostly involved in the binding of these cations (Figure 9).

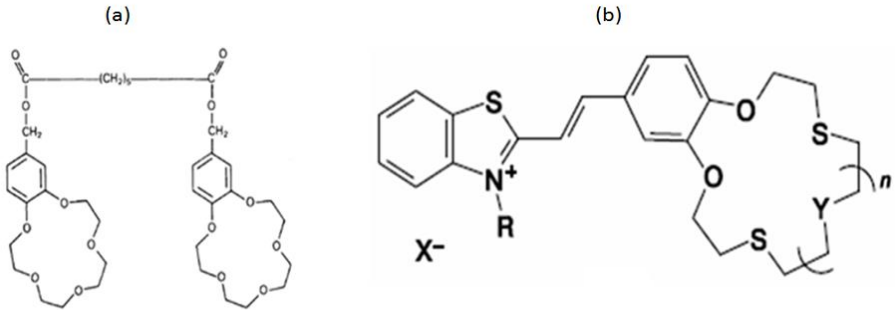

Figure 9. Bis[(benzo-15-crown-5)-4′-ylmethyl] pimelate for potassium detection (Moody, 1989) (a) and chromogenic benzothiacrown ethers where the sulfur atom is in conjugation with the chromophoric fragment for heavy metal detection (Vedernikov, 2010) (b)

Apart from ionophores, the membrane also contains plasticizer, additive and matrix, which are affecting the membrane performance. By changing the composition of the membrane, sensitivity, selectivity, mechanical stability, life and response times can be

modified. The choice of plasticizer is critical in the selective membrane preparation, because it connects all the components of the membrane creating a stabile membrane. Depending on its characteristics as lipophilicity, high molecular weight, low vapor pressure and high capacity for dissolving additives of the polymeric membrane, these parameters affect its permeability causing changes in sensitivity and stability (Oesch *et al.,* 1986). There are different plasticizers for this purpose such as chloronaphthalene (CN), dioctylpthalate (DOP), dibutyl butylphosphonate (DBBP), tri-n-butylphosphate (TBP) and o-nitrophenyloctylether (o-NPOE), bis(1-butylpentyl) adipate (BBPA) (Lee et al., 1998).

The membrane should be only permeable to the ions with the same charge as the primary ion, for this purpose the additives are used in the preparation of the ISE membrane. Additives repel oppositely charged ions, so that membrane has selective permeability. Normally, liphophilic anionic additives are used. Most employed ones for the determination of cations are potassium tetrakis (4-chlorophenyl) borate (KTpClPB) and sodium tetraphenylborate (TPBNa) (Figure 10). The presence of additives in the selective membrane increases the sensor selectivity by reducing interference. In addition, it enhances the sensitivity of the membrane and reduces the response time. However, an excess of salt amount can change the membrane mechanical stability and selectivity, so that additive concentration should be controlled carefully.

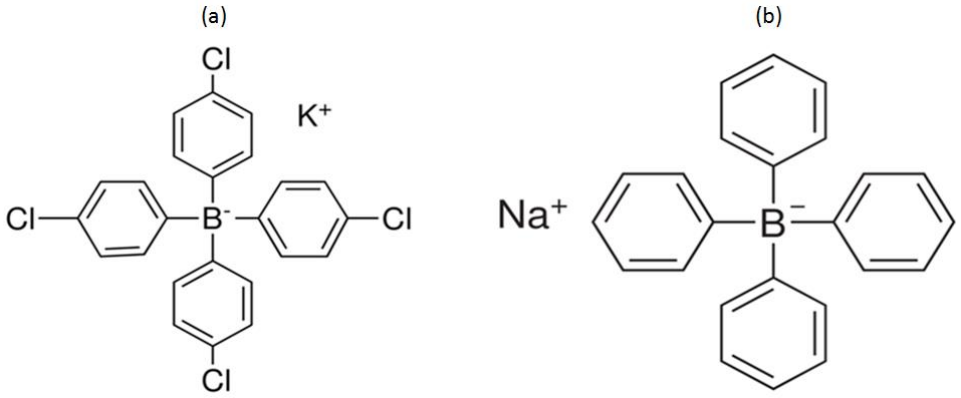

Figure 10. Structure of potassium tetrakis borate (KTpClPB) (a) and sodium tetraphenylborate (TPBNa) (b)

The matrix provides high mechanical and chemical stability to the membrane and it should be chemically inert. Most popular matrix is PVC, because of its chemical stability, biocompatibility and low price among the various compounds such as silicone, polyurethane, polystyrene, epoxy polymers used.

The last but not least part of the membrane is the solvent. It should solve all the membrane components. There are plenty of solvents such as tetrachloroethylene, toluene, turpentine, acetone, methyl acetate, ethyl acetate, hexane, petrol ether, ethanol

and water. However, the most used one to solve ISE membrane components especially with PVC based membrane is tetrahydrofurane (THF).

1.2.1.2. Properties and applications of all-solid state ISE sensors

Parameters such as detection limit, detection range, mechanical stability, response time, biocompatibility, reproducibility, selectivity, life time and sensitivity requirements should be defined before starting the design of an all-solid state ISE sensor.

Some challenges and needs of all-solid state electrochemical sensor can be listed as follows:

- The detection limit and signal to noise ratio should be very low and detection range should be as broad as possible. Also, high sensitivity is needed to distinguish low concentrations with close proximity. Moreover, high selectivity is required so that the device detects only the ion or metabolite of interest.

- Mechanical stability of the sensor must be strong, so that all-solid-state sensors should be stable on the WE surface for long sensor life time.

- The sensors performance should be reproducible and determine the right concentration of analyte with low standard deviation.

- The calibration of the electrochemical sensor should be simple and easy to perform. The signal obtained from the sensor response should be proportional to concentration of analyte in solution.

- The sensor should return to its baseline after measurement of the analyte, so that it can assure a repeatable response with low drift.

- The response time should be fast to use in real-time monitoring.

- The dimensions of the sensors must be as small as possible to reduce the sample volume.

- The sensors should have a long lifetime for continuous measurements and multisensor applications.

1.2.2. ISFET sensors

Ion sensitive field effect transistors (ISFET) are the further evolution of the ISEs. In a traditional field effect transistor (FET), the drain to source current flows through the conducting channel connecting the source and drain regions. The conductivity of a channel was controlled by an electric field between the gate and source terminals, so that gate electrode controls the conductivity by changing the electric field potential. For ISFET, gate electrode contains the analyte-selective membrane, which is brought into contact with the analyte solution (Errachid *et al.,* 2004). The membrane is selective to a specific ion so that the changes in these ion concentrations influence the accumulated charge carriers at the gate surface in proportion to the original analyte concentration. Hence, an electrical signal in the form of a measurable drain current is produced (Figure 11).

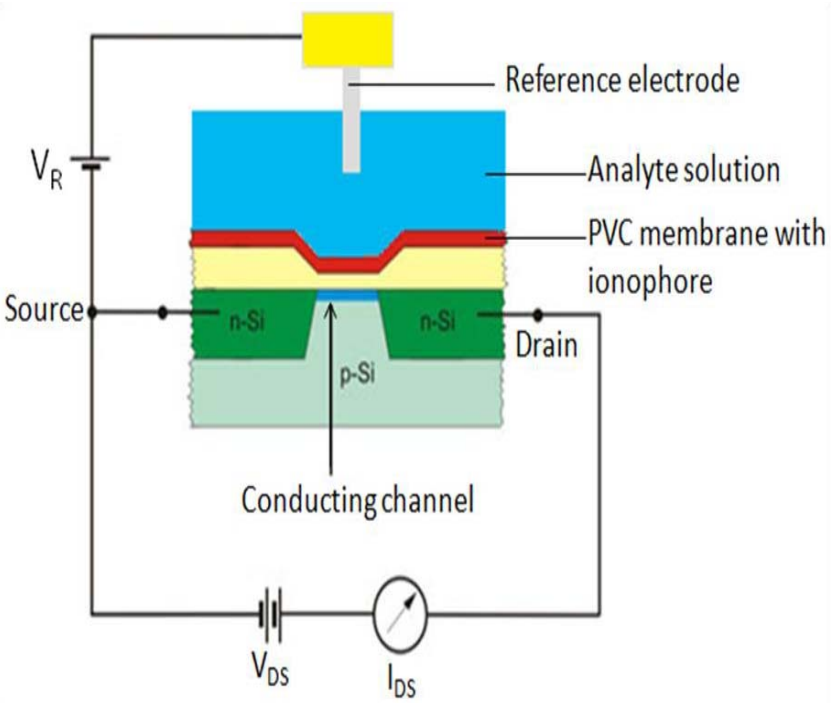

Figure 11. Scheme of an ISFET

The developments in the field were started in the beginning of 70´s by combining transistor and chemical sensor technology, for developing a field effect transistor sensitive to H^+ ions (Bergveld, 1970). At that time, this discovery was very important, because it provides the possibility to decrease the size of the existing diagnostic devices for biomedical applications. These sensors have a lot of important properties such as small size, robustness, fast response time and the possibility of mass production. Currently, there are ISFET sensors integrated with microprocessors, microcontrollers on the same chip (Figure 12) (Liu *et al.,* 2011, Goh *et al.,* 2011, Prodromakis *et al.,* 2011).

For pharmaceutical and biomedical industries, the main applications are directed to the clinical determination of gases (O_2, CO_2) and ions in biological fluids such as blood, urine, and sweat (Wang *et al.,* 1998, Vadgma *et al.,* 1991). These sensors have also used to detect myocardial ischemia by sensing potassium (K^+) and hydrogen (H^+) with multi ISFET sensors (Rai *et al.,* 2008).

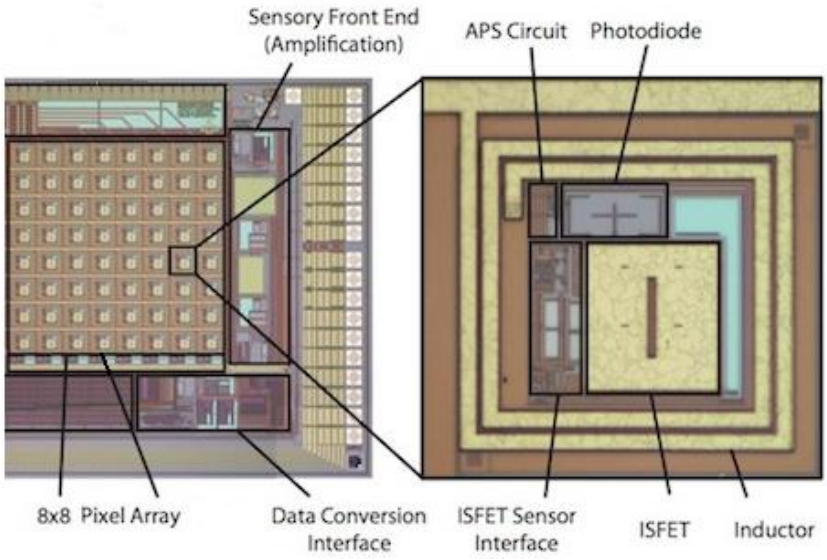

Figure 12. 64 ISFET sensor integrated with microprocessors, microcontrollers (Liu *et al.,* 2011, Goh *et al.,* 2011, Prodromakis *et al.,* 2011)

1.3. Impedance sensors

1.3.1. Impedance detection

Electrical impedance is the opposition of a current circuit during alternating current (AC) flow when a voltage is applied. Impedance is very valuable technique, since under direct current (DC) just information about the resistance of the circuit can be collected. However, under AC, other current impediments can be analyzed; the induction and the capacitance. Impedance is presented by real and imaginary parts. The current flow creates an electrostatic storage of charge induced by applied voltages called capacitance. The impedance caused by the capacitance, known as reactance, forms the imaginary part while the resistance forms the real part. Electrical impedance circuit can be presented as follows (Figure 13);

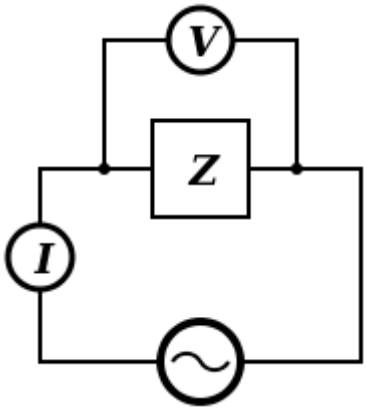

Figure 13. Representation of an impedance circuit

$$V=I\cdot Z \tag{2.1}$$

$$Z= R+ jX \tag{2.2}$$

$$j= \sqrt{-1} \tag{2.3}$$

$$X=1/ (2\pi fC) \tag{2.4}$$

where V is the voltage, I the current, Z the impedance, R the resistance, X the reactance, f the frequency and C the capacitance.

As can be seen from the formula (2.4), capacitive reactance is inversely proportional to the signal frequency and the capacitance, so that impedance can be defined as the frequency domain ratio of the voltage to the current. The magnitude of the complex impedance is the ratio of the voltage amplitude to the current amplitude and can be visualized in the figure 14, which shows the relation between reactance and resistance.

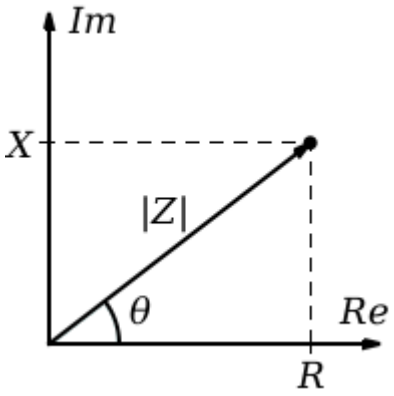

Figure 14. Representation of imaginary and real parts of the impedance

Θ is the phase shift of the complex impedance, that can be calculated by the delay time (d_t) between current and voltage (Ivorra, 2002). According to the relation;

$$\Theta = d_t * 360 * f \quad (2.5)$$

As can be seen from the equation (2.5), phase shift is depending on frequency and delay time (Figure 15). The change in the potential and current can be written as;

$$V(t) = V_0 * \sin(wt) \quad (2.6)$$

$$I(t) = I_0 * \sin(wt + d_t) \quad (2.7)$$

In this equation, w is the radial frequency, which is equal to:

$$W = 2\pi f \quad (2.8)$$

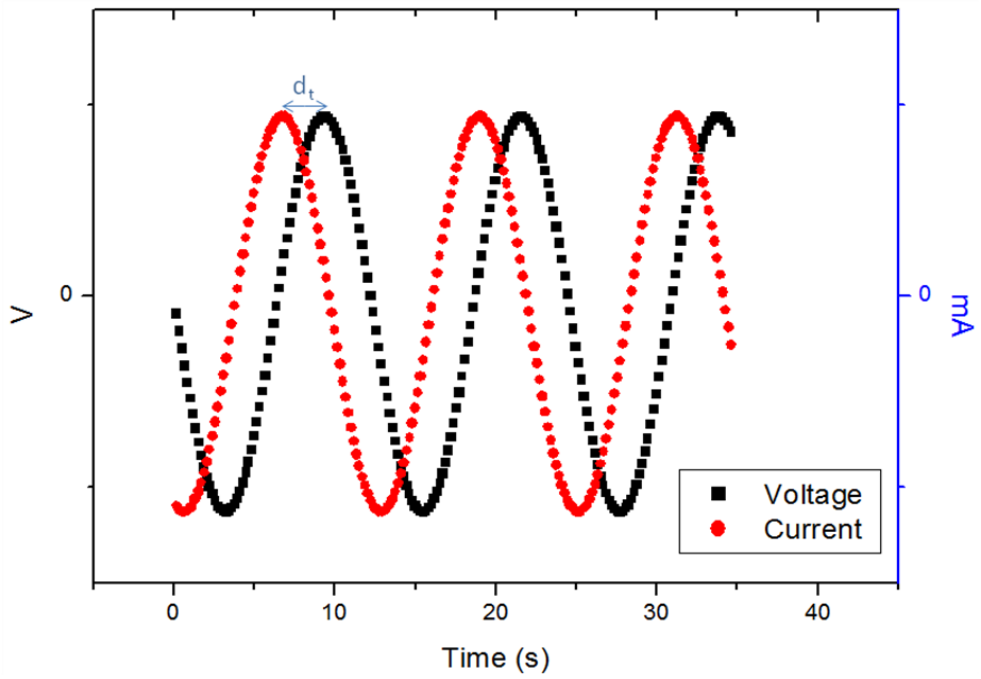

Figure 15. Plot of the voltage and current with a certain delay time

The magnitude of the impedance can be calculated according to the equation 2.9.

$$|Z|=\sqrt{ZZ^*}=\sqrt{(R^2+X^2)} \quad (2.9)$$

1.3.2. Bioimpedance

Impedance technique is used for electronics applications to measure elements like resistance, capacitance and inductance among others in electronics circuits. In the beginning of the 20th century, the scientific community started to be interested in this technique for being applied in biological samples such as cells, blood, tissues and organs. The charge carriers in living tissue are ions, which modify the pass of current in the solution changing the resistance. Thus, a cell membrane can behave as a capacitor. The cells can be considered as an electric circuit with serial and parallel connected resistance and capacitances (Figure 16). This idea motivated the scientists to make impedance measurements in biological elements and that was the birth of the bioimpedance field.

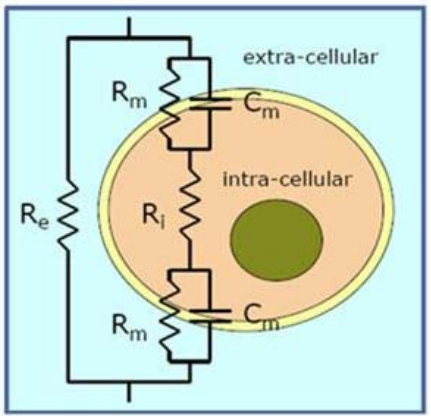

Figure 16. Representation of an electrical circuit across de cell

Since the intracellular and extracellular properties of the cells can change in case of different diseases. This technique allows the differentiation of healthy and sick tissue and provides the diagnosis of illness. The tissues behave differently according to the applied frequency. At low frequencies (<1 kHz), the cell membrane stores charge electrostatically behaving like a natural barrier for the current entrance. Thus, under low frequencies the applied current just flows in the extracellular matrix. However, at high frequencies (> 1 MHz), the current is able to cross the cell barrier, so that the current can flow through the cells (Figure 17). For frequencies between 1 kHz and 1 MHz, the current can flow through and around the cell, depending on the extracellular, intracellular ionic concentration and the membrane capacitance of the cell type. Hence, by alternating the frequency, normal and diseased cells can be distinguished as they have extra- and intracellular ion concentration and the deformation of the membrane.

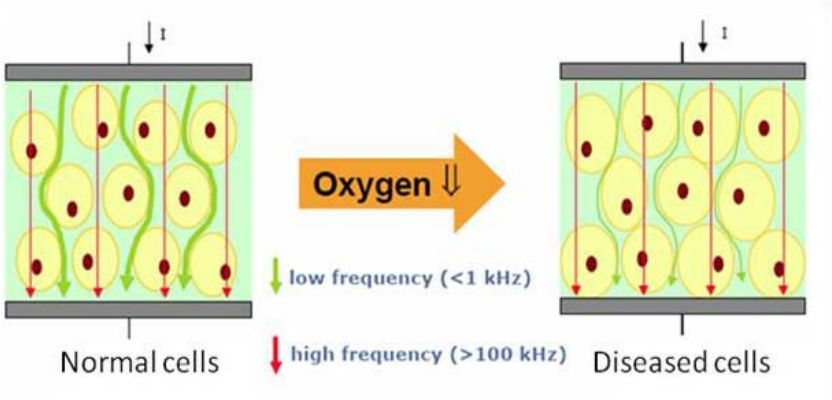

Figure 17. Behavior of cells at frequencies below 1 kHz and higher than 100 kHz for normal and ischemic tissue (Ivorra et al., 2002)

There are different methods to perform impedance measurements, depending on the number of electrodes used for this purpose (figure 18). Two-electrode experiments are the simplest cell setups, in which current carrying electrodes are also used for sensing, so that a polarization layer at a WE and RE to electrolyte interface is created. This situation is affecting the sensitivity of impedance measurements and makes complicated to analyze the results.

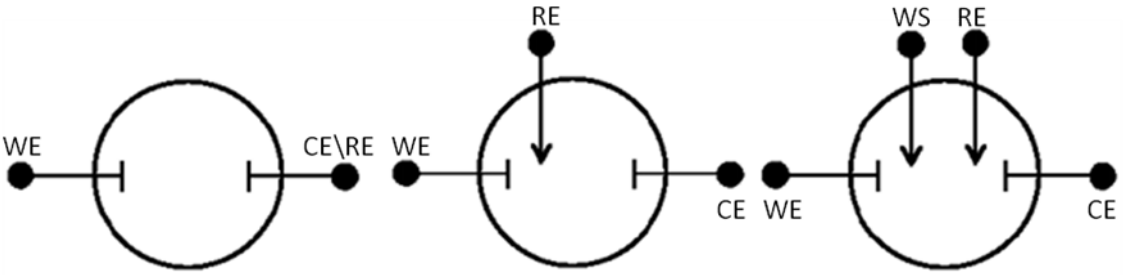

Figure 18. 2, 3 and 4 electrodes impedance measurements (Zou et al., 2003, Othman et al., 2003)

In three electrode models, the RE is separated from CE and connected to a third electrode measuring a point very close to the WE. In this way, the polarization effects were decreased using one half of the cell. Thus, just a polarization layer at a WE was created. In four electrode model, WE and CE are separated from RE and working sensing electrodes (WS) (Figure 18). Thus, four-electrode model has a distinct experimental advantage over two and three electrode setups, because WS and RE measure the potential changes independent from the polarizations of WE and CE. These properties make four electrodes system the best candidate for in-vivo experiments with its higher sensitivity and reliability (Zou *et al.,* 2003, Othman *et al.,* 2003). In four electrode systems, the current is injected by the outer electrodes and the voltage is recorded by the inner electrodes (Figure 19).

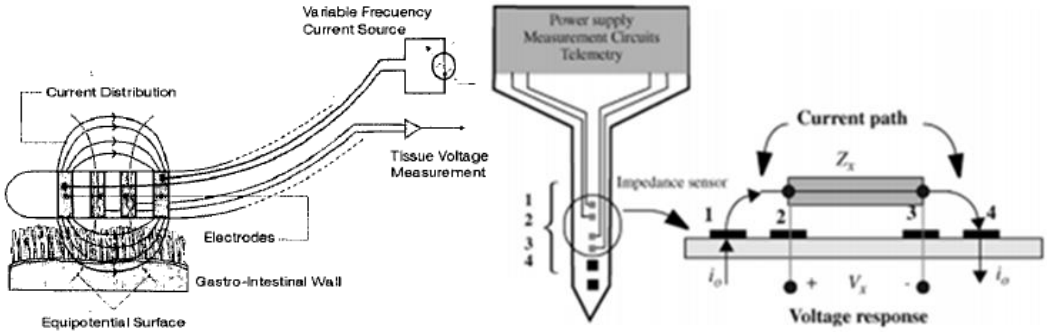

Figure 19. Reported examples of different configurations of 4 electrode impedance measurements(Zou *et al.,* 2003, Othman *et al.,* 2003)

1.3.3. Applications

Bioimpedance technology is an attractive tool, since it is safe, inexpensive, portable, rapid, convenient for use and highly reproducible. Because of these promising properties, a lot of different applications have been published in scientific journals in the last decade, using this technique. Bioimpedance had been focused in four different branches of biomedicine; estimation of body composition, wound healing, prognosis and detection.

Estimation of body composition consist in the assessment of fluid volumes and fat-free mass (FFM). Hoffer *et al.* found a significant correlation between healthy subjects and patients with fluid imbalance according to their total body water (TBW) volume, which was quantified by applying single frequencies to the whole body (Hoffer *et al.,* 1969). This idea was improved by others adding different variables such as body weight age and gender to have precise prediction (Lukaski *et al.,* 1985, Segal *et al.,* 1985, Kushner *et al.,* 1986, Lukaski *et al.,* 1988). However, there was a high variability between the group with healthy people and the group with obesity, chronic diseases and weight reduced people. For improving the method, multiple frequencies were started to be tested. At low frequencies (<1 kHz), the frequency just flows in the extracellular matrix, and so the extracellular water (ECW) can be determined. However, at high frequencies (> 1 MHz), the current is able to cross the cell barrier. Thus, the intracellular water (ICW) can be determined. TBW is the result of the summatory of ECW and ICW. By combining these techniques, high precision was achieved to predict assessment of body volumes. However, the topic is still controversial, because TBW and ECW results for people with severe obesity after weight loss were over predicted according to the impedance results (Cox-Reijven *et al.,* 2002). In contrary, TBW and ECW results were underestimated for patients with gastric bypass surgery (Mager et al., 2008)

Another important part of the body composition estimation is the analysis of FFM, which was done generally by applying 50 kHz between electrodes placed on the hand and the foot of a person. At 50 kHz, it measures the sum of ECW and ICW resistivities, because at this frequency the current is flowing through extracellular and intracellular matrix. This technique was named as FFM, because the adipose free mass compared with adipose tissue (fat tissue) has approximately six times TBW and twice the ECW content per unit weight (Wang, 1976). Although many impedance models are available to predict FFM, it is not reliable except among healthy adults. Predictions of FFM with these single-frequency bioimpedance models overestimate FFM in subjects with an expanded ECW. It is usual for congestive heart failure, severe obesity and hepatic disease patients or also this can be observed after weight loss or gain. So that it can be concluded that changes in the constancy of composition disturb the accuracy of the measurement.

Wound healing analysis is another important property, which can be analyzed noninvasively with single frequency, phase sensitive bioimpedance measurements. In

vitro experiments with cells and in vivo experiments with animal tissues have proved that increase of resistance can be interpret as cell growth and healing, at a certain frequency. In contrary, cell death or acute injury causes the decrease of resistance. Experiments of patients with high risk of pressure ulcer showed that their tissues reduced resistance and reactance compare to the control group. Processes during wound healing can be analyzed by bioimpedance noninvasively using the inverse relation of extracellular fluid volume and proportionality of fibrin clot formation to resistance. Also, cell mass is directly related with reactance. Thus, direct correlation between epidermal proliferation and granulation of the wound can be found with reactance. In conclusion, direct relationship between the bioimpedance results and healing can established and this advance system can be used for patient care (Spence *et al.,* 1996, Keese *et al.,* 2004, Lukaski *et al.,* 2012, Wagner *et al.,* 1996)

The last but not least, the prognosis and detection of diseases can be analyzed also with bioimpedance. Prognosis can be described as the way to predict possible future outcomes of an individual and detection can be described to find the existence of a disease. Prognostic accuracy is quiet strict to the statistical based methods with high dispersion, so that precision is quiet low taking into account the effects of age, gender, body mass index, nutritional status and physical activity. Whole-body bioimpedance technique was widely used as a predictor of morbidity and mortality in many types of chronic diseases by analyzing the phase angle. However, the range of phase angle is highly dependent on gender and age. Moreover, the survival possibility of advanced cancer patients can be analyzed by impedance. It has been shown that increase in phase angle after therapeutic intervention was associated with a 25% increase in survival. Furthermore, by applying radiofrequency current locally neuromuscular diseases can be recognized, due to radiofrequency current let to analyze the anomalies in neuromuscular disease, considering integrity and arrangement of cell membranes. In this case, the current is flowing along the muscle fiber, encountering less cell membranes compare to perpendicular. Thus, phase and resistivity are changing depending on the arrangement of the muscle fibers. Thus, bioimpedance gives the chance to analyze the anomalies of neuromuscular disease patients. (Lukaski, 2013)

Bioimpedance technique can also be used in detection of electrolytes and proteins in water and blood. Living cells must contain and are surrounded by aqueous electrolytes. In human blood, the most important ions are H^+, Na^+, K^+, Ca^{2+}, Mg^{2+}, HCO_3^-, Cl^- and HPO_4^-. Also, proteins contain in all the aminoacids, negatively charged carboxyl groups (COO^-) and positively charged amino groups (NH_3^+). In basic solutions, carboxyl groups are negatively charged and in acidic solutions, amino groups are protonated. Therefore, depending on the isoelectric point of each protein and the pH of its surroundings, proteins behave like a macro anion or cation, which can be dissolved in aqueous solutions. Hence, impedance of the solution starts to change depending on the concentration of these ions.

Impedance technique can also be used to detect bladder (Keshtkar *et al.,* 2012), breast ((Zou *et al.,* 2003) or skin cancer (Aberg *et al.,* 2005) among others. The cell has numbers of mechanisms for exporting ions, and a carrier-mediated system for exporting lactic acid. To maintain intracellular and extracellular concentration, ions should be pumped continuously from the cells. It is well known that cancer cells are poorly vascularized, so that interstitial fluid fails to equilibrate rapidly. Hence, cancerous tissue can be distinguished from normal tissue, due to the difference on the intracellular and extracellular environment (Griffiths et al., 1991. However, similar impedance properties of different staged cancer cells make in some cases hard to diagnose. Keshtkar *et al* studied different impedance behaviors of stomach cancer cells (Keshtkar *et al.,* 2012). Figure 20 shows the results obtained in that study, wherein the close impedance results for the cancer cells with different stages make hard to distinguish. Normal (blue) and abnormal; benign (green), tumoral (red) and dysplasia (magenta) cancer cells have nearly the same impedance values.

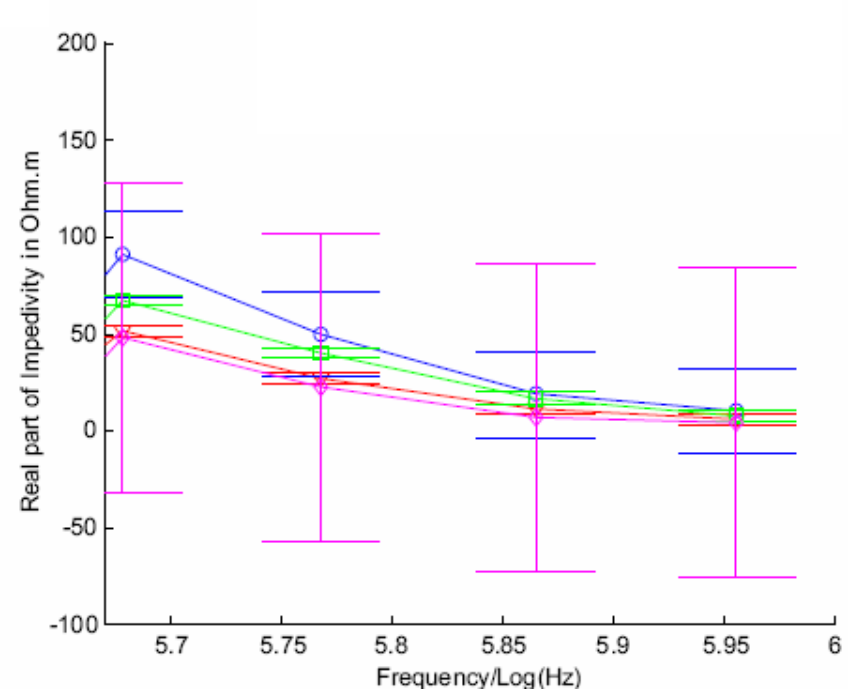

Figure 20. Electrical impedance results for normal and abnormal gastric tissue

The effect of mechanical stress is a limiting factor on impedance measurements for in vivo experiments. Mechanical stress alters the dimensions of the tissue continuously because of the respiration of the animal and creates a change in the tissue impedance. Also, the differences in the body fluids for some organs such as stomach can drastically change the detected signal causing irreproducibilities.

In conclusion, bioimpedance technique is very promising for estimation of body composition, wound healing, prognosis and detection. However, it is not totally optimized system and requires further improvements to solve the drawbacks commented and challenges to overcome.

1.4. Overview of ischemia

Ischemia is a lack of oxygen in the tissue, which can happen in any part of the body, but it is especially relevant in the case of brain, heart, bowel and stomach. 80% of all stroke produced in brain are because of ischemic stroke (Thrift et al., 2001), causing the 9% of deaths around the world, being higher in western countries (10–12%). The cost of stroke worldwide is around 2–4% of total health-care costs. The total costs per year of this disease is varying from country to country (£7, 6 billion in the UK, (AUS$ 1, 3 billion in Australia, and US $ 40,9 billion in the USA) (Donnan *et al.,* 2008).

Ischemic heart disease was the fifth most common cause of death in 1990 and is currently the leading cause of death in adults in developed countries. In 2020, it is estimated to be the most common disease of death (Menken *et al.,* 2000). Another kind of ischemia with high mortality rate is the acute mesenteric ischemia (bowel ischemia). Relative infrequency and non-specific clinical presentation cause delays in diagnosis and treatment and triggers high mortality rate (60–80%). Unfortunately, remarkable developments in medical and surgical aspects cannot help to improve the diagnostics of this disease (Oldenburg *et al.,* 2004, Assar et al. 2008). Furthermore, diagnosis of gastric ischemia brings more difficulties, since similar symptoms to other diseases delay its right diagnosis (Quentin *et al.,* 2006). The occurrence of gastric ischemia is mostly observed during morbid obesity surgeries. Sleeve gastrectomy (a surgical weight-loss procedure, in which the stomach is reduced to about 25% of its original size) and gastric bypass (reconnection of stomach and intestine) are safe and reproducible methods for morbid obesity surgeries (Jeffrey *et al.,* 2008, Dejardin *et al.,* 2013). However, lax gastric fixation or incorrect positioning of the stomach can lead to gastric volvulus (Dejardin *et al.* 2013). This may result in obstruction and impairment of the blood supply to the organ causing gastric ischemia (Kicsk *et al.,* 2007). Also, bowel obstruction due to internal hernia is another problem during gastric bypass, which can also cause severe ischemia (Peterson *et al.,* 2009, Aghajani *et al.,* 2012).

1.4.1 Biochemistry of ischemia

As we introduced, ischemia is a shortage of the blood supply to an organ. A prolonged ischemia condition causes severe tissue damage and failure of organs. Due to the lack of oxygen in the ischemic tissue, it turns from aerobic to anaerobic respiration. Under anaerobic respiration, the glucose is broken down to pyruvic acid and then converted to

lactic acid decreasing the pH of the tissue. The physiological concentrations of metabolites are maintained in a balance between the intra and extracellular medium through the action of ion pumps (Table 1).

cations (meq/L)			anions (meq/L)		
	extracellular	intracellular		extracellular	intracellular
Na^+	142	10	Cl^-	103	4
K^+	4	140	HCO_3^-	24	10
Ca^{2+}	5	10^{-4}	protein-	16	36
Mg^{2+}	2	30	HPO_4^{2-} + SO_4^{2-}	10	130
H^+	4×10^{-5}	4×10^{-5}	+ organic acids		
Sum	153	180	Sum	153	180

Table 1. Concentration of electrolytes in body liquids. (Grimnes, Martinsen., 2000)

This process requires metabolic energy from the adenosine triphosphates (ATPs), which is limited during ischemia. That causes the ion pumps to fail and due to the osmotic pressure ions move through the cell membrane according to the differences on ion concentration. Thus, under ischemic conditions potassium moves to extracellular fluid and sodium moves to intracellular (Songer, 2001). Moreover, the water penetrates into the cell generating the growth and filling of the extracellular space. That slows down the blood flow and decreases removal of carbon dioxide (CO_2) from the cells. The increased CO_2 pressure (pCO_2) creates a decrease of pH according Henderson-Hasselbalch equation (Hameed *et al.,* 2003);

$$pH = 6.1 + \log\left(\frac{[HCO_3^-]}{0.03 \times pCO_2}\right)$$

$$CO_2 + H_2O \rightarrow HCO_3^- + H^+$$ (Russel *et al.,* 1997)

All these changes cause an equilibrium shift and a new equilibrium is established under ischemic conditions. Oxygen, pH and glucose level decrease and ion pumps of these ischemic cells cannot work properly, creating a difference between intracellular and extracellular ions concentrations of sodium, potassium and chloride (Ammann et al., 1985).

1.4.2. Ischemia detection technologies

There are a lot of attempts to sense ischemia. The transduction methods reported are optical, magnetic and electronic. Noninvasive and non-touch optical detection of living tissues is getting more relevance. Oxygen is carried to tissues by the hemoglobin in blood, so, relative concentration of oxyhemoglobin determines the absorption of light in

the tissue. The optical method used for this detection is reflectance spectrophotometry, in which a light with specific wavelength is emitted to the tissue and the absorbance of the tissue is detected (Figure 21) (Friedland *et al.,* 2004). The different optical techniques reported are depending on the light source; basically LED with different frequencies at near infrared (Mirtaheri *et al,* 2004, Jafarzadeh and Rosenberg, 2009) or at visible light (Benaron *et al.,* 2004) and a photodiode as a receiver of signal.

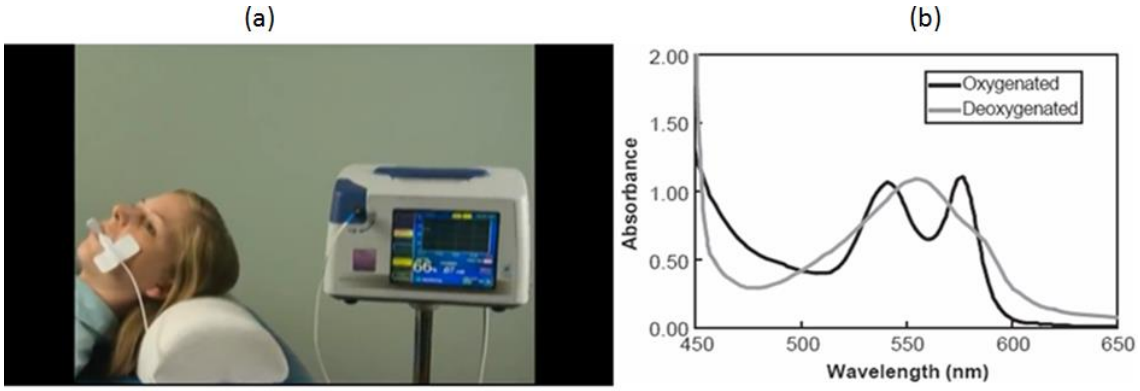

Figure 21. (a) Light with specific wavelength is emitted to the tissue and detected the tissue absorbance (b) Absorbance of oxygenated and deoxygenated tissue for different wavelengths.

Magnetic measurements are based on sensing the magnetic field created by the body electrical rhythm, which changes from ischemic and nonischemic tissue. The device used for this purpose is a superconducting quantum interference device (SQUID) (Figure 22 a) (Seidel *et al.,* 1999). The basic electrical rhythm (BER) is an electrical slow wave of the gastrointestinal tract, which generates a magnetic field. It characterizes the underlying electrical activity of the bowel. BER frequency is known to fall with ischemia (Figure 22 b).

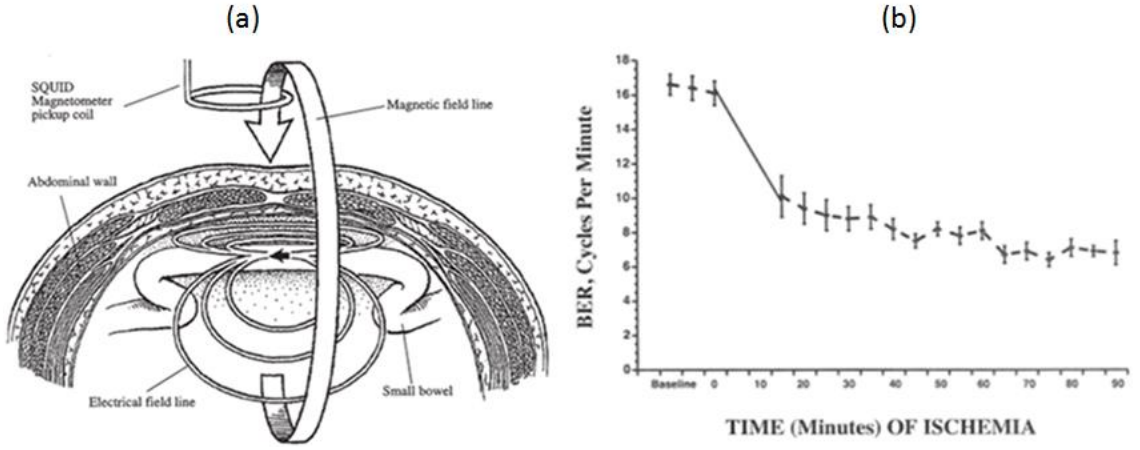

Figure 22. Demonstration of BER creating a magnetic field sensed by SQUID on small bowel. (a) Magnetic measurement of ischemia for 90 minutes (b)

Also, there are carbon dioxide sensors related with ischemia detection, which use air tonometry in order to measure the partial pressure of gastric carbon dioxide. Tonometry has a catheter with a gas permeable silicone balloon and the change in carbon dioxide pressure is sensed through the balloon. The disadvantage of air tonometry is the slow measurement rate which makes it unsuitable for short-term monitoring and for giving in real time the state of the patient (Mirtaheri *et al,* 2004, Herber *et al.,* 2005, Hameed and Stephen, 2003). Moreover, there are impedance sensors, which can analyze resistance and capacitance of the environment and cells membrane (Figure 23). The ion channels of the affected cells start to work differently, changing the concentration of ions inside and outside of the cells (Beltran *et al.,* 2005, Othman *et al.,* 2003).

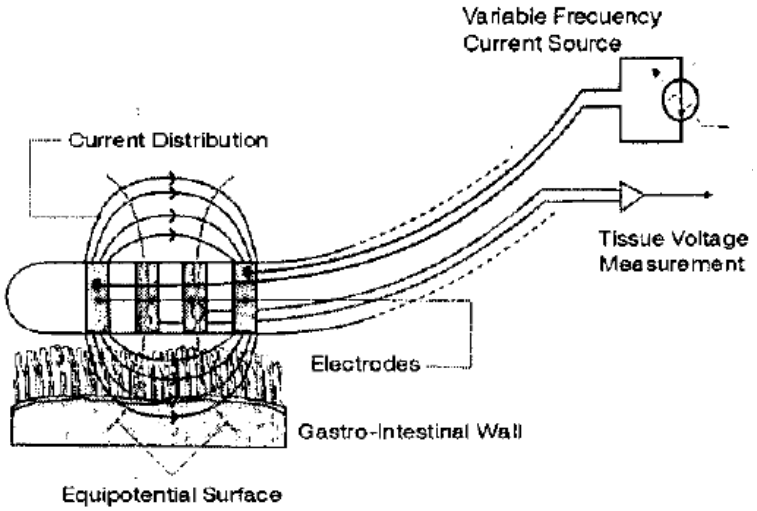

Figure 23. Four electrodes impedance detection of ischemia on small intestine tissue

There are commercial pH glass electrodes sensors for measuring stomach pH, being directly in contact with stomach tissue. Hydrogen ions (H^+) flow from the tissue through the glass membrane and create a potential difference. However, these kinds of sensors are breakable, hard to miniaturize and to apply for multisensing, (Mclaughlan *et al.,* 1987). Combined with impedance sensors, independent conventional potassium and pH ISE sensors with commercial RE were used in the detection of ischemia on kidney. The different sensors used for this application neither integrated nor implanted into the organ (Ivorra *et al.,* 2003) (Figure 24).

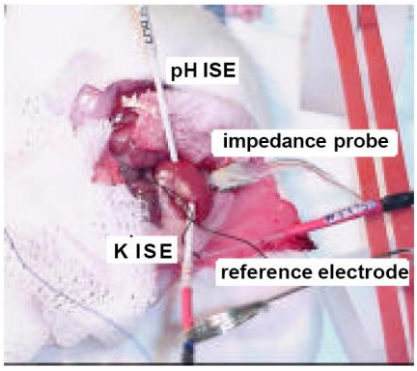

Figure 24. Developed impedance sensors and commercial pH, potassium sensors and RE electrode for sensing ischemia on kidney tissue (Gomez et al. 2001)

There are nearly no examples of whole integration of the ISE or impedance WE with the RE in the same device. One example is the system developed by Cosofret et al., where a thick film H^+ and K^+ selective sensor arrays combined with solid state RE based on solvent polymeric neutral carrier membranes for ischemia detection was developed. This platform was performed for detection near to physiological pH (7,4), but not for low pH, close to the needs of stomach detection (Cosofret et al., 1995). This system was improved (Marzouk et al., 2002) adding lactate sensors to the existing pH and potassium selective sensors, since exist an interdependency of potassium and lactate concentration during ischemia.

1.5. Objectives of this thesis

1.5.1. General objectives

This thesis was performed into the framework of the European Union project ARAKNES (Array of Robots Augmenting the KiNematics of Endoluminal Surgery). The idea of this project is to transfer the technologies of bi-manual laparoscopic surgery to the endoluminal surgical by integration of advanced micro-nano-bio technologies and electronics.

With the advances in technology, the surgical methods were altered in the last decades. By the introduction of laparoscopic techniques, the traditional methods for surgery were completely modified, focusing in scarless and/or minimal invasive methods. Laparoscopy uses the natural orifices in order to reduce the necessity of opening the body and reduce the surgery risk and the post operatory, for this reason was called natural orifice translumenal endoscopic surgery (NOTES). Laparoscopy instruments

use tools such as camera, light, energized dissection devices and staplers, actuated by the surgery with bi-manual tools.

In ARAKNES project all these technologies were integrated to a robotic system, controlled by the surgery by means of remote joysticks an 3D vision on a console, where also integrates the monitoring of the sensors. The laparoscopic robot was developed for morbid obesity surgery introduced through the esophagus to the stomach in a scarless way (Figure 25).

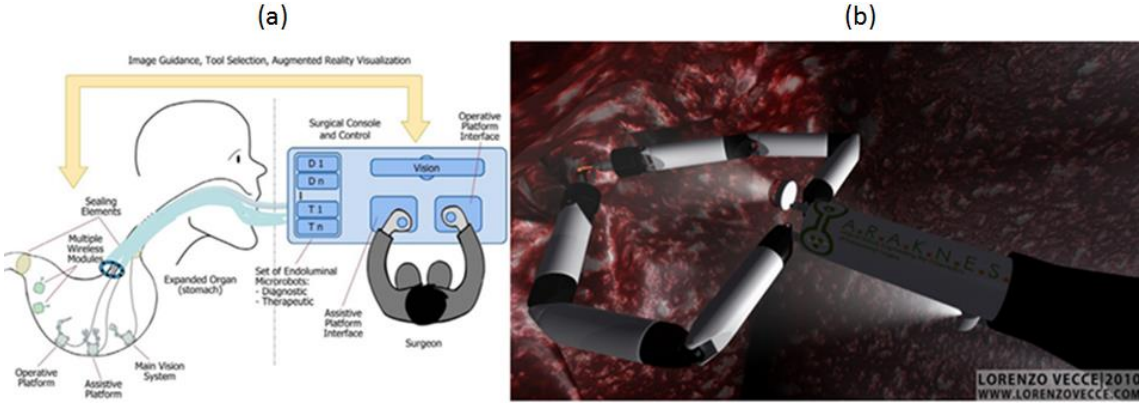

Figure 25. Scheme of the devices inserted through the gastroendoscope and the control console developed in the ARAKNES project (a). Simulation of the ARAKNES robot working inside the stomach (b)

1.5.2. Specific objectives

In the present work, an electrochemical multi-sensors array platform for real-time monitoring of ischemia for laparoscopic applications was designed and developed. For this goal, sensors based on ion-selective microelectrodes for pH and potassium detection and a bioimpedance based sensors have been integrated with a RE in a functional array. ISE technology has been chosen because of its unique characteristic enabling a direct measurement of extracellular ionic activities, which give direct information about the patient state with a low cost device. Meanwhile, impedance technique was used to sense extra- and intracellular ionic activities to support the ISE sensors. These sensors are particularly interesting for direct and local ionic measurements without the need of markers or reagents, and permit the real time monitoring of some diseases such as cancer and ischemia.

This thesis presents a bioimpedance sensor and potentiometric all-solid-state ISE approaches for pH and potassium detection integrated in an array miniaturized, mass producible at low cost for monitoring ischemia at low pHs (0.7–2.5) on stomach and small intestine tissue. This sensor was designed for being inserted into the stomach for endoluminal monitoring, which was integrated on miniature manipulators endoscope modules, in order to sense the evolution of the patient during scarless noninvasive stomach surgery (figure 26).

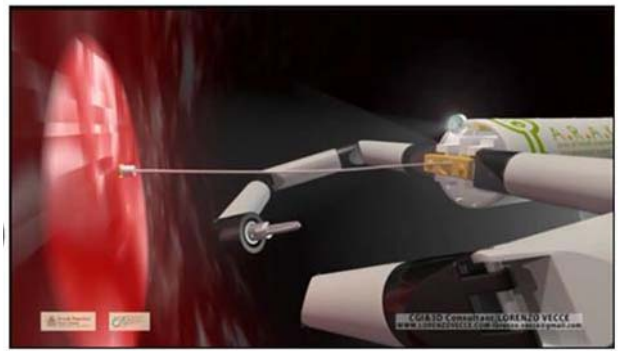

Figure 26. Simulation of the ARAKNES robot and the electrochemical array inserted through the gastroendoscope, sensing on the stomach tissue

References

A. Errachid, N. Zine, J. Samitier, J. Bausells Electroanalysis., 16 (2004), 1843

A.G. Thrift, H. M. Dewey, R.A Macdonell, J. J. McNeil, G. A. Donnan Stroke., 32 (2001), 1732

A. Hoffer, C. K. Meador, D.C. Simpson, J Appl Physiol., 27 (1969), 531

A. Ivorra Bioimpedance Monitoring for physicians: an overview (2002)

A. Ivorra, R. Gómez, N. Noguera, R. Villa, A. Sola, L. Palacios, G. Hotter, J. Aguiló Biosensors and Bioelectronics., 19 (2003), 391

A. Keller, P. Leidinger, A. Bauer, A. El Sharawy, J. Haas, C. Backes, A. Wendschlag, N. Giese, C. Tjaden, K. Ott, J. Werner, T. Hackert, K. Ruprecht, H. Huwer, J. Huebers, G. Jacobs, P. Rosenstiel, H. Dommisch, A. Schaefer, J. Müller-Quernheim, B. Wullich, B. Keck, N. Graf, J. Reichrath, B. Vogel, A. Nebel, S. Jager, P. Staehler, I. Amarantos, V. Boisguerin, C. Staehler, M. Beier, M. Scheffler, M. Büchler, J. Wischhusen, S. Haeusler, J. Dietl, S. Hofmann, H. Lenhof, S. Schreiber, H. Katus, W. Rottbauer, B. Meder, J. Hoheisel, A. Franke, E. Meese Nature Methods, 8 (2011), 841

A. Keshtkar, Z. Salehnia, A. Keshtkar, B. Shokouhi., Patholog Res Int., 2012 (2012), 1

A. Keshtkar, Z. Salehnia, M. H. Somi, and A. T. Eftekharsadat, Physica Medica, 28 (2012) 19–24

A. N. Assar, C. K. Zarins British Journal of Hospital Medicine., 69 (2008), 12

A.W.J. Cranny, J.K. Atkinson Measurement Science and Technology, 9 (1998), 1557

A.W. Hassel, K. Fushimi, M. Seo Electrochemistry Communications, 1 (1999), 180

C. M. Peterson, J. S. Anderson, A. K. Hara, J. W. Carenza, C. O. Menias, Radio Graphics., 29 (2009), 1281

C. P. Shelor, P. K. Dasgupta Analytica Chimica Acta., 702 (2011), 16

C. R. Keese, J. Wegener, S.R. Walker, I. Giaver, Proc Natl Acad Sci., 101 (2004) 1554

D. A. Benaron, I. H. Parachikov, S. Friedland, R. Soetikno, J. Brock-Utne, P. J. A. van der Starre, C. Nezhat, M. K. Terris, P. G. Maxim, J. J. L. Carson, M. K. Razavi, H. B. Gladstone, E. F. Fincher, C. P. Hsu, F. L. Clark, W. Cheong, J. L. Duckworth, D. K. Stevenson Anesthesiology., 100 (2004) 1469

D. A. MacInnes, and M. J. Dole Am. Chem. Sot., 62 (1930), 29

D. Ammann, P. Anker, E. Metzger, U. Oesch, W. Simon, 1985. Ion Measurements in Physiology and Medicine, in: Kessler, M., Harrison, D.K., Höper, J. (Eds.), Springer-Verlag., Berlin, 102.

D. Déjardin , F. Sabench Pereferrer, M. Hernàndez Gonzàlez, S. Blanco, A. Cabrera Vilanova Surgery., 153 (2013), 431

D. Grieshaber, R. MacKenzie, J. Voros, E. Reimhult Sensors, 8 (2008), 1400

D.J. Harrison, L.L. Cunningham, X. Li, A. Teclemariam, D. Permann Journal of the Electrochemical Society., 135 (1988), 2473

D.R. Theavenot, K. Toth, R.A Durst, G.S. Wilson, Pure Appl. Chem., 71 (1999), 2333

D. R. Wagner, K.F. Jeter, T. Tintle, M. S. Martin, J.M. Long Adv. Wound Care., 9 (1996), 30.

D. W. Spence, B. Pomeranz, Physiol Meas., 17 (1996), 57

E. Aghajani, H. J. Jacobsen, B. J. Nergaard, J. L. Hedenbro, B. G. Leifson, H. Gislason J Gastrointest Surg., 16 (2012), 641

E. C.V Butler, R. M Gershey Analytica Chimica Acta., 164 (1984), 153

F. Haber, Z. Klemensiewicz Physik. Chem., 67 (1909), 385

G. A. Donnan, M. Fisher, M. Macleod, S. M Davis Stroke Lancet., 371 (2008), 12

G. Blackburn, J. Janata Journal of the Eletrochemical Society., 129 (1982), 2580

G. Harsányi, “Sensors in biomedical applications. Fundamentals, technology and applications.” CRC Press, USA (2000)

G. J. Alegret S, M. R, De Román, M., Leija, P.R. Hernández , M Del Valle Anal Bioanal Chem., 377 (2003), 248

G. J. Moody, B. B. Saad, J. D. R. Thomas, Analyst., 114 (1989)

G. Kicsk, M. S. Levine, S. E. Raper, N. N. Williams AJR., 189 (2007); 1469

G. Mclaughlan, J. M. Rawlings, M. L. Lucas, R. F. Mccloy, G. P. Crean, K. Mccoll Gut., 28 (1987), 935

G. S. Grimnes, O. G. Martinsen, ‘Bioimpedance & Bioelectricity Basics’, Academic Press, (2000).

H. C. Lukaski, P.E. Johnson, W.W. Bolonchuk, G.I. Lykken Am J Clin Nutr., 41(1985), 810

H.C. Lukaski, W.W. Bolonchuk, Aviat Space Environ Med., 59 (1988), 1163

H.C. Lukaski, M.M. Moore J. Diabetes Sci Technol., 6 (2012) 209

H C Lukaski European Journal of Clinical Nutrition., (2013), 67

H.J. Lee, U.S. Hong, D.K. Lee, J.H. Shin, H. Nam, G.S. Cha Analytical Chemistry., 70 (1998), 3377

H. Kim, J. W. Hummel, K. A. Sudduth, P. P. Motavalli Soil Sci. Soc. Am. J., 71, (2007), 1867

H. Suzuki, H. Shiroishi, S. Sasaki, I. Karube Analytical Chemistry, 71 (1999), 5069

H. Jafarzadeh, P. A. Rosenberg JOE., 35 (2009), 3

I. Vedernikov, L. G. Kuzmina, Y. A. Strelenko, J. A. K. Howard, S. P. Gromov Russian Chemical Bulletin., 59 (2010), 927

J. A. Russell, Intensive Care Med., 23 (1997), 3

J. A. Tice, L. Karliner, J. Walsh, A. J. Petersen, M. D. Feldman, The American Journal of Medicine., 121 (2008), 885

J. Bobacka, A. Ivaska, A. Lewenstam Chemical Reviews., 108 (2008), 2

J. M. Esson, M. E. Meyerhoff Electroanalysis., 9 (1997), 1325

J.R. Griffiths Br. J. Cancer., 64 (1991), 425

J.R. Mager, S.D. Sibley, T.R. Beckman, T. A. Kellogg, C.P. Earthman Clin Nutr., 27 (2008), 832

J. Ruzicka, J. Chem. Ed., 74 (1997), 2

J. Saurina, E. López-Aviles, A. Le Moal, S. Hernández-Cassou Analytica Chimica Acta., 464 (2002), 89

J. Songer, 2001. Thesis: Tissue Ischemia Monitoring Using Impedance Spectroscopy: Clinical Evaluation

J. Wang, Electroanalytical techniques in clinical chemistry and laboratory medicine. Wiley –VCH, New York, (1998)

J. Wang, The Journal of Nutrition., 106 (1976), 1687

K. Joung, H. J. Yoon, H. Nam, K. Paeng Microchemical Journal., 68 (2001), 115

K. R Segal, B. Lutin, E. Presta, J. Wang, T.B. Van Itallie, J Appl Physiol., 58 (1985), 1565

L. Pivarnik, P. Ellis, X. Wang, T. Reilly Journal of food science., 66 (2001), 945

M. Cremer, Z. Biol., 47 (1906), 562

M. Menken, T. L. Munsat, J. F. Toole Arch Neurol., 57 (2000), 418

M.P. Mattson Nature, 430 (2004), 631

N. Abramova, A. Bratov Sensors., 9 (2009), 7097

N. Beltrán, G. Sánchez-Miranda, M. Godínez, U. Díaz, E. Sacristán IEEE Engineering in Medicine and Biology 27th Annual Conference., (2005)

P. Åberg, P. Geladi, I. Nicander, J. Hansson, U. Holmgren, S. Ollmar Skin Research and Technology., 11 (2005), 281

P. Bergveld, IEEE Trans. Biomed. Eng., 17 (1970), 70-71

P. C. Hauser, D.W.L. Chiang, G. A. Wright Analytica Chimica Acta., 302 (1995), 241

P. E. Jackson Encyclopedia of Analytical Chemistry R.A. Meyers (Ed.) (2000), 2779

P. L. Cox-Reijven, B van Kreel, P.B. Soeters, J. Parenter Enteral Nutr., 26 (2002), 120

P. Mirtaheri, (2004). Thesis: A novel biomedical sensor for early detection of organ ischemia

P. Rai, S. Jung, T. Ji, V. K. Varadan Proc. of SPIE ., (2008), 6931

R. F. Kushner, D.A. Schoelller, Am J Clin Nutr., 44 (1986), 417

R. Gómez, N. Noguera, A. Ivorra, R. Villa, J. Aguiló, J. Millán, J. López, L. Palacios, A. Sola, G. Hotter. Semiconductor Conference, Proceedings, (2001), 261

R. Martínez, N. A Sanz, and J. M. Albero Rev Esp Cardiol, 56 (2003), 850

R. S. Hutchins, L. G. Bachas Analytical chemistry., 67(1995), 1654

P. Vanysek The Electrochemical Society Interface., (2004) 19

P. Vadgma, M.A. Desai, I. Christie, Z. Koochaki, Pure Appl. Chem., 63 (1991), 1147

R. W. Cattrall and H. Freiser, Analytical Chemistry, 43 (1971), 1905

S. A. Glazier, M. A. Arnold Analytical chemistry., 60 (1988), 2540

S. Alegret, E. Martínez-Fàbregas Biosensors., 4 (1989), 287

S. A. Marzouk, R.P. Buck, L.A. Dunlap, T.A. Johnson, W.E. Cascio Anal Biochem., 308 (2002), 52

S. A. Seidel, L. A. Bradshaw, J. K. Ladipo, J. P. Wikswo, W. O. Richards, Journal of vascular surgery., 30 (1999), 309

S. Friedland, R. Soetikno, D. Benaron, Gastrointest Endoscopy Clin., 14 (2004), 539

S. Herber, J. Bomer, W. Olthuis, P. Bergveld, and A. van den Berg Biomedical Microdevices., 7 (2005), 197,

S. Li, A. Simonian, B. A. Chin The Electrochemical Society Interface., (2010), 41

S. M. Hameed, S. M. Cohn, Chest., 123 (2003) 475

S. Othman, E. Sacristan, C. A. Gonzalez, J. Pinz, J. Aguado, P. Flores, O. Infante Proceedings of the 25' Annual lntemational Conference of the IEEE EMBS (2003)

T. Prodromakis, Y. Liu, T.G. Constandinou, P. Georgiou, C. Toumazou IEEE Electron Device Letters, 31 (2010), 1053

U. Anastasova-Ivanova, A. Mattinen, J. Radu, A Bobacka, A. Lewenstam, J. Migdalski, M. Danielewski Sensors and Actuators B., 146 (2010), 199

U. Oesch, Z. Brzbzka, X. Aiping, B. Rusterholz, G. Suter, P.H. Viet, D.H. Welti, D. Ammann, E. Pretsch, W. Simon Analytical Chemistry, 58 (1986), 2285

U. Oesch, D. Ammann, W. Simon, Clin. Chem., 32 (1986), 1448-1459

V. Cosofret, M. Erdosy, T.A. Johnson, R.P. Buck Analytical Chemistry, 67 (1995),1647

V. Quentin, N. Dib, F. Thouveny, P L'Hoste, A. Croue, J. Boyer J. Endoscopy., 38 (2006), 529

W.A. Oldenburg, L. L. Lau, T.J. Rodenberg, H.J. Edmonds, C. D. Burger Arch Intern Med 164., 10 (2004), 1054

W.C. Stadie, J. Biol. Chem., 83 (1929), 477

W.L. Elder, W.H. Wright, Proc. Natl. Acad. Sci., 14 (1928), 936

W. Nernst, Ber. Dtsch. Chem. Ges., 30 (1897), 1547

Y. Lin, Z. Sun Journal of Endocrinology, 204 (2010), 1

Y. Liu, P. Georgiou, T. Prodromakis, T. G. Constandinou, C. Toumazou, IEEE Transactions on Electron Devices., 58 (2011), 4414

Y Zou, Z Guo Medical Engineering & Physics., 25 (2003), 79

Z. D. C. Goh, P. Georgiou, T. G. Constandinou, T. Prodromakis, C. Toumazou IEEE International Symposium on Circuits and Systems (ISCAS) (2011), 1997

Z. Stefanac, W. Simon, J. Microchem., 12 (1967), 125

CHAPTER 2

Development of Ion Selective Sensors

2.1. Introduction

The fields of chemical sensors based on microelectronic devices have increased its important role in the last decade (Grieshaber et al., 2008). It has been largely focused on all-solid-state electrochemical ISE sensors, in which all the ISE compounds are integrated into a polymeric matrix and attached in direct contact with the metal electrode. This interest arises from certain advantages of all-solid-state ISEs such as the low cost, the miniaturability and the possibility of multi-sensing and mass fabrication (Kwon et al., 2005). All-solid-state ISE with its advantageous properties can be used to sense gases, electrolytes and metabolites in vivo and in vitro for different kinds of applications. Medical diagnosis is one of the field that exploits the resources of the ISE, since the changes in these parameters are directly related with disease occurrence such as cancer (Keller et al., 2011), diabetes (Lin and Sun, 2010), neurological disorders (Mattson, 2004), and ischemia (Ammann et al., 1985), among others.

The most common plasticizer used in all-solid-state ISE sensors is PVC. However, this membrane has poor adhesion to the electrode surface, which inhibits its applications in implantable sensors (Piao et al., 2003). Therefore, scientific works focused on solving the adhesion problem with different approaches such as UV light photocuring techniques (Abramova and Bratov, 2009), fabrication of suspended mesh for the

attachment of the membrane mechanically (Blackburn and Janata, 1982), chemical modification of PVC by modifying its structure with carboxylic acid groups (PVC–COOH) (Cosofret et al., 1995) and anchoring chemically PVC membranes containing OH^- groups to an oxide surface (Harrison et al., 1988). However, the hard analytical conditions and low pH of the stomach complicate the adhesion of PVC to the electrode surface.

Ionophore protonation is another limiting factor for the usage of ISE electrodes at low pH. Sensors based on ISE membranes have selective ionophores for trapping ions, which create a concentration difference between ions within the ISE membrane and solution. At low pH, ionophores start to get affected by anion interference due to the high protonation. This issue was partially solved by using neutral carrier based membranes for conventional ISE electrodes (Oesch et al., 1986), where the membrane glass base is in electrical contact through an inner electrolyte solution with the RE (Bobacka et al., 1995), but these conventional ISE electrodes are fragile and hard to miniaturize. Thus, anion interference is still inevitable for all-solid-state ISE sensors at low pH. Other sensors devoted to low pH detection were developed by Zine et al. (Zine et al., 2006) and Won-Sik Han et al. (Han et al., 2001). The first was based on PPy[3,3′-Co(1,2-C2B9H11)2], reaching a working range of 3.5–11 while the second was developed with tribenzylamine neutral carrier in a PVC membrane with a poly (aniline) solid contact electrode, obtaining a lower detectable pH of 2.48. However, a work that reports lower pH detection is the one reported by Anastasova-Ivanova et al. where 2–9 range of pH was observed in a miniaturized all-solid-state potentiometric sensor. However, this sensor cannot be used at pH below 2, since the signal starts to go down below this pH (Anastasova-Ivanova et al., 2010).

Anion interference is also a drawback in all-solid-state REs based on Ag/AgCl that are not in contact to an internal electrolyte, which could cause a voltage change due to the variations of anion concentration on the electrode surface (Simonis et al., 2004). The anion interference problem was solved for commercial glass REs by keeping them in saturated KCl solutions to minimize liquid-junction potential. However, solution based systems have a lot of drawbacks as introduced with the conventional glass based ISEs. Therefore, different strategies were followed to fabricate miniaturized REs as explained in the first chapter. The problems of these strategies are their insufficient stability when the electrolyte and the Ag/AgCl layer are placed in contact and their potential short life at pH below 2 (Blaz et al., 2005, Kisiel et al., 2005, Piao et al., 2003 and Rius-Ruiz et al., 2011). Due to these reasons, no integrated RE and all-solid-state ISE for in situ detection inside the stomach has still been reported.

This chapter describes the fabrication and characterization of needle shaped, miniaturized all-solid-state potassium and pH sensors based on ISE membranes, integrated in an array with all-solid-state RE, for detecting ischemia at low pH (0.7–2.5) on stomach tissue. For achieving this, the adhesions of ISE membrane on different solid surfaces were studied and improved to choose the suitable interface for a stable

and durable ISE sensor under strong acidic conditions. In this platform, the problem of anion interference on ISE sensors has been studied and solved by using an all-solid-state RE, which is affected by anions, in the same tendency as that of the ISE, canceling the anion interference in the differential potentiometric measurement. Also, the sub-nernstian behavior of the all-solid-state pH sensor was fixed by increasing the concentration of lipophilic anions in the ISE membrane.

2.2. Materials and methods

2.2.1. Material

Silversulfate (Ag_2SO_4), silver chloride (AgCl), sodium thiosulfate, potassium metabisulfite, uracil, 1,3-diaminopropane, polyethyleneimine-1800 (PEI) potassium tetrachloroplatinate(II) (K_2PtCl_4), (Bis[(benzo-15-crown-4)-4'-ylmethyl]pimelate), valinomycin, hydrogen ionophore IV (Octadecyl isonicotinate), PVC high molecular weight, 2-nitrophenyl octyl ether, potassium tetrakis (4-chlorophenyl) borate (KTClPB), bis(1-butylpentyl) adipate (BBPA) and perfluorinated ion-exchange resin (Nafion) were obtained from Sigma. Tetrahydrofurane (THF), tris(hydroxymethyl) aminomethane, KCl, NaCl, HCl LiOH, NaOH and KOH were received from Panreac. RbOH and CsOH were supplied by ABCR. Ag/AgCl, gold and carbon inks were purchased by Dupont. MCS 5 and 12 series electrode arrays were bought from Omnetics Connector Corporation and resin hardener complex (EPOTEK 301-2) was provided by Epoxy Technology.

2.2.2. Characterization techniques

2.2.2.1. Cyclic voltammetry

Cyclic voltammetry (CV) is one of the most versatile electroanalytical techniques for the study of electroactive species. It has been used widely in the fields of electrochemistry, biochemistry, inorganic and organic chemistry. This technique has the capability for rapidly observing the redox behavior over a wide potential range. Thus, it is usually the first electrochemical method to characterize an electrode surface. CV measures the resulting current from a redox molecule during its potential cycles on the WE. The current is applied in the electrochemical cell through the CE and the WE response is measured *versus* the RE, which is Ag/AgCl the most widely used.

The cyclic voltammetries performed for the characterization of the fabricated electrodes in this project, were performed in potassium ferrocyanide solution with 5 mM of $K_3Fe(CN)_6$ and 0,5 M KCl.

.

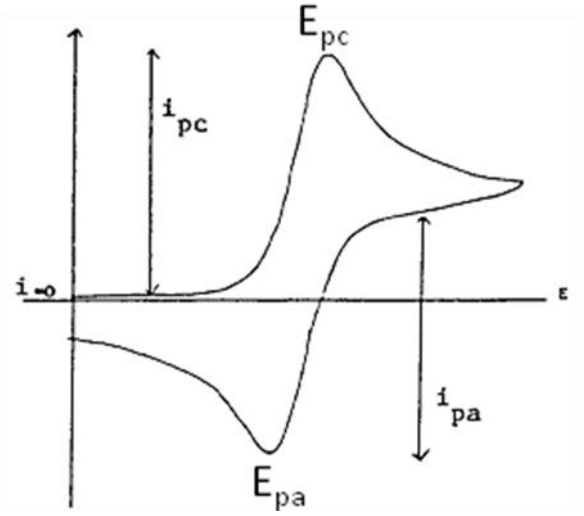

Figure 1. Example of CV

When the potential is sufficient to reduce $Fe^{III}(CN)_6^{3-}$, cathodic current (I_{pc}) increases rapidly, until a peak value (E_{pc}), where the concentration of $Fe^{III}(CN)_6^{3-}$ at the electrode surface starts to diminish.

$$Fe^{III}(CN)_6^{3-} + e^- \rightarrow Fe^{II}(CN)_6^{4-}$$

The same process is also valid for anodic current, where the contrary effect is observed in the positive current axes. In this case, when the potential is enough to oxidize $Fe^{II}(CN)_6^{4-}$, the anodic current (I_{pa}) increases rapidly, until a peak value (E_{ac}). These oxidation and reduction peaks are characteristic of the redox molecules *versus* a specific RE. The potential distance between $|E_{pc} - E_{pa}|$ shows the electron transfer quality of the redox reaction (Figure 1.). If the potential distance increase, it corresponds to poorer electron transfer (Kissinger et al., 1983). I_{pA} value is related with the concentration of the measured redox molecule and to the electrode area, thought Cottrell equation, which is very valuable for quantitative analytical analysis and to measure the real electrode area;

$$I_{pa} = nFAC_jD_j^{1/2}(\pi t)^{-1/2}$$

Where *n* is the number of electrons interchanged on the redox reaction, *F* is the Faraday constant, *A is* the WE area, *C* is the concentration and *D* is the diffusion coefficient of the redox species and t is the time.

2.2.2.2. Time-of-Flight Secondary Ion Mass Spectrometry (ToF-SIMS)

ToF-SIMS is a technique that uses pulsed ion beams of cesium (Cs) or gallium (Ga) to hit the surface to characterize and remove atoms or molecules from the top of the sample surface. Depending on the charge and the mass of the removed particles, they have different reach time to the detector. Thus, the surface composition of the material can be characterized using this surface sensitive technique (Figure 2).

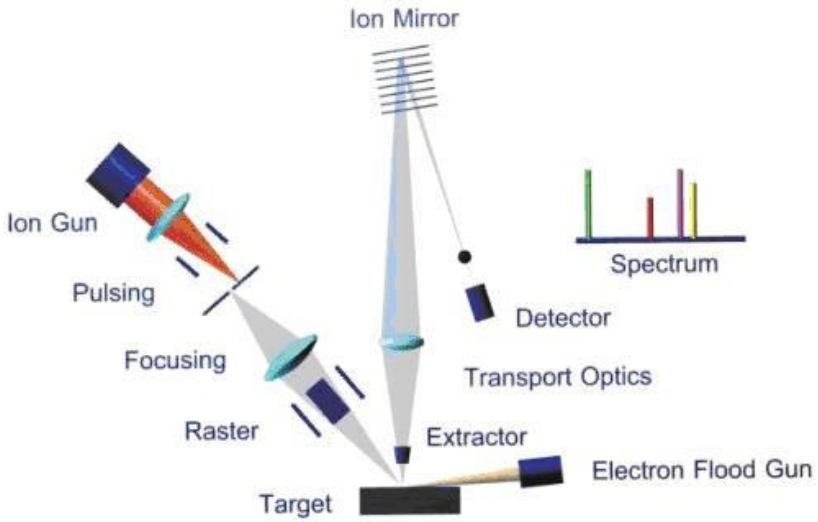

Figure 2. Scheme of the work principle of ToF-SIMS.

2.3. ISE microelectrodes fabrication process

2.3.1. Array design

The main application of the array developed in this project was endoscopic surgery, so its design was limited for this purpose. Hence, the next specifications of the array where followed;

- The diameter of the array should be appropriate for its insertion inside commercial endoscopes.

- The electrodes are designed in a needle shape instead of planar electrodes for a full contact with the tissue.

- The parts of the sensor that touches the stomach tissue should be biocompatible.

- The sensor array should be designed to be partially disposable and interchangeable for reducing the costs.

- Each electrode should be distanced enough to each other in order to avoid crosstalks between the electrodes.

- The sensor array should be designed in a way that contains pH and potassium all-solid-state ISE sensors, all-solid-state REs and 4 electrodes in a row for the bioimpedance sensor.

To achieve these properties, an array with 12 needles for ischemia detections by means of potentiometry and impedance was designed and fabricated. 3 WEs were dedicated to detect pH and 2 WEs to detect potassium. 2 REs were shared for pH detection and 1 RE was used for potassium detection. The last four electrodes were used for impedance measurements. The diameter of the needles was 600 µm with 3 mm length. The diameter of the entire array sensor was 7 mm. The diameter of the wires was 2 mm for its insertion into the 2.5 mm insertion tool of the commercial endoscope, which were sealed in order to ensure the water tightness. In order to reduce the cost of the sensor, it was designed in two parts. One part of the sensor, which touches the tissue, can be packaged and stored separately and discarded after used. The other part connects the sensor array with the electronics equipment. This part is not in contact with the sample, so that it can be reused (Figure 3).

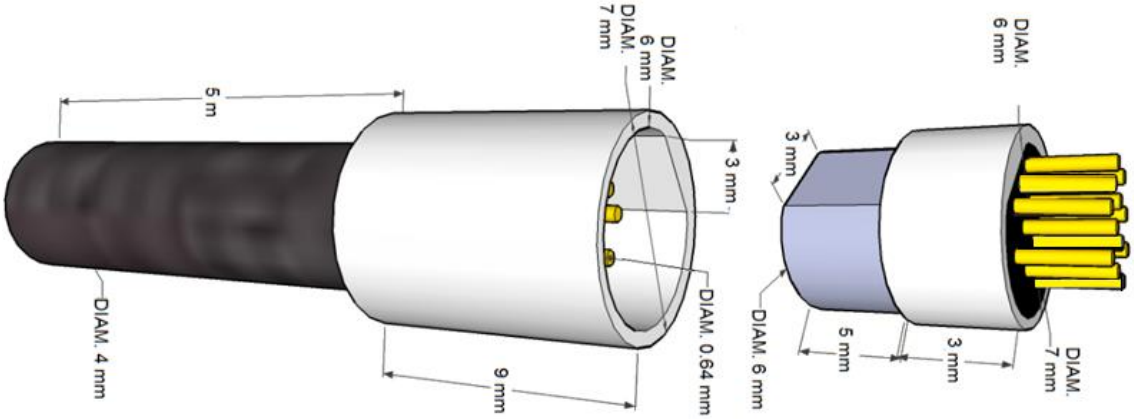

Figure 3. Scheme of the array design with the dimensions of the two sensor parts.

In order to make functional the electrodes needles, the pins sides need to be insulated, and the WE and RE electrodes surfaces properly functionalized.

2.3.2 Insulation

Insulation of all the metallic part of the electrode pin that is not going to be used for sensing is very relevant to reduce the background noise and to delimitate the sensing area to achieve reproducible results.

For this purpose, prior to the insulation, the array was washed with double deionized (MilliQ) water and dried under nitrogen atmosphere. The sides of the electrodes pins were insulated with different materials to choose the best candidate (Figure 4). Before the testing of any liquid polymer, a thermoretractable plastic was used. This plastic tube retracts fitting onto the pin when it is heated. However, it was not perfectly fitting to the sides of the pin and it was removed easily. Thus, liquid polymers were started to test for finding the optimum insulation. Poly(methyl methacrylate) (PMMA) is a transparent synthetic thermoplastic. This plastic has an appropriate density to facilitate the soaking of the array into the polymer and also it has good biocompatibility for in-vivo application and impact strength higher than glass. However, it has poor resistance to solvents and other chemicals like acids, so it makes difficult its application into the stomach. Polydimethylsiloxane (PDMS) is a polymer with appropriate density and also has a good biocompatibility. However, it is soluble in some organic solvents and was the polymer with lower mechanical strength comparing the other polymer tested. As can be appreciated in figure 4 due to its weak mechanical resistance after polishing, part of the polymer on the tips was lost. The commercial polymer araldit was also tested for pins insulator. Although this polymer shows a very good mechanical and chemical resistance, it is not biocompatible and its density is too high to soak and bound properly all the pin side. The commercial epoxy 2014 polymer shows a biocompatibility and higher mechanical strength with excellent chemical resistance. The density of the polymer is sufficiently low for a good soaking of the pins into the polymer and it shown a very good distribution of the polymer all the pin along. This polymer presented the better coating and delimitation of the electrode area with good balance between the mechanical, chemical resistance and biocompatibility. However, the polymer density did not allow insulating pins separately, in case the pins were very close to each other.

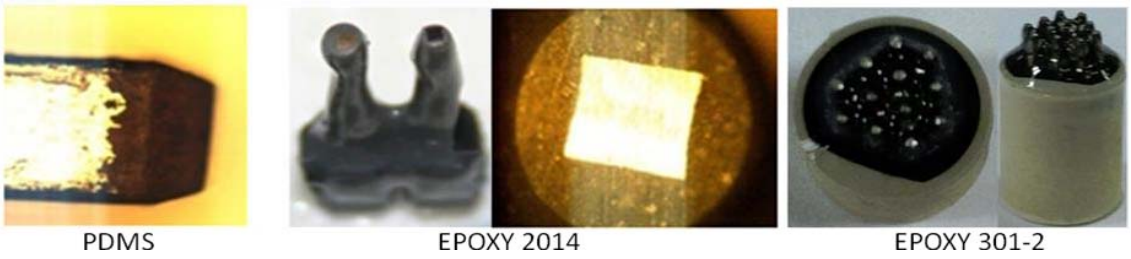

Figure 4. Insulated electrodes with different insulation materials

Thus, from broad range of insulators (Table 1) epoxy 301-2 resin was chosen as the best insulation materials.

Polymers	Density	Drying	Hardness	Resistance	Biocomp.	Remarks
Thermo retractile plas.	-------	80ºC 30 sec	Medium	High	High	Bad fit in
Araldit rapid	High	5h RT	High	High	Low	High density
PDMS	Low	90ºC 1h	Low	Medium	High	Too soft
PMMA	Medium	90ºC 1h	High	Low resist. to chemicals and solvents	High	Low resistance to acid
Epoxy 2014	Medium	60ºC 30 min	High	High	Medium	Good coating
Epoxy 301-2-8OZ	Low	80ºC 3h	High	High	High	Good coating

Table 1. Different properties of the insulation materials tested.

The side pins insulation reduces the background noise signal and brings high biocompatibility, mechanical strength and chemicals resistance to the electrodes. Electrodes were completely covered by soaking the pins inside the insulator and cured at 80 °C for 3 h. 600 µm of beryllium copper diameter electrode area was delimited after polishing the electrodes tips (Figure 5).

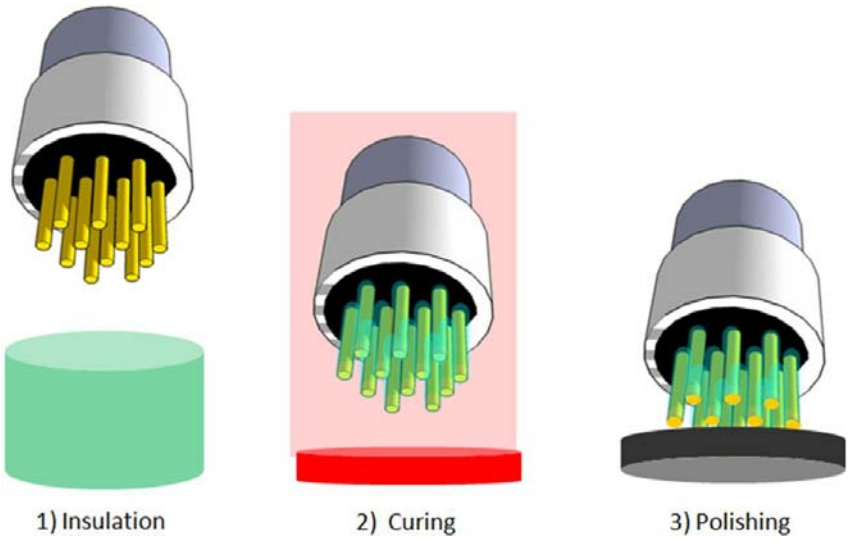

Figure 5. Insulation and polishing steps for the electrodes fabrication

2.3.3. Metallization

The polished electrode tips were fabricated with a copper-beryllium alloy, which is easy to oxidize even on air and is highly unstable under the acidic conditions of further applications. For this reason, the sensing area was modified with platinum and silver by electrodeposition technique to cover the electrodes with noble metals to improve its resistant to corrosion and oxidation (Figure 6). For the construction of the REs, silver metallization was chosen to achieve an Ag/AgCl electrode and platinum metallization was chosen for the WEs.

Electrodeposition was chosen as surface modification for its advantages in an array format, where each microelectrode is modified in a controlled way by applying current or voltage in a specific electrode and no spontaneous reaction on the rest of microelectrodes in the array should be observed. Different protocols for silver and platinum metallization were tested to optimize the best condition.

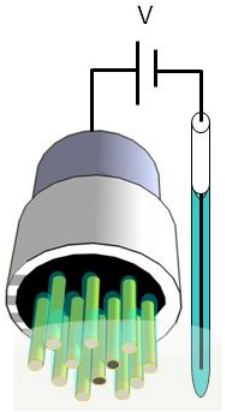

Figure 6. Scheme of silver and platinum electrodeposition versus and external Ag/AgCl RE electrode,

2.3.3.1. Metallization and characterization equipments

Electrometallization of silver and platinum was performed with a CH instruments electrochemical workstation. For this purpose, a current or voltage was applied in a specific electrode in order to attract the positive metal ions to this electrode. The characterization of the metalized surface was done with electrochemistry with the previous equipment. CV technique brings information about the electrode surface area and composition, so we can measure the coverage of the metallization and the reproducibility of this coverage.

Another technique used for surface characterization was ToF-SIMS. With this technique elementary analysis of the surface will give us information about the metal ions deposited on the electrode surface specifically by the electrodeposition and nonspecifically by the spontaneous deposition, as well as the percentage of copper alloy coverage.

Once the electrode surface is characterized, the electrodes were modified with ISE sensors to test the stability of the electrode surface with the ISE membrane and under low pH conditions. Potentiometry is an electrochemical method used for the ISE detection, where voltage difference is measured between the RE and WE. In the ISE sensors, WE is modified with a PVC membrane that contains a ionophore that bind specifically with the ion of interest. The attachment of charged ions on the membrane generates a potential difference respect to the RE. An ideal potentiometry measurement system should have very high input impedance, in order to create less disturbance of the circuit. In this thesis, a palmsense potentiostat was chosen for potentiometry experiments, because of their high impedance, multiplexer properties and portability. Multiplexer properties provide array applications, allowing up to 16 sensors detection together, but sequentially. The small size of this device was relevant for this project, since it allows easy transportation for in-vivo experiments.

2.3.3.2 Platinum electrometallization

Platinum and platinum alloy films electrodeposited from conventional aqueous electrolytes find wide range of applications. However, the surface composition is affecting tremendously the quality of the electrodeposition. In our experiments, firstly we used a solution of 0.01 g of chloroplatinic acid and 1 g of lead acetate diluted in 100 ml water (Feltham et al., 1971). The array was soaked into this mixture and connected as WE with an external platinum CE and Ag/AgCl RE. Current density of 15 mA/cm^2 was applied for 12 cycles of 10 s each followed by 10 s of ultrasound agitation. This protocol works properly for inert materials like gold. However, the stability of the

deposited platinum was very low for non-inert materials such as beryllium copper. Because of this reason, the platinum metallization solution was changed to another one based on potassium tetrachloroplatinate. The protocol followed was the next; 51 ml of 1,3-diaminopropane and 51ml of water were mixed and heated at 60^0C. 40 g of K_2PtCl_4 was added to the solution and the pH adjusted to 11.5 by adding KOH. Current density of 0.5 mA/cm^2 was applied for 200 s. The quality of electrodeposition was characterized by TOF-SIMS. According to TOF-SIMS measurements, good results were achieved following this protocol. A complete coverage of the copper surface and negligible contamination by spontaneous electrodeposition of the platinum on the neighboring pins was achieved (Figure 7).

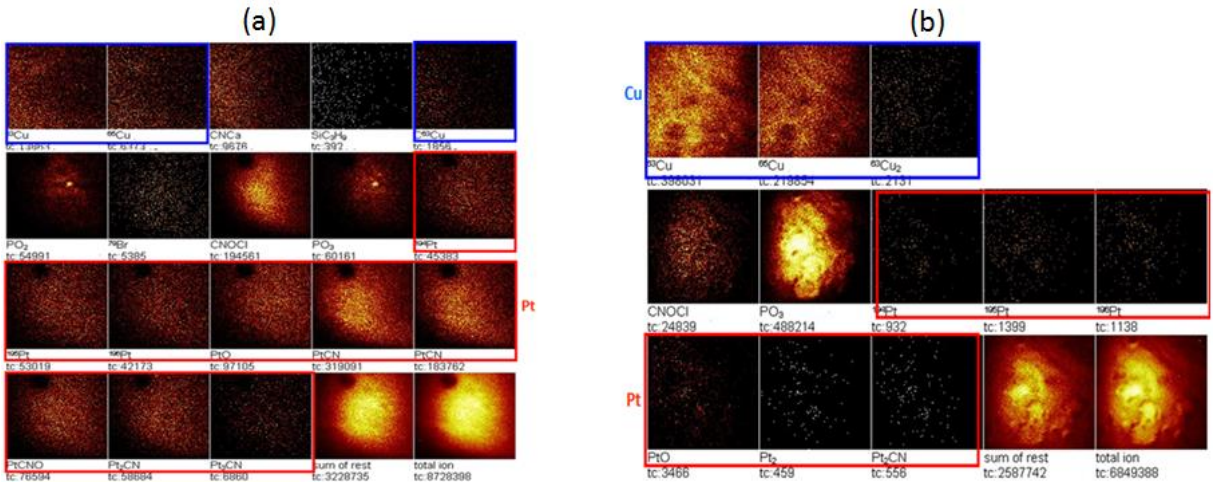

Figure 7. ToF-SIMS characterization of specific coverage of platinum on the copper pin (a) and negligible nonspecific adsorption of platinum on the neighboring pins (b)

As can be appreciable in figure 7a, the amount of copper ions in platinum metallized pins is very low comparing with the unmodified pin in figure 7b. While the amount of different platinum ions in this pin is higher comparing with the unmodified one, being the spontaneous deposition of platinum negligible.

2.3.3.3. Silver electrometallization

The electrodeposition of silver from cyanide solutions is a well-known process. In fact, the silver electrometallization process in commercial applications is nearly similar to the first patent, more than a century ago (Elkington et al., 1840). Although, this process based on cyanide has a low cost and high quality, delicate handling during the process of production and storage is needed because of the high toxicity of cyanide based solutions. Hence, alternative silver electrodeposition techniques were researched for decades. Thiosulfate based techniques are the most widely used silver electrodeposition

without cyanide (Leahy et al., 1978; Sriveeraraghavan et al., 1989; Foster et al., 2003; Foster et al., 2005; Su et al., 2005). Thus, one of the thiosulfate based protocols was followed by mixing; 0.5 gr of silver chloride, 5 gr of sodium thiosulfite and 0.3 gr of potassium metabisulfite in 10 ml of water. Current density of 0.2 mA/cm^2 was applied for 20 s, changing from positive to negative currents for five times. The interchanges of positive and negative currents were applied for avoiding the deposition of anion on the surface. However, low stability of silver on the surface was observed. Deposition tried to be optimized without negative repulsion of the positive ions, but then high depositions of other positive ions besides silver were observed (Figure 8).

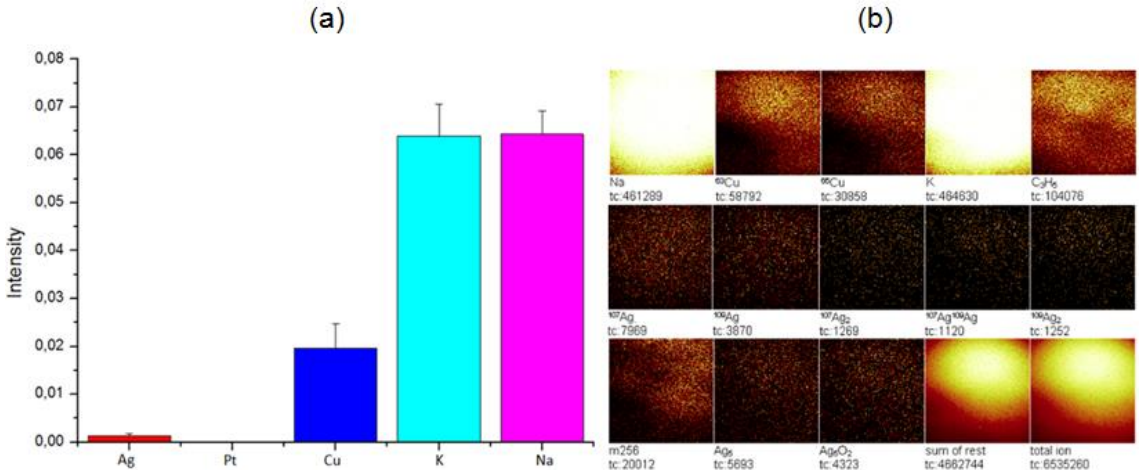

Figure 8. ToF-SIMS characterization of electrodeposition of silver by means of thiosulfate based solution.

Thus, comparing to cyanide solution, thiosulfate based silver deposition needs a separate striking previous process to make a thin layer of silver without contaminations.

With this purpose, uracil biomolecule was chosen as silver complexing agent, avoiding the contamination of other cation (Figure 9). Uracil has a heterocyclic structure that coordinates metal ions in basic solutions. Thus, it is not required a previous striking, since the displacement rate is slower and a silver deposition on copper surface was successfully achieved with uracil-silver plating bath.

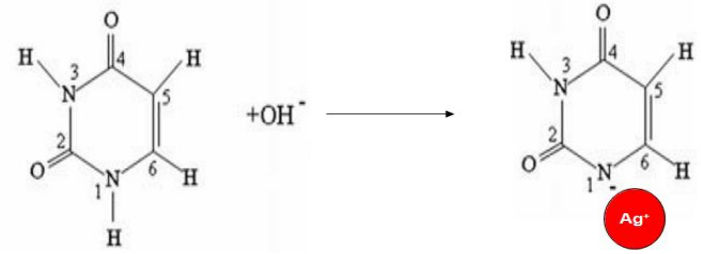

Figure 9. Uracil silver complexing agent at basic solutions

This protocol was chosen as silver electrodeposition method in our studies. The protocol followed is the next; a solution of 0.075 M Ag_2SO_4, 0.36 M uracil, 0,022 M PEI in water was prepared and pH was regulated to 13 by addition of KOH. The electrodes were soaked into the solution and connected as WE in the electrochemical cell and it was applied a voltage of -0.65 V for 150 s for silver deposition (Xie et al., 2009). During this reaction, uracil has complexing capability with silver, so that it increases silver solubility, improving its deposition on the electrode. However, there is still high deposition of potassium together with silver (Figure 10).

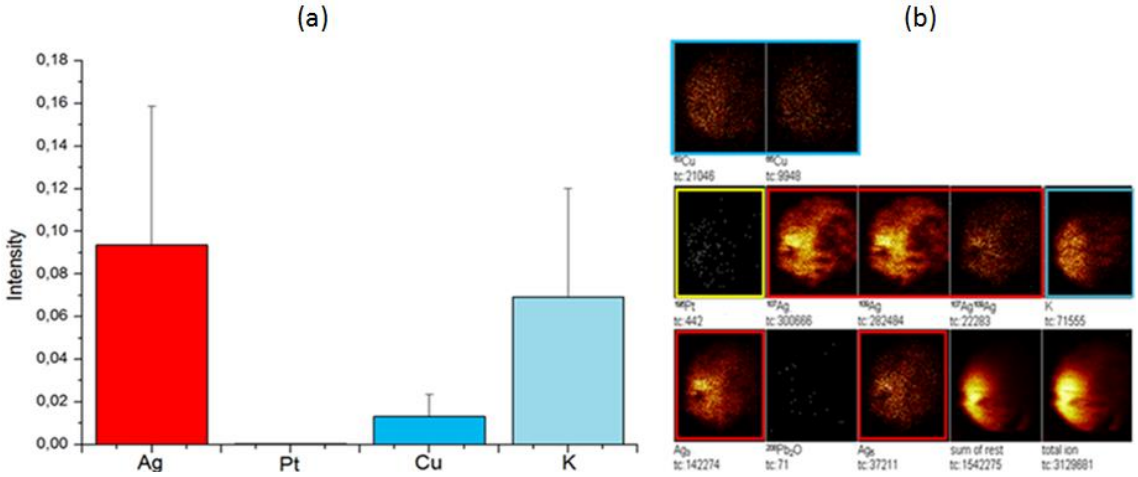

Figure 10. TOFsims results of silver electrodeposited electrode with uracil protocol

2.3.3.3.1 The effect of hydroxide counterions on silver electrodeposition based on uracil

The uracil-silver complex has the formula AgLOH, where L is uracil. According to this approximation, uracil-silver complex should not be affected by the base counterions. However, a deeper study of the complex structure showed us the contrary.

Under basic pH (pH=13), the nitrogen atom of the uracil loses the proton and is charged negatively. Depending on which amino group is charged, they are named as tautomer I or tautomer II. The positively charged silver ions are electrostatically attached to the charged amino groups, creating the uracil-silver complex (Figure 11).

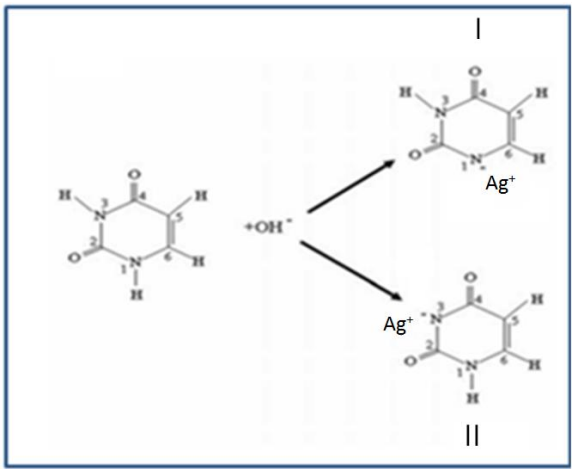

Figure 11. Formation of the tautomers on the silver-uracil complex under basic pH

Silversulfate, the salt used for the electrodeposition of silver in this protocol, is poorly soluble in water. However, the complex formed with uracil, helps increasing the solubility of silver in water. However, we observed that the solubility of silver is not just affected by uracil molecule, but also it is directly related with the counter ion of the base. Uracil solution is insoluble in water a neutral pH but starts to be soluble at basic pH and completely solubilized, independently of the base counterion. However, in the case of silver, its solubility is directly related with the counterion present in the solution. While the silver solutions containing Cs^+, Rb^+ or K^+ ions are perfectly solubilized, the same solutions but prepared with LiOH or NaOH do not allow silver solubilization (Figure 12). These experimental results suggest that silver-uracil complex cannot be explained just with $AgLOH^-$ formula and a deeper study about the reaction is needed.

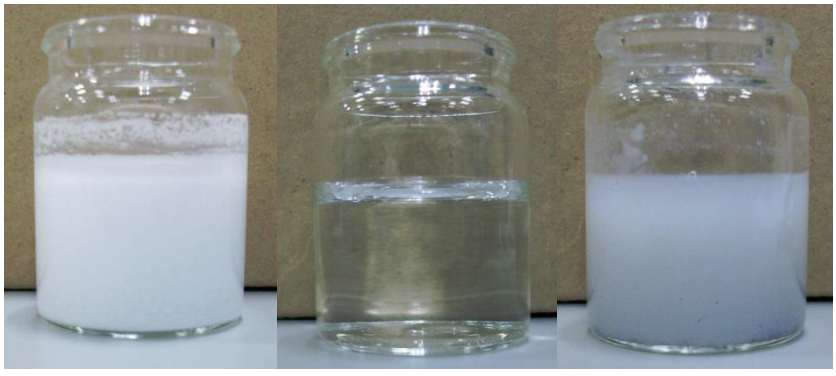

Uracil Uracil+LiOH/NaOH Uracil+LiOH/NaOH+Ag^+

Uracil Uracil+KOH/RbOH/CsOH Uracil+ KOH/RbOH/CsOH $+Ag^{+}$

Figure 12. Uracil-silver complex prepared with different bases

In the literature, there are some works devoted in the study of the uracil behavior with different bases. Electrospray ionization (ESI) in combination with mass spectrometry (MS) experiments gives the opportunity to study complex structure of biomolecules such as uracil, guanine, cytosine and thymine (Koch et al., 2002). With these techniques, it has been proven that uracil is mostly stable in trimeric structure when it is combined in solution with lithium ion, tetrameric structure when it is combined with sodium ion and pentameric structure in the case of potassium, rubidium and cesium ions (Qiu et al, 2009). Looking on the structures of this counter ions, seems that its molecular structure could be related with the complex formed with uracil, since the ions with smaller radius (Li<Na<K<Rb<Cs) creates smaller structures.

Our results support the notion that silver-uracil complex is just stable when it is combined with potassium, rubidium and cesium bases, which are the counter ions that supports the formation of a stable pentameric structure. We can hypothesized that silver ions in the uracil complex left less space, which makes unstable the formation of polimetric structures smaller than 5 molecules (figure 13). Thus, the trimeric cluster stabilized with lithium and the tetrameric structures formed with sodium are not able in a complex with silver ions attached to the uracil.

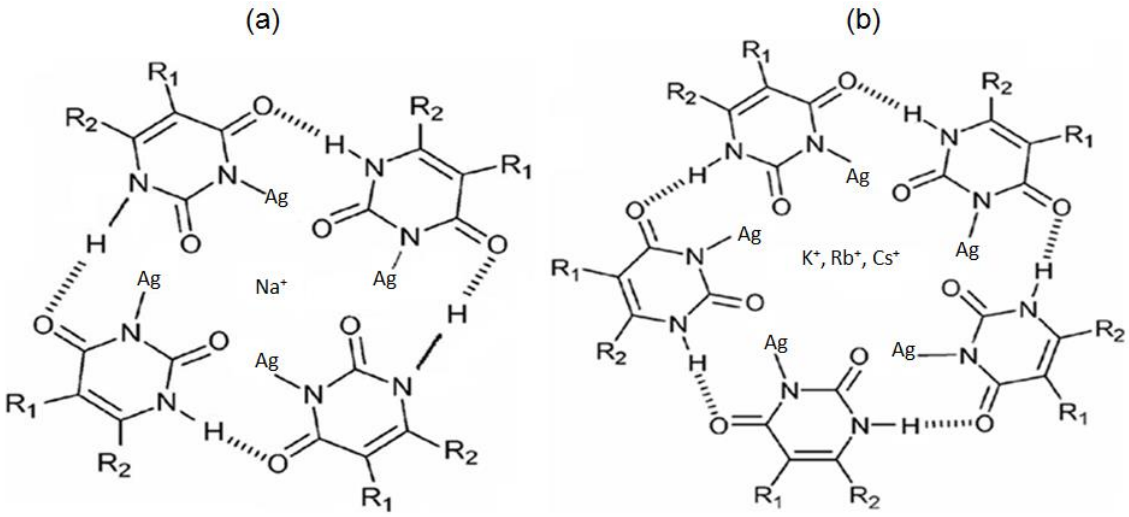

Figure 13. Tetrameric structure formed with uracil and sodium ions (a) and pentameric structure created with potassium, rubidium and cesium in the presence of the silver-uracil complex (b)

2.3.3.3.2 Silver metallization characterization

After the electrodeposition, the electrodes were characterized by CV, connecting silver electrodeposited electrodes as WE, and closing the electrochemical cell with commercial RE and CEs in ferrocyanide. Single peaks around -0.1 V and 0.3 V showed that silver covered entirely copper surface (Figure 14a). For the first cycle, just a single peak at -0,08 V (silver peak) was observed. But with increasing number of cycles, a second peak started to grow at -0,18V (copper peak) and silver peak started to disappear, being completely flat after 40 cycles. Silver deposited layer is not enough stable to bear the current applied and the ferrocyanide, which etched silver from the surface (Figure 14b). Although ferrocyanide also etches noble pure metals as gold, it is the most widely method for measuring the electrode area, but in the case of deposited metals and silver that is less inert than gold, this method is not working properly.

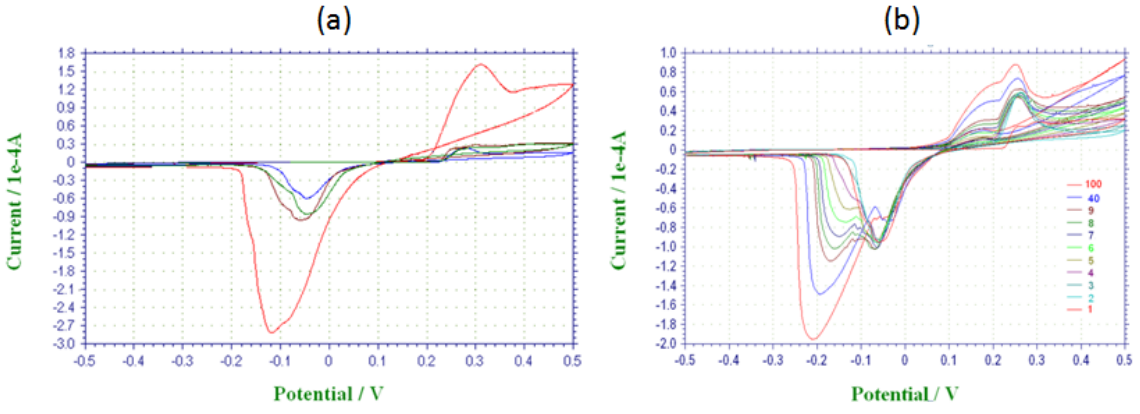

Figure 14. CV results of electrodeposited silver in ferrocyanide for few (a) and many cycles (b)

Therefore, an alternative strategy was applied. Also CV technique was used, but avoiding the effects of the current through the deposited silver, it was connected as RE, and commercial gold WE and platinum CE were used inside ferrocyanide. Thus, the currents are just affecting the WE and CE, and depending on the silver layer on the RE a different reference voltage was observed, and the reproducibility of the deposition can be evaluated, without effects on the deposition.

Initially, the electrodepositions were done inside glass beaker containing the array and the RE and CE commercial electrodes. However, the silver layers obtained were highly irreproducible, as shows the shifted voltages obtained in the characterization of different arrays (Figure 15).

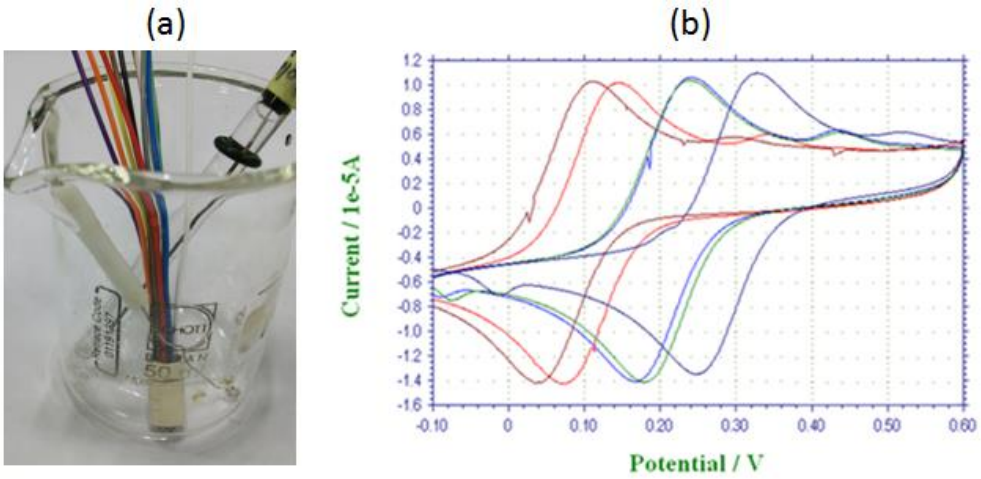

Figure 15. Silver electrodeposition inside a glass beaker (a) and CV characterization of the deposited layer (b)

During electrodepostion, the current coming from the CE to the WE is creating an electric field that drives the ions of interest to the WE surface. Therefore, for achieving a reproducible method; the CE and WE electrodes area, shape and distance needs to be fixed. For this purpose an electrochemical cell was designed, in which the position of the three electrodes was fixed as well as the cell volume. In one of the sides of the cell the platinum CE is inserted, on the other side the Ag/AgCl RE and the designed array for the project was placed on the upper part of the cell. The solution was pumped inside the chamber with the help of a syringe in the batch system or by means a pump in the fluidic system. Comparing with previous results, performing the electrodeposition inside the cell brings a highly reproducible silver deposition, as shows the stable voltage on the silver deposited in figure 16.

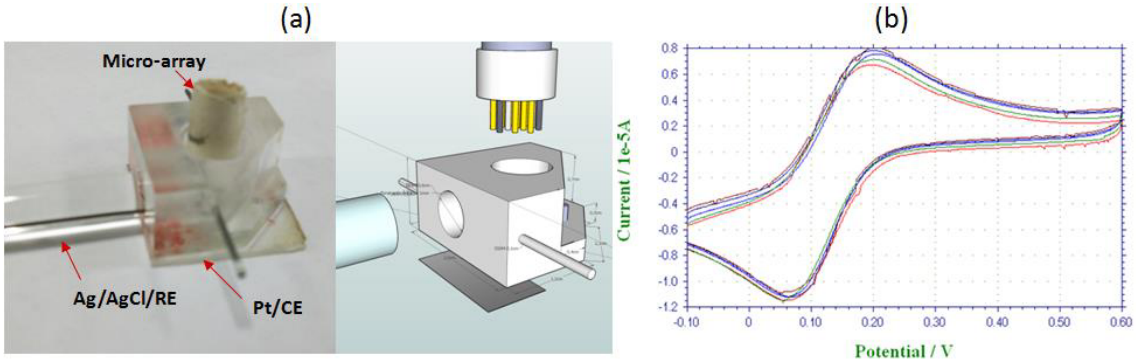

Figure 16. Cell designed for the reproducible Silver electrodeposition (a). CV characterization of the deposited layer in the cell (b)

The silver electrodeposition based on uracil was tested with different bases; KOH, NaOH, CsOH. After the deposition, the electrodes were rinsed for 2 minutes inside double deionized (MilliQ) water to remove physical attachment.

The electrodeposition surface coverage was tested with ToF-SIMs. The results show that beryllium copper pins were perfectly covered with silver, except in the case of NaOH. The reason may be found in the fact that the solubility of silver is lower with bases based on sodium and lithium and so its deposition. Besides silver deposition, it was observed also the nonspecific absorption of the base counter ions. The higher nonspecific absorption was obviously observed in the case of sodium, in which the silver was not solubilized and so, another positive ion; sodium, has free line for its adsorption on the electrodes. In the case of potassium and cesium, which both creates a pentameric structure with uracil-silver complex, the reason could be found in the higher reactivity of cesium and its bigger radius that could destabilize more the pentameric structure (Figure 17). Finally, the protocol choice for silver deposition was based on uracil and KOH.

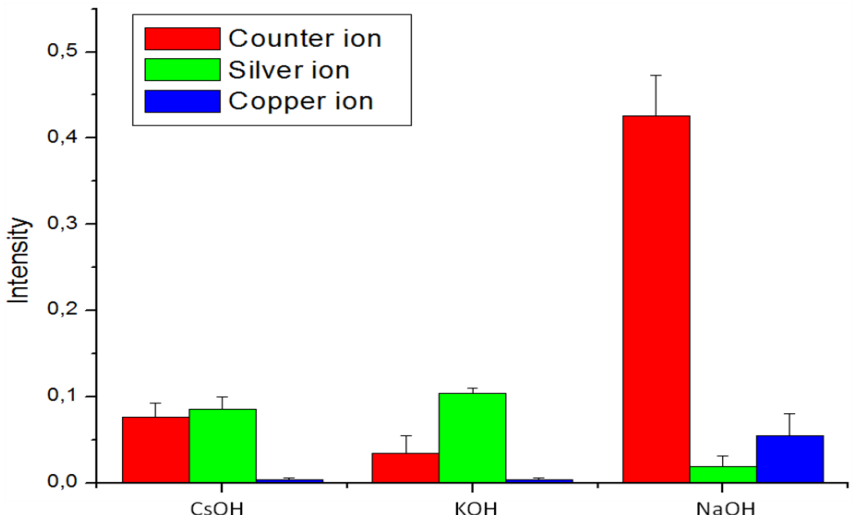

Figure 17. ToF-Sims results of silver deposition with different bases in uracil solution.

The optimized platinum and silver electrodeposition techniques were used on the array, where some of the pins were selectively electrodeposited with silver and others with platinum (Figure 18).

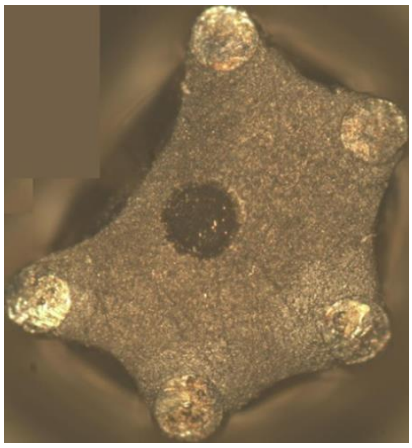

Figure 18. The site selective electrodeposited electrode with silver and platinum in the middle of the array

After the reproducible and selective electrodeposition of silver and platinum on the electrodes, ISE membrane was placed on top of the electrode to check their performance as all-solid-state pH sensor electrode. ISE membrane was prepared with a mixture of 1.0 wt% hydrogen ionophore IV, 1.33 wt% KTClPB, 68.0 wt% 2-nitrophenyl octyl ether, and 29.67 wt% PVC of high molecular weight. 300 mg in total of these chemicals was dissolved in 3 mL of freshly distilled THF (Oesch et al., 1986).

Silver and platinum electrodes serve well as support for all-solid state pH sensor at physiological pH, but the membrane lost its stability on the electrodes surface at low pH (Figure 19), since electrometalization did not bring a stable surface for low pH environment.

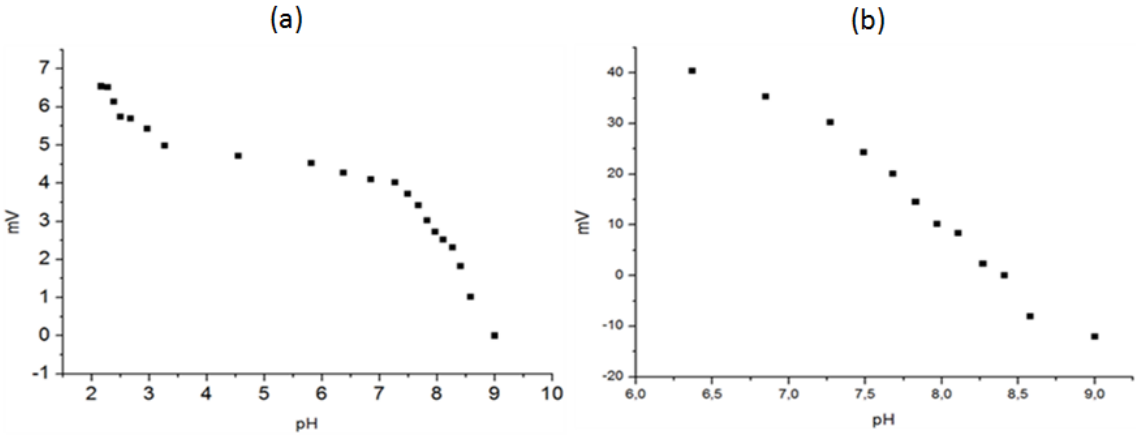

Figure 19. ISE pH measurement on electrodeposited platinum (a) and silver (b) electrodes

2.3.4. Conductive ink for electrode surface fabrication

Due to the instability of the silver and platinum metalized electrode surface tested under low pHs, the electrode surface modification strategy was changed. To achieve a conductive and stable surface under strong acidic conditions, the electrode surfaces were treated with a conductive paste used commonly in the production of screen printed electrodes.

With this method, same insulation and polishing steps were used as in the previous system. Afterwards, beryllium copper pins surface were covered with a controlled thickness of ink. It was first covered by carbon paste by soaking the tip of the electrodes in a homogeneous thin ink layer with 17 µm thickness created by spin coating under 4000 rpm for 1 minute and left to dry at 130 °C for 6 min. Once carbon surface was dried, it was covered by Ag/AgCl ink by soaking the tip of the electrodes in a thin ink layer of Ag/AgCl with 33 µm thickness created by spin coating under 1500 rpm for 4 minutes and left to dry at 130 °C for 6 min. The modified electrodes were characterized by connecting it as reference electrode, and commercial gold WE and platinum CE closing the electrochemical cell. CVs were performed in ferrocyanide to test the reproducibilty of the modified surface. CV results in figure 20 shows that AgCl ink coverage was reproducible for different electrodes, proved by the aligned oxidation and reduction peaks of the CVs.

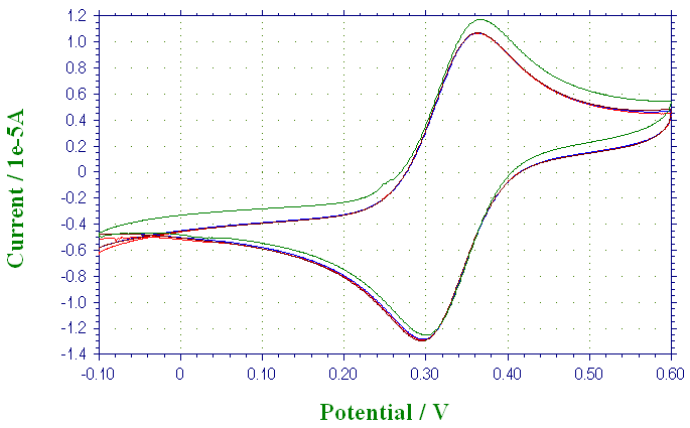

Figure 20. Reproducible CV for ink modified electrodes, tested in ferrocyanide

Besides the reproducibility of the electrode surface fabrication, the material used for the electrode modification should tolerate the strong acidic conditions of the measurement. An appropriate adhesion between the electrode surface and PVC based ISE membranes are of great importance for achieving highly stable sensors.

The adhesions of these kinds of membranes were tested on different solid supports (gold, Ag/AgCl and carbon ink) in order to choose the suitable surface for a stable attachment of ISE membranes. The same ISE membrane was attached on different

surfaces and potentiometry was used to measure the potential difference created by the specific attachment of proton ions on the sensor surface. Potentiometric curves show that gold (hydrophilic) and carbon (hydrophobic) surfaces with PVC coverage have a good response, but the adhesion between the electrode surface and the ISE membrane is totally lost at pH below 2 (Figure 21). Hydrophobicity of PVC membrane is highly dependent on pH (Pascoe et al., 2003). For this reason, the severe hydrophobicity change at low pH causes the detachment of the membrane from gold and carbon surfaces. However, adhesion failure is not observed for Ag/AgCl surface (Figure 21 C). This surface was fabricated with a conductive ink containing micro-particles bound with branched acrylic polymers. Its grafted copolymer has a linear backbone with hydrophilic carboxylic acid-pendant groups and side chains of hydrophobic monomers (Chan et al., 1996). Those hydrophilic and hydrophobic groups into the Ag/AgCl surface provide a strong adhesion, almost unaffected by the low pH.

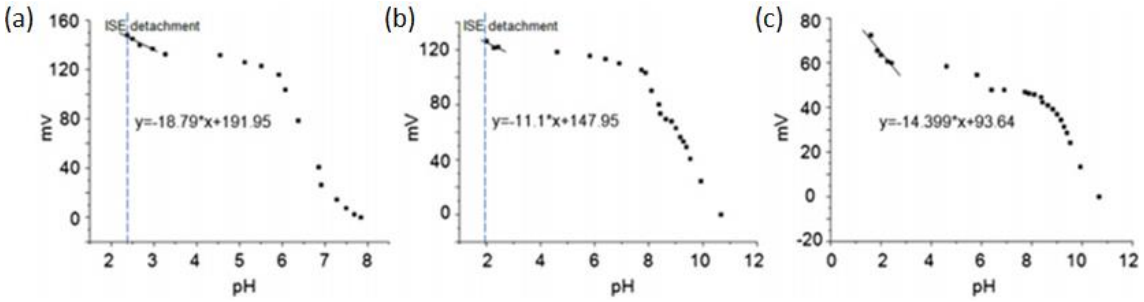

Figure 21. Potentiometry response curves of carbon (a), gold (b) and Ag/AgCl (c) layer with ISE membrane *vs.* external RE for different pH values.

2.4. pH ISE Detection

2.4.1. Study of all-solid-state RE and ISE polymeric membranes

The results mentioned above indicated that the high adhesion between Ag/AgCl and ISE sensor makes it a perfect candidate as ISE pH sensor substrate at low pH. In order to test the performance of this sensor, potentiometry measurements were performed at low pH (0.7–2.5). Figure 22 shows the response sensed at different concentrations of KTClPB and the signal observed on bare electrodes.

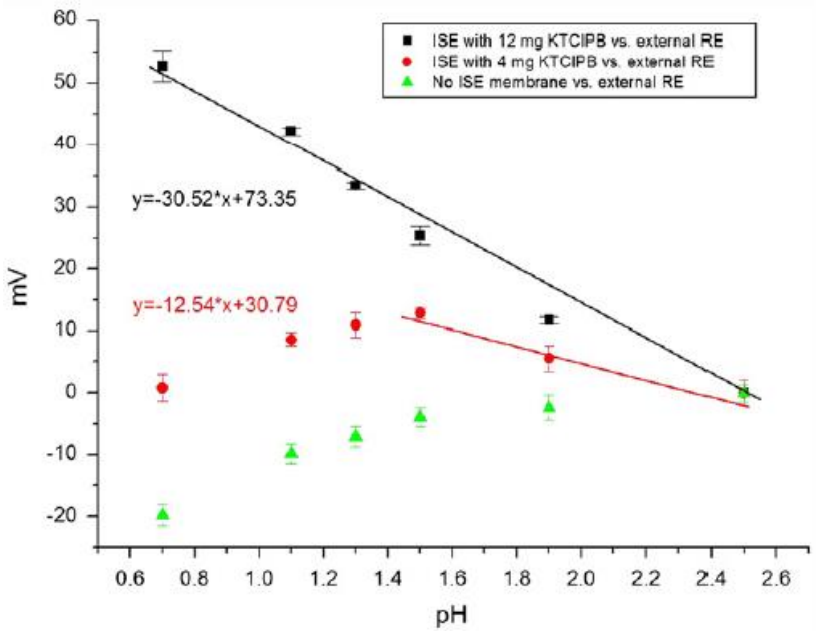

Figure 22. Potentiometry response curves for all-solid-state ISE under low pH for different KTCIPB concentrations and the absence of ISE membrane *vs*. external Ag/AgCl commercial RE (n=2).

The negligible potential recorded on this control shows the selectivity and functionality of the ionophore in the ISE membrane for pH sensing. However, at pH lower than 1,5, the high protonation starts to dominate and the anion interference is visible in the reduction of the potential measured. Two clear tendencies, in which protons and anions compete, are observed; until pH 1,5, protons are dominant and below this value, anions start to be sensed, as shows the decay on the voltage signal.

Two different strategies have been proposed for reducing the anion interference at low pH. First is based on the amount of KTCIPB used in the mixture of the ISE membrane. KTCIPB is a liphophilic anion that charges negatively this membrane, preventing the entrance of external anions (Cardwell et al., 1992). As can be appreciated in Figure 23, the increase of KTCIPB from 4 to 12 mg blocks the anion access to the ISE sensor, having a fully functional pH sensor also at pH below 1,5. Higher concentrations of KTCIPB were also tested. However, at concentration above 12 mg, the ISE membrane lost its mechanical stability, being degraded under these conditions.

The alternative strategy for canceling the anion interference is to take the advantage from the potentiometry measurements. In this technique, is measured the voltage difference generated between WE and RE due to the absorption of the ions on the ISE membrane surface. When WE and RE have the same surface nature, the tendency of non-specific absorbed anions on the surface is the same, and this undesired adsorption is cancelled in voltage difference between RE and WE electrodes. For this reason, WE and RE used in this platform were fabricated in the same manner and integrated in an array.

A layer of conductive Ag/AgCl paste was used for this purpose, since it was demonstrated to be the best support for a stable attachment of the ISE membrane. This Ag/AgCl paste is used commonly in the fabrication of screen printed RE. However, this standard RE under low pH conditions was demonstrated to be unstable. The stability of the integrated RE was measured inside a solution of 20 mM KCl and pH of 1,9 for 1 h, showing a decay of 7 mV, as already reported (Matsumoto et al., 2002). While the same RE protected with a Nafion layer gave a stable signal under the same conditions. The stability of the Ag/AgCl RE signal with and without the protecting Nafion layer was tested at different pH. Figure 23 shows the decay voltage signal observed for the platform with unprotected RE at pH below 1, due to the leakage of chloride ions from the Ag/AgCl ink. Meanwhile the Nafion protected RE shows a stable and repeatable tendency under all the pH ranges of interest.

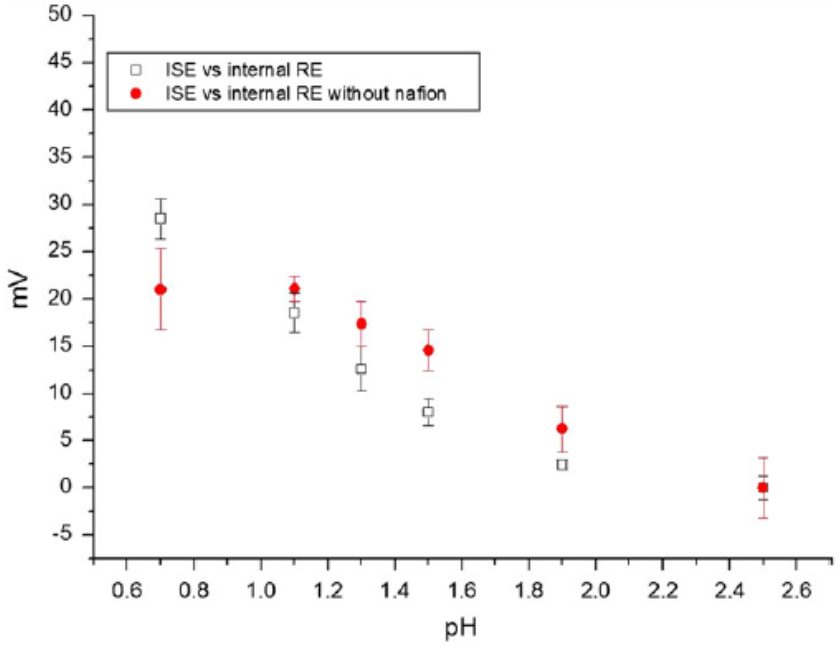

Figure 23. Potential response curves for all-solid-state ISE membrane with 4mg of KTCIPB *vs.* internal RE with and without Nafion (n=2).

The same Ag/AgCl paste substrate was used for the attachment of the ISE membrane and both electrodes were integrated in the array. In Figure 24 can be appreciated the advantages of this platform, where the anion interferences at low pH observed in the ISE measured with external commercial RE (figure 22), were completely eliminated. This result is very obvious in the control without the ISE membrane, where no affect of the ions is observed in the flat baseline. Also, in the case of the ISE sensor integrated with the RE in the array, no decay of the signal is observed at pH below 1.5.

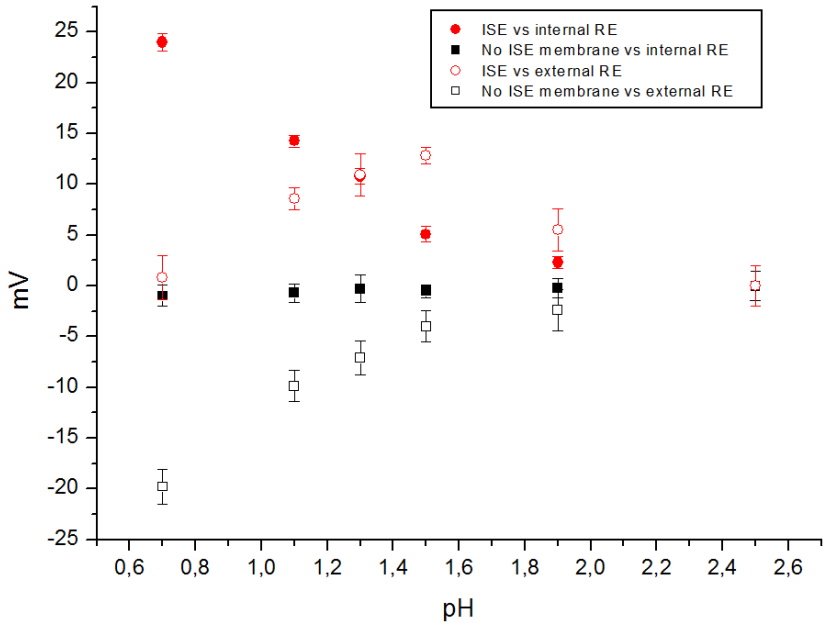

Figure 24. Potential response curves for all-solid-state ISE membrane with 4mg of KTCIPB *vs*. internal RE and external RE

An improvement of the protons signal and an increase of the slope were observed for both ISEs fabricated with increasing KTCIPB concentrations. The ISE fabricated with 12 mg of KTCIPB shows a nernstian behavior slope close to that usually observed under physiological conditions, but still not reported under this highly acidic environment (Figure 25).

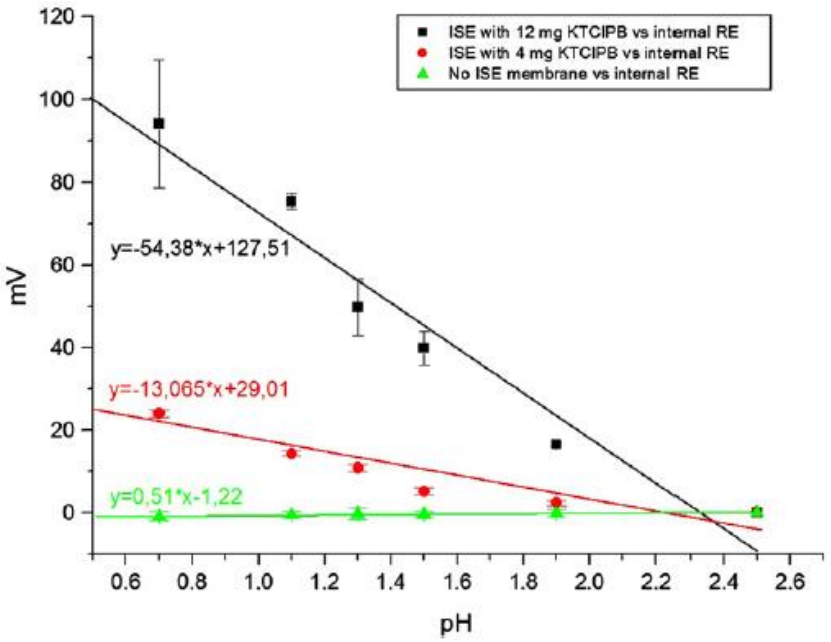

Figure 25. Potentiometry response curves for all-solid-state ISE under low pH for different KTCIPB concentrations and the absence of ISE membrane *vs*. internal RE (n=3)

Thus, the charged structure of the KTCIPB plays an important role in the sensor behavior. For this reason a deeper study of the concentration of this molecule into the ISE membrane was performed. 4, 6, 8, 10, 12, 15, 18 and 20 mg of KTCIPB were inserted into the ISE membrane mixture and different membranes were tested in the pH range of 0.7–2.5. The slope obtained for each sensor is compared in Figure 26. The results show an increase of the pH sensor response slope by increasing the amount of KTCIPB. The KTCIPB concentrations from 8 to 12 mg are closer to a Nerstian behavior and its higher slope brings an improvement in the sensor sensitivity. However, at concentration from 8 mg to higher ones the irreproducibility of the response increase because of lower mechanical stability, being the ISE membrane totally degraded at concentrations above 15 mg KTCIPB.

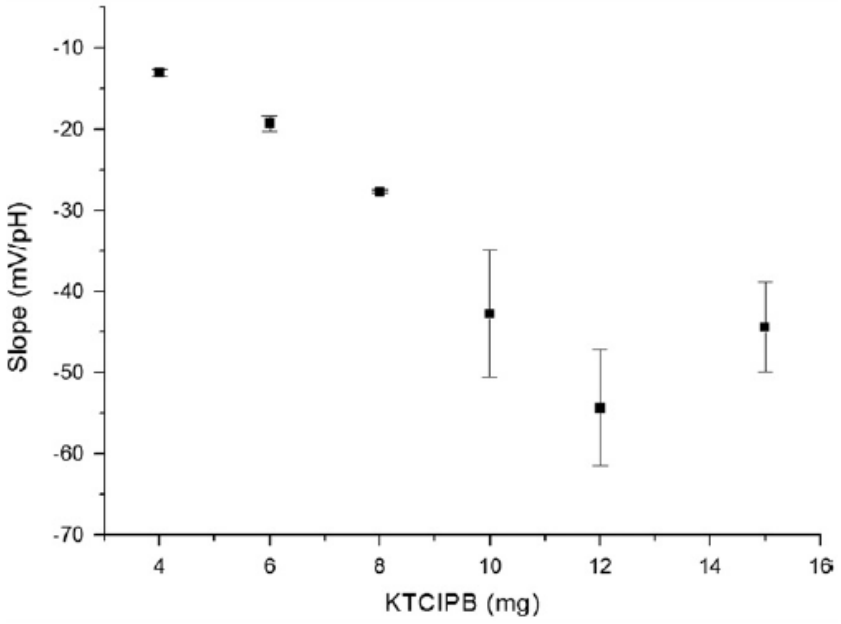

Figure 26. Slope of potentiometric response of pH sensor at different concentrations of KTCIPB (n=3)

The reproducibility of all-solid-state ISE fabrication on the same array with the integrated RE, containing 4 mg of KTCIPB, were tested. Calibration curves at low pH were obtained and the slopes of the curves were compared, obtaining a good reproducibility (−12.4±1.8 mV/pH). Also, the reproducibility of different pH sensors on different arrays was tested, showing also a good response (−13.065±0.4 mV/pH). However, as was observed on the bigger error bares in figure 27, the reproducibility of the all-solid-state ISE containing 12 mg of KTClPB is much worse (−54.38±7.15 mV/pH).

2.4.1.1. Interferences study

The selectivity of the developed pH ISE sensor was tested with other cations similar to the target of interest; Na^+ and K^+, which are also the cations with higher concentration in the stomach (Watson et al., 1996). Selectivity coefficients ($K_{A,B}$) were calculated according to the mixed solution method (Ekmekci et al., 2000). Table 2 summarizes the $K_{A,B}$ values for the ISE fabricated with 4 and 12 mg of KTCIPB. The table shows that cation interference of all-solid state ISE containing 12 mg of KTCIPB is approximately eight times higher than the ISE containing 4 mg. The reason of the higher cation interference in the ISE with increased concentration of KTClPB is due to the chemical nature of this molecule, which is a liphophilic anion that charges negatively the ISE membrane, attracting positive ions, as reported in the literature (Cardwell et al., 1992).

Table 2
A = hydrogen ion, B = interfering ions.

Selectivity coefficients	Na^+	K^+
$K_{A,B}^{4\ mg}$	10.4×10^{-2}	10.3×10^{-2}
$K_{A,B}^{12\ mg}$	77×10^{-2}	78×10^{-2}

So, increasing concentrations of KTCIPB have a double effect preventing the access of anion interference, but also, this negatively charged surface deteriorates the proton detection due to cation interference. On the contrary, although all solid-state ISE containing 4 mg of KTClPB has a lower potential response slope, it has negligible potential increase due to KCl and NaCl interferences. Figure 27 shows the difference in signal due to the cation interference at different pH and KTCIPB concentrations. The interference of NaCl and KCl is higher under 12 mg KTCIPB ISE membrane, being more betrayed at lower pHs.

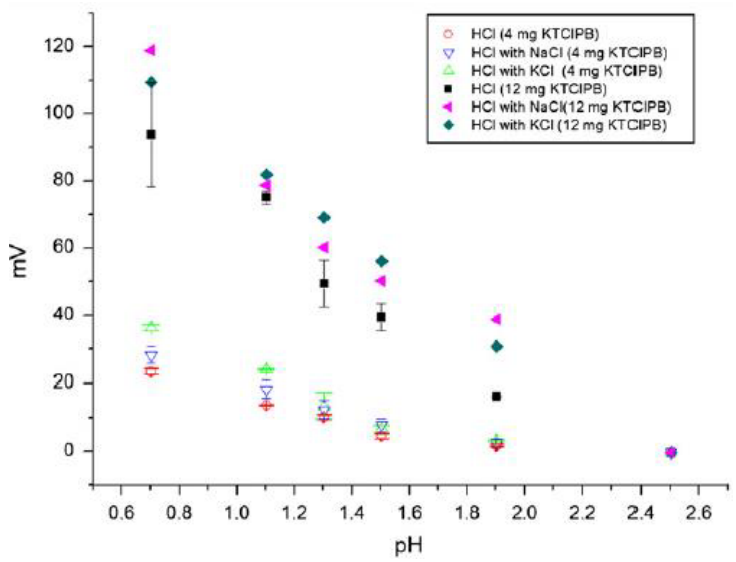

Figure 27. Potential response curves for all-solid-state ISE *vs*. internal RE under 20mM KCl or NaCl interference (n=3).

2.4.1.2. Evaluation of the response time

Besides the sensitivity and selectivity, the time for sensor responding is another relevant feature of this analytical devices. The response time was calculated as the required time for achieving 90% of the steady state potential after the HCl injection. The response time observed with the pH sensor with 4 mg KTCIPB was longer for lower pHs, since the proton concentrations was higher and the ISE membrane took longer for the stabilization. The average of the response time was in the range of 17.86±7,3s, which is in between the literature results for other reported all-solid-state pH sensors: 8s in the system developed by Won-Sik Han et al. (Han et al., 2001) and 45 s in the sensor developed by Zine et al. (Zine et al., 2006) (Figure 28).

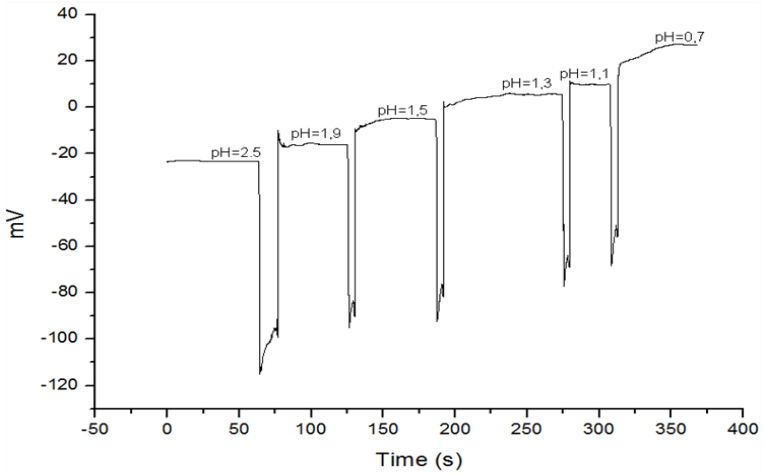

Figure 28. Response time of all-solid-state pH sensor developed for this project.

2.4.1.3. Long life response of the pH ISE sensor

The longevity of the fabricated ISE sensors is also extremely relevant for devices that have a future commercialization. Thus, these sensors need to be stable for certain time, because a shorter degradability do not allows a competitive entrance in the market.

For this purpose, different arrays were fabricated, kept and measure every week. The sensors, which kept in open air, were oxidized after 4 weeks, starting to be affected its pH detection ability (Figure 29).

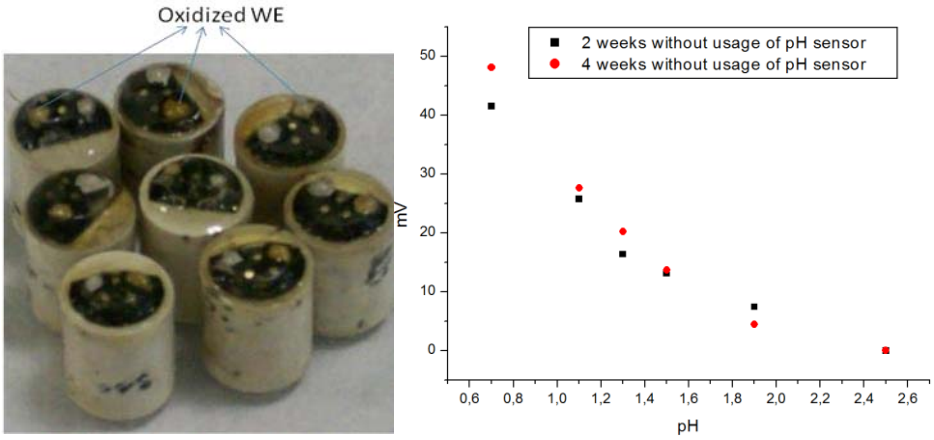

Figure 29. pH response of oxidized of all-solid-state pH sensors after 2 and 4 weeks in open air.

In order to improve the stability fabricated sensors, the arrays were kept in argon to stop oxidation effects. pH measurements were done every 2 weeks for 12 weeks. Figure 30 and 31 show the long time response observed with these arrays kept under argon. The storage of the arrays under these conditions was demonstrated to be a suitable system to save the arrays for the degradability and so they can be commercialized and used minimum for 12 weeks kept in argon.

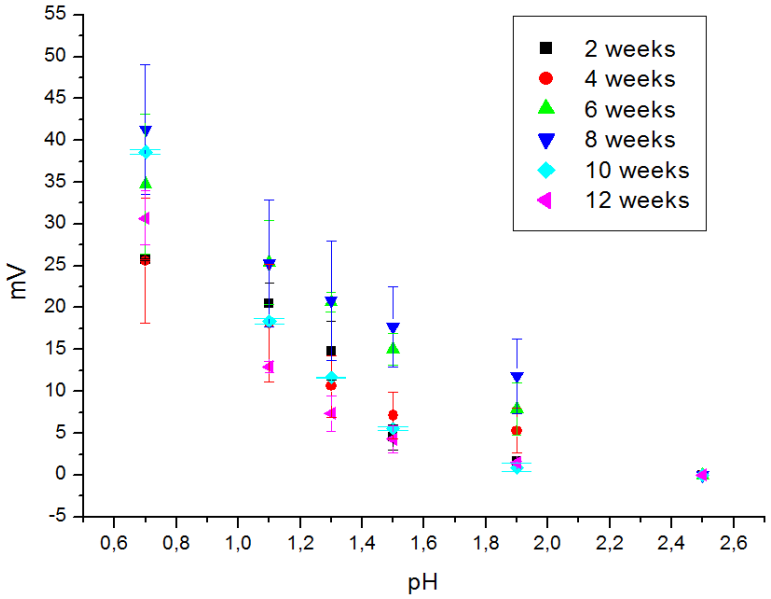

Figure 30. Long time response of fabricated pH sensors kept under argon.

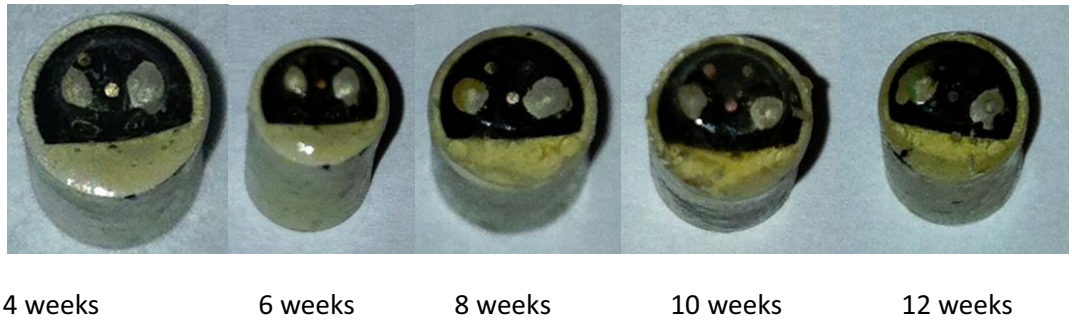

Figure 31. Pictures of the arrays used for the long time response kept under argon.

2.4.1.4. Applications for physiological pH range

The all-solid-state array developed for this project had an initial application for ischemia detection on the stomach tissue. For this reason, all the efforts were focused in the stability of the sensors under this strong acidic conditions. However, it is important to show that this sensor is also useful under physiological pH, since many other applications can be found for this sensor, as will be presented in chapter 4 and 6.

Since the array integrates the all-solid-state ISE but also the RE, which is in the same way affected by the pH, the effect of the integrated RE (Ag/AgCl ink with Nafion) was tested and compared with unprotected RE and commercial RE under all the pH range.

As can be appreciated in figure 32, reproducible stable response for Ag/AgCl electrode covered by nafion membrane was achieved between the pH values of 2 to 8.

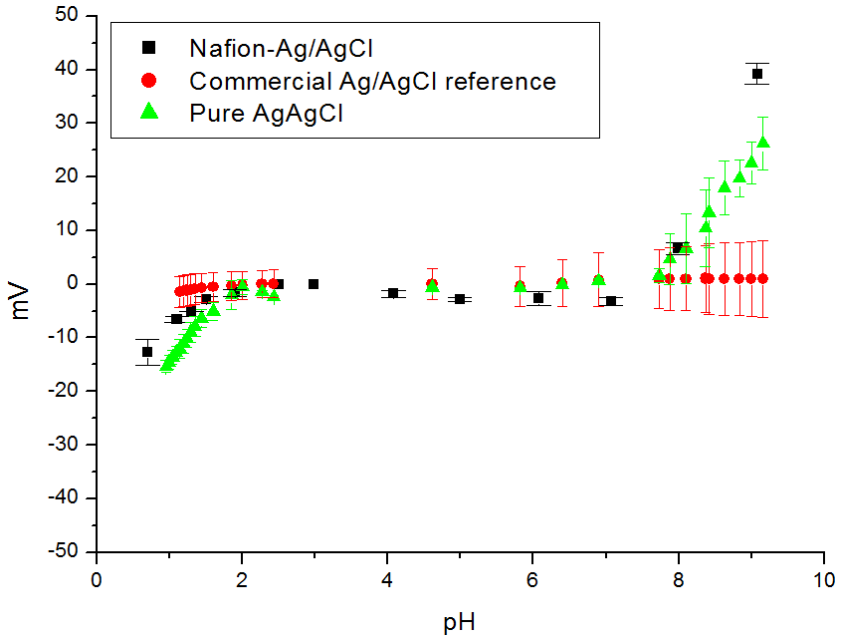

Figure 32. Potentiometry response curves for different RE under physiological pH *vs*. external Ag/AgCl commercial RE (n=2).

Thus, the same working range was tested with the developed all-solid-state pH ISE sensor. The results in figure 33 shows that besides the ability of this sensors for measuring at low pHs also in physiological pH; from 6.5 to 8, this sensor can be used, because the active working range is determined by the ion-to electron transfer, which depends on the pH and the material and membrane choice.

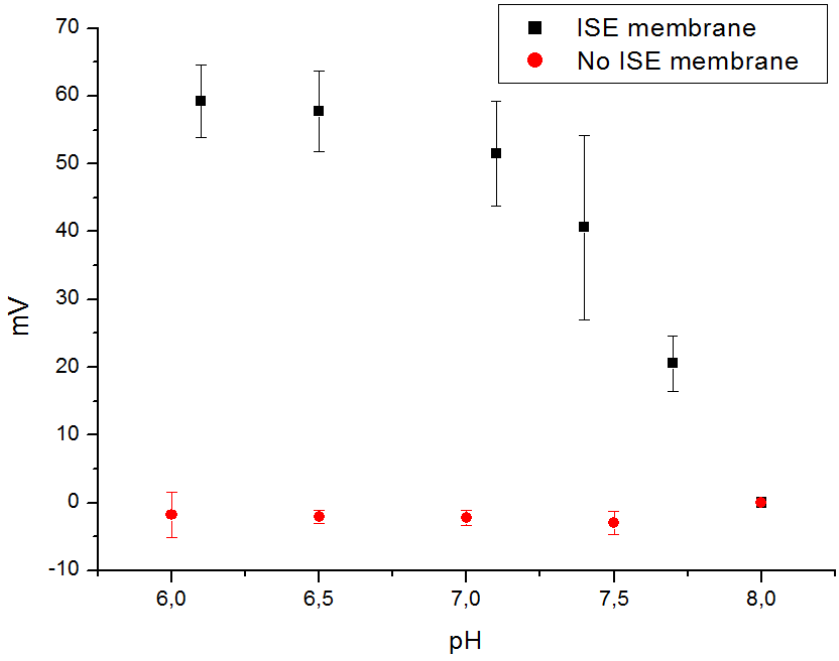

Figure 33. Potentiometry response curves under physiological pH for all-solid-state pH ISE *vs*. internal RE (n=2)

2.5. Potassium ISE Detection

2.5.1. Potassium ISE results at different pH

The optimizations of surface electrodes and integrated RE performed for the pH sensor, were applied for all-solid-state potassium sensors. Ag/AgCl ink surface covered with nafion was used as RE and Ag/AgCl ink surface covered with ISE membrane was used as WE and these two electrodes were integrated on the designed array. The potassium ISE membrane ionophore (Bis[(benzo-15-crown-4)-4-ylmethyl]pimelate) was used, following next protocol; Potassium ISE membrane was prepared with a mixture of 1.0 wt% potassium ionophore (Bis[(benzo-15-crown-4)-4'-ylmethyl] pimelate), 0,3 wt% KTClPB, 68.0 wt% 2-Nitrophenyl octyl ether, 30.7 wt% PVC high molecular weight. 300 mg in total of these chemicals were dissolved in 3 mL of freshly distilled THF (Tamura et al., 1983)

The results obtained with this potassium ionophore are presented in figure 34, where good results were observed for potassium sensing at physiological and basic solutions.

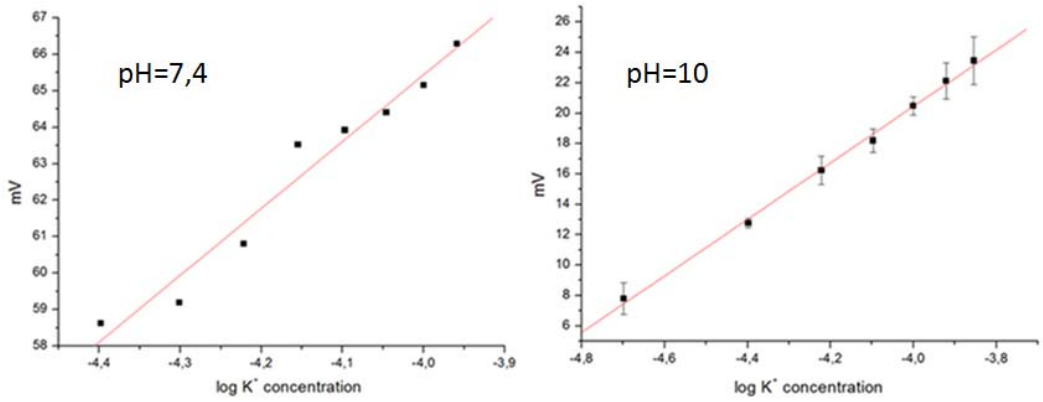

Figure 34. Potentiometry response curves for all-solid-state potassium ISE at pH7.4 and 10 *vs*. internal RE (n=2)

However, the developed potassium ISE membrane was detached from the surface at low pHs, which is the main working range for this sensor. For these reasons, the ionophore was changed to valinomycin, which was reported to be applied at low pHs. The alternative protocol was; 2 wt% potassium ionophore valinomycin, 65.0 wt% Bis(1-butylpentyl) adipate (BBPA), 0,5 wt% KTClPB, 32,5 wt% poly (vinyl chloride) (PVC). 200 mg in total of these chemicals were dissolved in 2 mL of freshly distilled THF (Hauser et al., 1995).

The potassium detection obtained with this ionophore at 1,9, 1,6 and 7,4 pH is shown in figure 35. The reproducibility of the sensor is high at any potassium concentration and pH. The sensor response is much sensitive at pH 1,9, losing its sensitivity at lower and higher pHs, because the sensitivity of the potassium sensor is highly dependent on the

solution pH. The active working range is determined by the ion-to electron transfer, which depends on the pH, the material and membrane choice. Thus, it affects tremendously sensitivity, selectivity and working range. In figure 35, it can be appreciated that the results are very obvious in the control without the ISE membrane, where no effects of the ions is observed in the flat baseline at low pH and also at physiological pH values proving that the sensitivity of the sensor is because of potassium selective membrane.

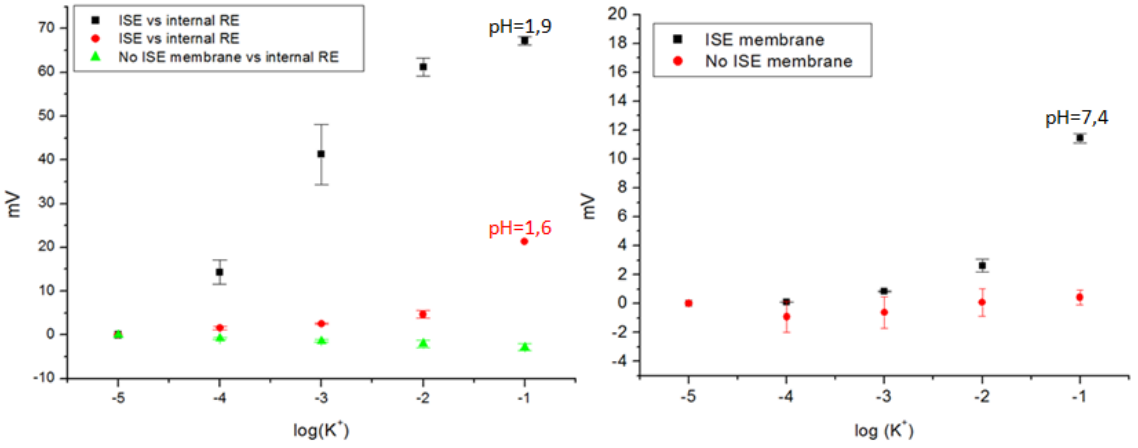

Figure 35. Valinoycin based potassium ISE integrated in the project array at pH 1,6, 1,9 and 7,4 (n=3)

2.5.2. Long time response of the sensors

As was previously reported for the pH developed ISE sensors, long time responses of all-solid-state potassium sensors in different weeks were also analyzed.

From the experience with all-solid-state pH sensors, all-solid-state potassium sensors were kept inside argon. However, in the case of potassium senor, although kept under argon, these sensors got oxidized after 2 weeks (Figure 36).

Figure 36. Oxidized all-solid-state potassium sensors kept under argon for 2 weeks

The potentiometry results agree with oxidation pictures, shown noisy and unstable potentiometry signal. The reason behind this effect is the ionophore used inside the ISE membrane. Valinomycin molecule contains amide groups, which are very weak bases that can react with oxygen causing the formation of nitriles. That process results with the formation of mixed oxides of nitrogen (NO_x) on time.

References

A. Keller, P. Leidinger, A. Bauer, A. El Sharawy, J. Haas, C. Backes, A. Wendschlag, N. Giese, C. Tjaden, K. Ott, J. Werner, T. Hackert, K. Ruprecht, H. Huwer, J. Huebers, G. Jacobs, P. Rosenstiel, H. Dommisch, A. Schaefer, J. Müller-Quernheim, B. Wullich, B. Keck, N. Graf, J. Reichrath, B. Vogel, A. Nebel, S. Jager, P. Staehler, I. Amarantos, V. Boisguerin, C. Staehler, M. Beier, M. Scheffler, M. Büchler, J. Wischhusen, S. Haeusler, J. Dietl, S. Hofmann, H. Lenhof, S. Schreiber, H. Katus, W. Rottbauer, B. Meder, J. Hoheisel, A. Franke, E. Meese Nature Methods, 8 (2011), 841

A. Kisiel, H. Marcisz, A. Michalska, K. Maksymiuk, Analyst., 130 (2005), 1655

Ammann, E. Pretsch, W. Simon, Analytical Chemistry., 58 (1986), 2285

A.M. Feltham and M. Spiro Chemical Reviews., 71 (1971), 177

A. Simonis, H. Luth, J. Wang, M. J. Schoning Sensors and Actuators B.,103 (2004),429

A.W.J. Cranny, J.K. Atkinson, Measurement Science and Technology., 9 (1998), 1557

A. W. Hassel, K. Fushimi, M. Seo Electrochemistry Communications., 1, (1999) 180

B. J. Polk, M. Bernard, J. J. Kasianowicz, M. Misakian, M. Gaitan, J. Electrochem. Soc., 151 (2004), 559

B. Qiu, J. Liu, Z. Qin, G. Wang, H. Luo ChemComm., 20 (2009), 2863

B. Reents, W. Plieth, V. A. Macagno, G. I. Lacconi, J. Electroanal. Chem., 453 (1998), 121

B. Xie, J. Sun, Z. Lin, G. Chen Journal of the Electrochemical Society, 156 (2009) 79-83

Chan, M., 1996. Water-based silver–silverchloride compositions. US Patent: US 5,565,143A.

D. Ammann, P. Anker, E. Metzger, U. Oesch, W. Simon, (1985). In: Kessler, M.,

Harrison, D.K., Hoper, J. (Eds.), Ion Measurements in Physiology and Medicine. ¨

Springer-Verlag, Berlin.

D. G. Foster, Y. Shapir, and J. Jorne, J. Electrochem. Soc., 150 (2003), 375

D. G. Foster, Y. Shapir, and J. Jorne, J. Electrochem. Soc., 152 (2005), 462 (2005).

D. Gonullu, Y. Yankol, F. Isiman, A. Igdem, O. Yucal, F. N. Koksoy, Turkish

Journal of Trauma and Emergency Surgery., 13 (2007), 261

D. Grieshaber, R. MacKenzie, J. Voros, E. Reimhult Sensors, 8 (2008), 1400

D. J.Harrison, L. L. Cunningham, X. Li, A. Teclemariam, D. Permann, Journal

of the Electrochemical Society., 135 (1988), 2473

E. P. Leahy, G. A. Karustis, US Pat. 4,067,784 (1978).

F.X. Rius-Ruiz, D. Bejarano-Nosas, P. Blondeau, J. Riu, F.X. Rius. Analytical Chemistry., 83 (2011), 5783

G. Blackburn, J. Janata, Journal of the Eletrochemical Society., 129 (1982), 2580

G. Elkington, H. Elkington, Br. Pat., 8 (1840) 447

G. Ekmekci, G. Somer, Analytical Sciences., 16 (2000), 307

G. Gunawardena, G. Hills, and I. Montenegro, J. Electroanal. Chem., 138 (1982), 241

G. M. de Oliveira, L. L. Barbosa, R. L. Broggi, I. A. Carlos, J. Electroanal. Chem., 578 (2005), 151

H. F. Osswald, R. Asper, W. Dimai, W. Simon Clin Chem., 25 (1979) 39

H. J. Lee, U. Hong, D.K. Lee, J.H. Shin, H. Nam, G.S. Cha Analytical

Chemistry, 70 (1998), 3377

H. Suzuki, H. Shiroishi, S. Sasaki, I. Karube, Analytical Chemistry., 71 (1999),5069

H. Tamura, K. Kumami, K. Kimura, T. Shono Microchimica Acta., 80 (1983), 287

J. Bobacka, T. Lindfors, M. McCarrick, A. Ivaska, A. Lewenstam, Analytical

Chemistry., 67 (1995), 3819

K. J. Koch, T. Aggerholm, S. C. Nanita, R. G. Cooks J Mass Spectrom., 37 (2002), 676

L. Tymecki, E. Zwierkowska, R. Koncki, Analytica Chimica Acta., 526 (2004), 3

M. Chan, Water-based silver–silverchloride compositions. US Patent: US

5,565,143A (1996)

M. Miranda-Hernández, I. González, J. Electrochem. Soc., 151 (2004), 220

M. P. Mattson, Nature., 430 (2004), 631

M. Piao, J. Yoon, G. Jeon, Y. Shim, Sensors., 3 (2003), 192

N. Abramova, A. Bratov, Sensors., 9 (2009), 7097

N. Kwon, M. Won, D. Park, Y. Shim Electroanalysis., 17 (2005), 641

N. Kwon, K. Lee, M. Won, Y. Shim, Analyst., 132 (2007), 906

N. Kwon, K. Lee, M. Won, Y. Shim Analyst., 132 (2007), 906

N. Zine, J. Bausells, F. Teixidor, C. Viñas, C. Masalles, J. Samitier, A. Errachid Materials Science and Engineering C, 26 (2006), 399

O. Azzaroni, P. L. Schilardi, R. C. Salvarezza, A. J. Arvia, Langmuir., 15 (1999) 1508

P. T. Kissinger, W. R. Heineman, Journal of Chemical Education., 60 (1983), 702

R. D. Pascoe, B.O. Connell, Waste Management., 23 (2003), 845

R. J. Morrissey, WO Pat. 083,156 (2005).

R. Lars, A. Jenkins Bioelectrochem., 70 (2007), 387

S. J. Watson, R.H. Smallwood, B. H. Brown, P. Cherian, K.D. Bardhan, Physiological Measurement., 17 (1996), 21

S. Jayakrishnan, S. R. Natarajan, K. I. Vasu, Met. Finish., 94 (1996), 12.

S. Masaki, H. Inone, H. Honma, Met. Finish., 96 (1998), 16

S. Sriveeraraghavan, R. M. Krishnan, and S. R. Natarajan, Met. Finish., 87 (1989), 115

T. Blaz, J. Migdalski, A. Lewenstam, Analyst., 130 (2005), 637

T. J.Cardwell, R.W. Cattrall, L.W.Deady, K.A. Murphy, Australian Journal of

Chemistry., 45 (1992), 435.

T. Matsumoto, A. Ohashi, N. Ito, Analytica Chimica Acta., 462 (2002), 253

ToFSIMS, (2012)
http://serc.carleton.edu/research_education/geochemsheets/techniques/ToFSIMS.html

U. Anastasova-Ivanova, A. Mattinen, J. Radu, A Bobacka, A. Lewenstam, J. Migdalski, M. Danielewski Sensors and Actuators B., 146 (2010), 199

U. Oesch, Z. Brzbzka, X. Aiping, B. Rusterholz, G. Suter, P.H. Viet, D.H. Welti, D. Ammann, E. Pretsch, W. Simon Analytical Chemistry., 58 (1986), 2285

V. Cosofret, M. Erdosy, T. A. Johnson, R.P. Buck, Analytical Chemistry., 67 (1995), 1647

W. Han, M. Park, M, K. Chung, D. Cho, T. Hong, Electroanalysis., 13 (2001), 955

Y. Lin, Z. Sun, Z, Journal of Endocrinology., 204 (2010), 1

Y. T. Su, D. H. Cheng, K. J. Li, T. H. Cao, and W. Y. Xu, Chin. Plat. Finish., 27 (2005) 161

CHAPTER 3

Bioimpedance sensor for ischemia detection

3.1. Introduction

This chapter describes the fabrication and measurements with four electrode impedance sensor for the final purpose of ischemia sensing on the stomach tissue by means of endoscopy tools for vivo experiments.

Bioimpedance sensor was first optimized in vitro with different solutions of ions concentration. Also, for mimic the tissue detection, tissues with different nature were differentiated with the sensor. For this purpose, fat and breast chicken tissues were taken as a model for mimicking non-ischemic and ischemic states respectively. The effect of electrodes insulation on impedance signal as well as the pressure applied on the tissue was studied. The sensitivities of the impedance device were determined and the right injection frequency was chosen for in vivo experiments.

3.2 Materials & Methods

3.2.1. Materials

KCl, NaCl and HCl were received from Panreac. Ag/AgCl and carbon inks were supplied by Dupont. MCS 12 series electrode arrays were obtained from Omnetics Connector Corporation and resin hardener complex (EPOTEK 301-2) was provided by Epoxy Technology.

3.2.2. Microelectrodes fabrication

The electrochemical sensor array was composed of 12 electrode pins of beryllium copper alloy. Prior to the modification, they were washed with double deionized (MilliQ) water and dried under nitrogen atmosphere. The sides of the electrodes pins

were insulated with a commercial biocompatible resin mixed with a hardener complex (as was already explained in chapter 2). This insulation reduces the background noise signal and brings high biocompatibility and chemical resistance to the electrodes. 600 µm of beryllium copper diameter electrode area was delimited after polishing the electrodes tips. Afterwards, they were cleaned by sonication inside pure ethanol for 2 min and remaining contaminants were removed under nitrogen gas. Beryllium copper surface was first covered with carbon paste by soaking the tip of the electrodes in a homogeneous thin ink layer with 17 µm thickness created by spin coating under 4000 rpm for 1 minute and left to dry at 130 °C for 6 min. Once carbon surface was dried, it was covered with Ag/AgCl ink by soaking the tip of the electrodes in a thin ink layer of Ag/AgCl with 33 µm thickness created by spin coating at 1500 rpm for 4 minutes and left to dry at 130 °C for 6 min.

3.3. Detection

3.3.1 Impedance device

In the literature, there are 2, 3 and 4 electrodes systems for impedance measurements. 4 electrodes system was chosen for in vitro and in vivo experiments, because this system prevents polarization at metal electrolyte interface by injecting current with outer electrodes and by recording voltage with inner electrodes as explained in the introduction section. In case of this impedance experiments, it were done in extremely noisy environments such as organs or tissues. Thus, lock-in amplifiers were necessary to extract a signal with a known carrier wave from the noisy environment to distinguish the real signal, and also to measure phase shift (Odry et al., 2011). For this purpose, a custom made impedance device developed by SIC-BIO (Instrumentation Systems and Communications and Biomedical) was used for the impedance measurements. Impedance and phase of the tissues were determined by injecting a fixed AC current and recording voltage (figure 1).

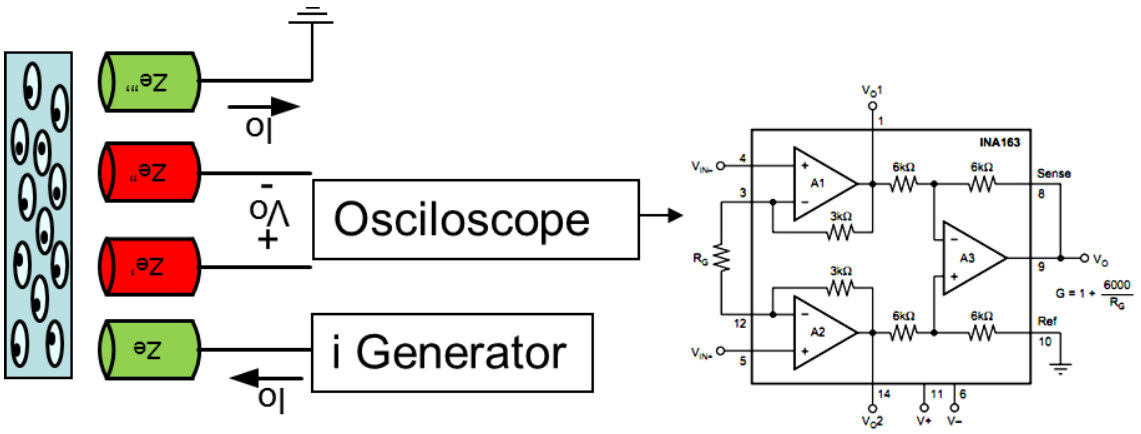

Figure 1. Scheme of the 4 electrodes for bioimpedance measurement.

3.3.2. Conductivity tests in different solutions

When ionic compounds are dissolved in solution, the positive and negative ions of this compound start to move freely carrying positive and negative electrical charge, conducting electrical current. These electrically charged ions are called electrolytes. When the concentration of electrolyte starts to increase, the conduction of the current through the solution is higher with the subsequent reduction of impedance. This fact was used to check, if the designed impedance device is working properly in tris buffer solutions (0,1M) with different pH values adjusted with HCL. The electrodes were immersed into the solution and impedance measurements were performed. As it is expected, the results proved that the impedance is decreasing at lower pH values (higher H^+ concentration). A clear trend is observed in the response as well as good reproducibility in the signal (Figure 2).

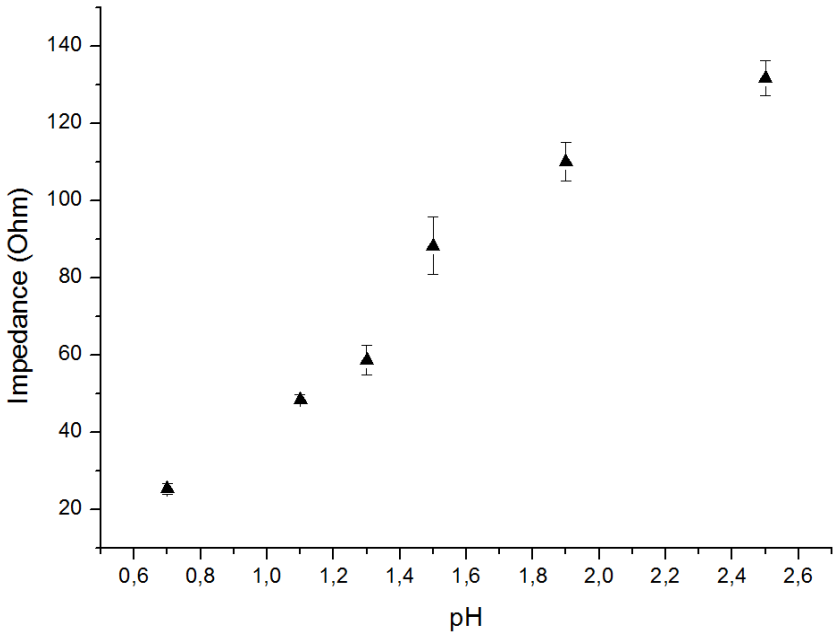

Figure 2. Impedance measurement of different pH solutions (n=5)

3.3.3. Impedance measurements on different tissues

The feasibility of the impedance sensor was first tested on different tissues. For mimicking the ischemic and normal states of the tissue, chicken fat (adipose tissue) and chicken breast (muscle tissue) were chosen. Adipose tissue can barely hold water, meanwhile muscle tissue can hold high amount of water (Wang and Pierson, 1976), in the same way that ischemic tissue can hold more than normal tissue (De oliveira et al., 1960). The electrodes were put in contact with different tissues (fat, breast chicken and liver) and impedance measurements were performed with 4 pin electrodes in a row applying 100 kHz and injecting current of 3 mA peak to peak (3 mAp-p). The

impedance results proved that these tissues can be distinguished from each other with the impedance device (Figure 3).

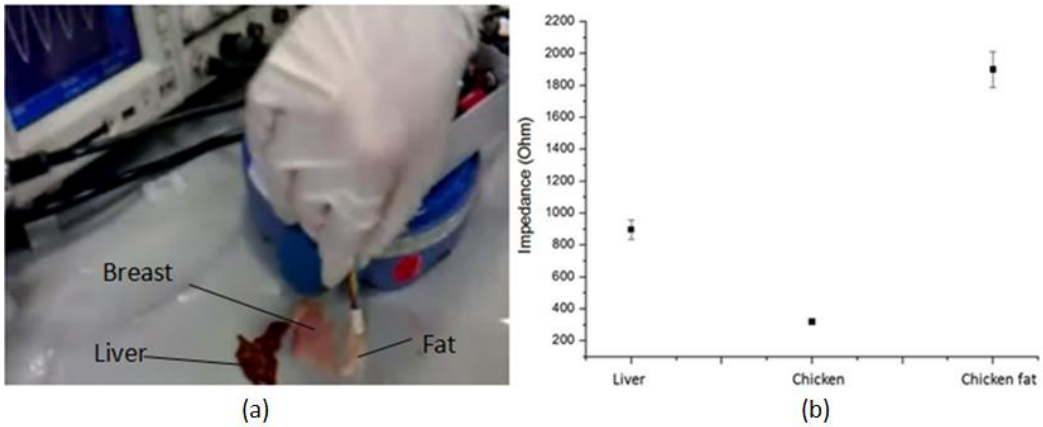

Figure 3. Impedance measurements on chicken fat, breast and liver.

In order to keep closer to the stomach model, the tissue was covered with a solution mimicking the gastric juice, which has very high conductivity; around 14 mS. For simulating the gastric juice, HCL and KCL solutions with similar concentrations and conductivity found in the stomach were prepared (Watson et al., 1996). Chicken fat and breast were put inside a glass vial containing tris based HCL or KCL solution with a final conductivity of 14 mS (figure 4).

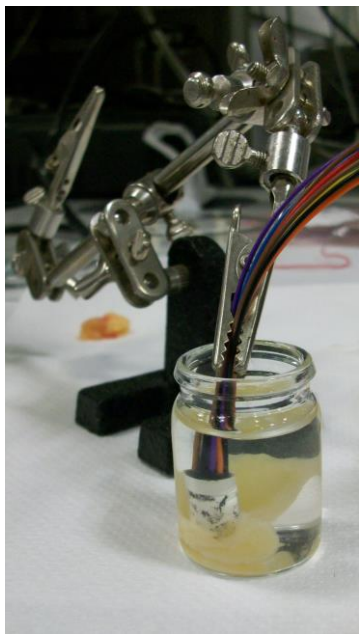

Figure 4. Chicken breast detection in 14 mS conducting solution

Impedance measurements were performed in air, KCL and HCL tris based solutions with 14 mS conductivity. Two types of pin electrodes were compared. Ones were pure beryllium copper alloys with any pin insulation, while the second type of pins were

covered with the epoxy insulation and covered with Ag/AgCl ink on the top as explained in materials and methods section (figure 5).

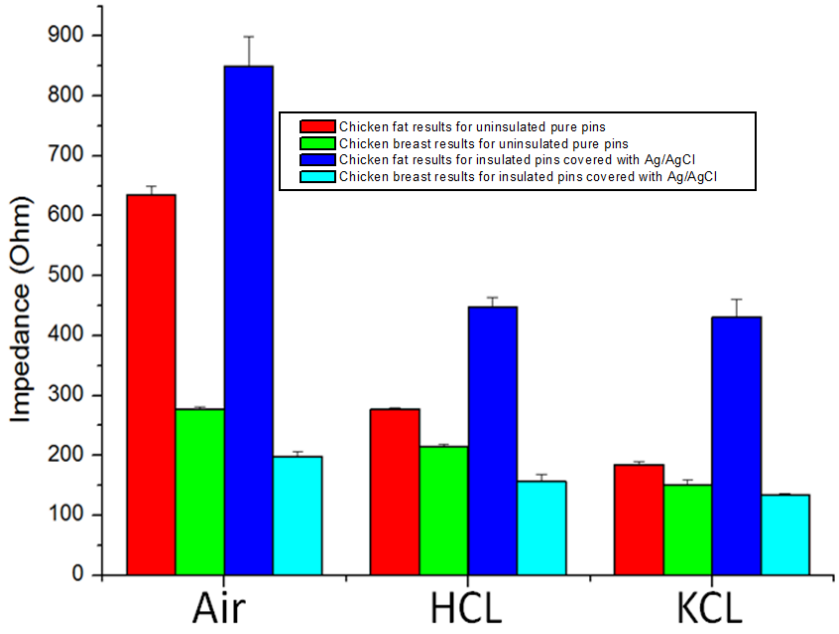

Figure 5. Impedance results for chicken breast and chicken fat for insulated, Ag/AgCl covered pin electrodes and uninsulated pin electrodes

As expected, the impedance difference for chicken fat and breast is higher in air than HCL and KCL , since in air all the current flow through the tissue and when the tissue was in conductive HCL and KCL solutions, current was flowing through both; the tissue and the solution, which makes the current difference smaller between the two tissues. Comparing the two types of pins, the ones insulated brought higher difference between the two tissues, because with these electrodes the top of the pins was the only uncovered part of the electrode, which is the one that touched the tissue. Therefore, the part that was not sensing was covered reducing the background noise. Thus, it was decided to do further experiments with insulated Ag/AgCl covered electrodes.

3.3.4. Frequency optimization for in vivo experiments

The differentiation of tissues are directly related to the frequency applied to the tissue. Thus, it is very relevant to choose the right frequency for the detection. For this purpose chicken breast and fat were measured inside different pH solutions at different frequencies; between 10-250 KHz (Figure 6).

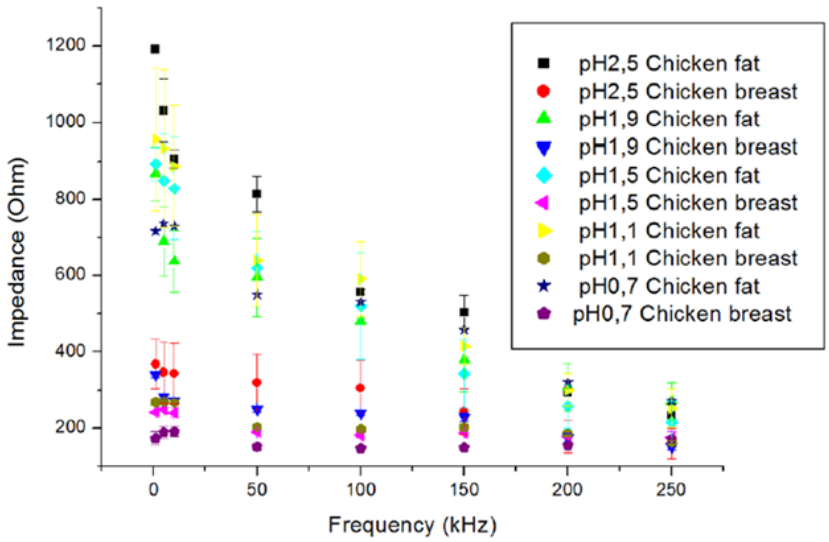

Figure 6. Impedance results for chicken breast and chicken fat under different pH and frequencies at 3 mAp-p (n= 2)

In Figure 6, it was clear the dependence of the impedance response with the frequency, since at higher frequency it was hard to differentiate the two tissues, while at lower frequencies was very clear this differentiation.

In order to choose the best conditions for the stomach tissue detection, different frequencies were tested for the measurement of the tissue differentiation under gastric juice conductivity; 14 mS. Figure 7 shows the results of impedance and phase under the described conditions.

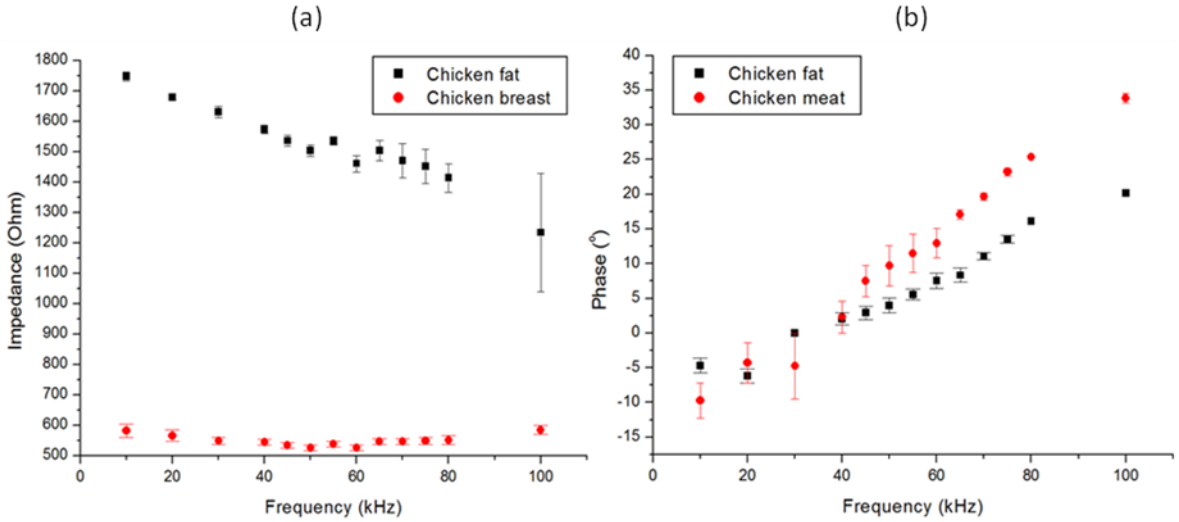

Figure 7. Impedance and phase results for chicken fat and breast under 14 mS at different frequencies (n=2)

Taking into account the phase and impedance results of the measured solution in figure 7, 70 kHz was chosen as the better conditions for this detection.

The achieved results were also supported by the literature, which had shown 68 kHz as the best frequency to distinguish ischemic and nonischemic tissues on small intestine (Othman et al., 2003) (Figure 8).

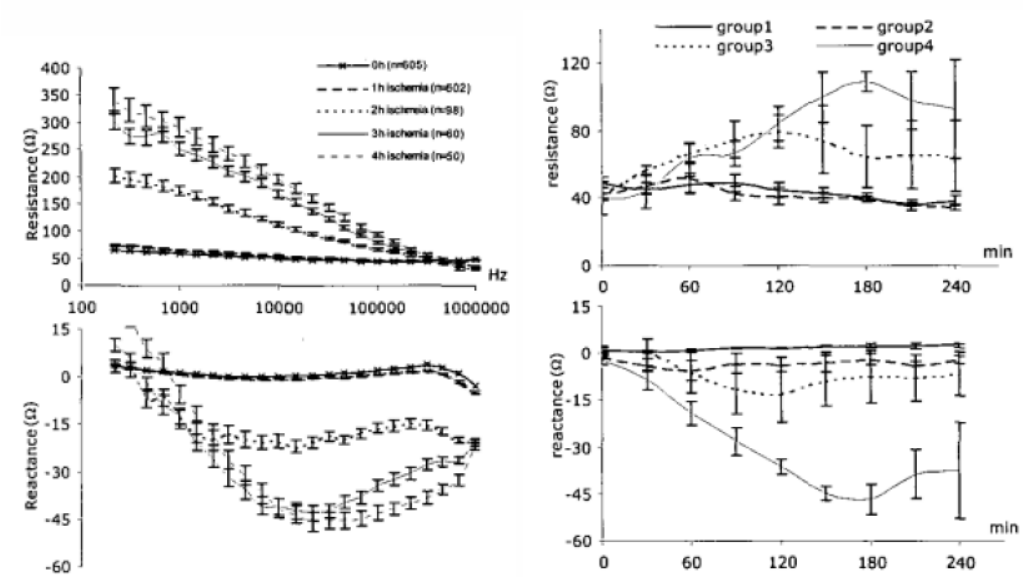

Figure 8. Resistance and reactance tests for ischemic and non ischemic intestine tissues

References

J. M. de Oliveira, M. N. Levy, American Heart Journal, 60 (1960) 106

J. Wang, R.N. Pierson Journal of Nutrition 106 (1976), 1687

K. Máthé IEEE 9th International Symposium on Intelligent Systems and Informatics, Subotica, Serbia., (2011) 407

O.S. Sacristán, E. Gonzalez, C.A. Pinzón, J. Aguado, J. Flores, P. Infante, Annual International Conference of the IEEE Engineering in Medicine and Biology – Proceedings., 4 (2003) 3207

P. Odry, F. Henézi, E. Burkus, A. Halász, I. Kecskés, R. Márki, B. Kuljić, T. Szakáll, S.J. Watson, R.H. Smallwood, B.H. Brown, P. Cherian, K.D. Bardhan Physiological Measurement., 17 (1996), 21

CHAPTER 4

Sensors integration and in vivo experiments

4.1. Introduction

Humans´ life standards were drastically improved from the beginning of the last century with the help of modern technology. With the advancement in medicine, many diseases were cured and life expectancy of the human was enhanced. However, humans were started to struggle with other problems such as depression, cancer, diabetes, heart disease, dementia, and obesity, among others (Mathers *et al.,* 2001, Mir *et al.,* 2012). Considerable numbers of people are affected by morbid obesity in Europe and just in USA more than two hundred thousand operations for morbid obesity were performed in 2006. Different surgical operations were developed to fight against morbid obesity such as bariatric surgical procedures, sleeve gastrectomy and gastric bypass. However, although these techniques are the most safe and reproducible for stomach reduction (Karliner *et al.,* 2007; Dejardin *et al.,* 2013), they have also complications such as volvulus of stomach. The twisting of the stomach produced in gastric volvulus is due to the lax gastric fixation or incorrect positioning of the stomach (Dejardin et al., 2013). This may result to the shortage of the blood supply to the organ causing to gastric ischemia (Kicska *et al.,* 2007; Borum *et al*., 2009). Also, intestine obstruction due to internal hernia is another problem during gastric bypass. That can also cause severe ischemia (Borum *et al.,* 2009; Steinemann *et al.,* 2011). Local tissue ischemia in gastric bypass may happen due to anastomotic stricture on bowel and stomach (Chung *et al.,* 1988; Songer *et al.,* 2001). Because of these reasons, ischemia monitoring on stomach and intestine tissue is relevant during sleeve gastrectomy and gastric bypass based bariatric surgery.

There are few examples of commercialized ischemia sensors. The typical commercialized ischemia sensors are based on optical detection. A light with specific wavelength is emitted to the tissue and the changing absorbance of the normal and

ischemic tissue is detected (Benaron *et al.,* 2004). Although electrochemical sensors have a lot of advantages comparing with the optical sensors, such as low cost, fast response, and miniaturization, there are no commercialized devices and few examples in the literature about full integrated electrochemical sensors for ischemia detection.

Conventional potassium and pH ISE sensors, combined with impedance sensors, were used in the detection of ischemia on kidney (Ivorra *et al.,* 2003). The RE utilized for this detection was also a commercial RE. Thus, the different sensors used for this application were neither integrated nor implanted into the organ. Another example of all-solid-state potassium and pH ISE was reported for sensing myocardial ischemia on the beating heart (Cosofret *et al.,* 1995). A sensor array with thick-films of pH and potassium selective sensor arrays were fabricated for this purpose and used for measuring the beating pig heart. This system was improved by Marzouk et al. (Marzouk *et al.,* 2002) adding lactate sensors to the existing pH and potassium selective sensors taking into account the interdependency of potassium and lactate concentration during ischemia. However, none reported examples of all-solid-state sensors published were applied for ischemia detection on the stomach tissue. Probably, the reason behind the fact is the measurements needed to be performed under strong acidic and corrosive environment and such a condition makes the development of a reliable and stable sensor more complicated (Tahirbegi *et al.,* 2013).

This chapter describes the integration of all solid state ISE pH and potassium sensors with the all solid state RE and bioimpedance sensor. All of them developed for its application in endoscopic systems for in vivo detection of ischemia inside the stomach and small intestine. For this purpose, an electrochemical array was designed and developed, being the disposition of the sensors, the shape and size of the array and the stability on the tissue studied for reliable detection under endoscopic in vivo detection. Once the integrated array was tested in vitro, some experiments in vivo inside the stomach of pigs were performed, where the performance of the array was tested.

4.2. Array design and fabrication for endoscopic applications

4.2.1. Array design

The sensor array was designed for the detection of ischemia inside the stomach by means endoscopic systems in a reliable and low cost way. For this reason, the shape and size of the sensor array was designed for being adapted to the commercially available gastroendoscopes.

The array was a round shaped cylinder of 7 mm. For the sensor insertion inside the commercially available gastroendoscope, which have an inner 2,5 mm cavity for the external tools insertion, the wires of the sensor array was changed with thinner ones; 150 μm diameter each wire, with a final diameter of 2 mm and a total length of 2 m. All the electrical connections and wires were sealed with heat shrink tubes in order to ensure the water tightness and to prevent any short circuit in highly reactive gastric juice of the stomach. The electrodes were fabricated under a needle configuration rather than a planar to improve the connectivity of all the electrodes with the tissue. The array contained 12 needle electrodes with 600 μm diameter each. The electrodes were functionalized as; 3 RE, 3 pH and 2 potassium all-solid-state sensors and 4 electrodes in a row for impedance measurements. Each electrode was distanced enough to each other in order to avoid crosstalks between the electrodes. For reducing the cost, the sensor array was designed to be partially disposable and interchangeable. The array part, which touches the patient tissue, can be easily disconnected from the 2 m reusable cable (Figure 1). The sensing part was packaged and stored separately for being discarded after used. While the 2 m wire connecting the transducer and the sensor array can be reused. The two sensor parts tightly bound avoiding the entering of fluids inside the connections. Potentiometric electrochemical detection method was chosen for being easily miniaturizable and for having low cost fabrication.

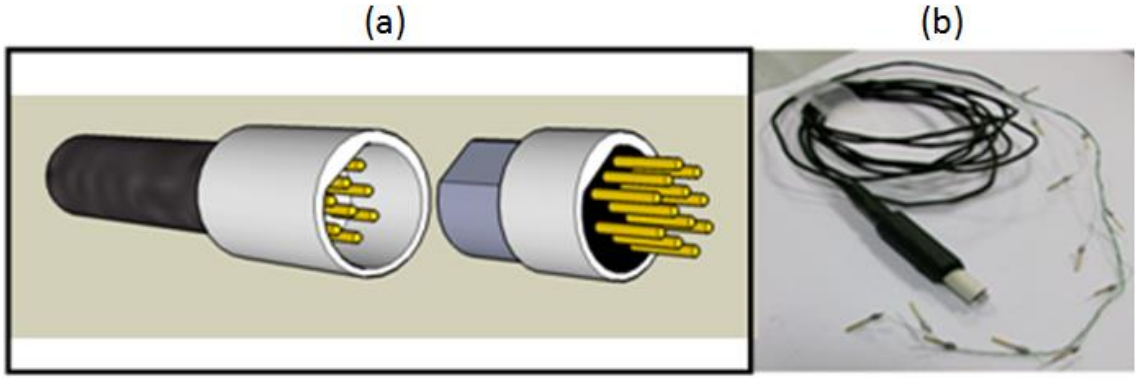

Figure 1. Scheme of the designed array sensor (a). Picture of the fabricated sensor array (b)

4.2.2. Distribution of the sensors on the array

For the prototype developed, some repetitions of each sensor were required for the optimization and for testing the reproducibility of the in vivo detection. For this reason, 2 potassium and 4 pH sensors with its respective RE were integrated. Due to the distribution and the limitation of array size, just one 4 electrodes in a row for the bioimpedance sensors was available in the array (figure 2). Distribution of the sensors on the array can drastically influence the sensors feasibility and sensitivity, mainly due to the electric field created by impedance sensors, which can affect in the differential voltage measured between the RE and the ISE sensors.

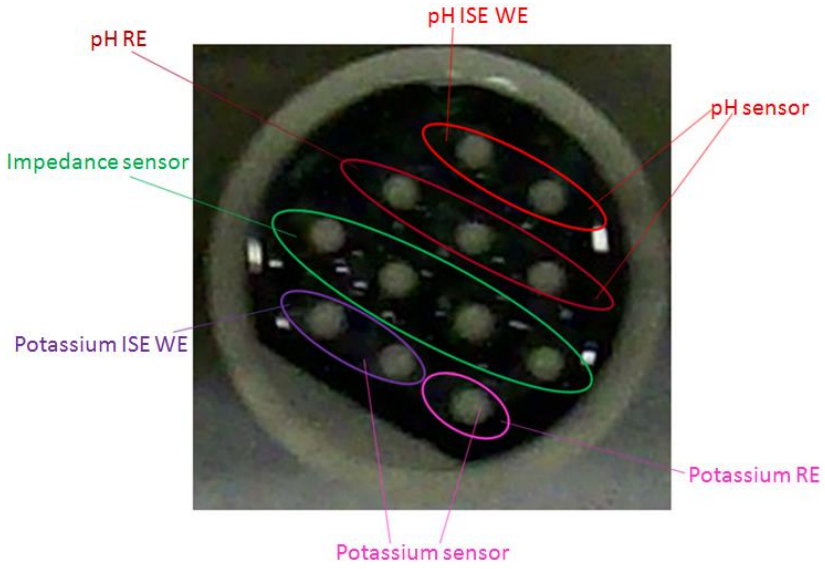

Figure 2. Distribution of the WE ISE sensors, RE and bioimpedance sensor in the array.

For testing the electric field effect on sensor behavior, it was measured the difference on the potentiometry measurement between two type of ISE electrodes distribution respect to the bioimpedance electrodes. For this purpose, two sets of experiments were designed. In one set of experiment, the pH sensors WE (Figure 2, red circle) and the RE (Figure 2, Dark red circle) were close to each other, while in the second set of experiment, the pH sensors RE was in the other side of the array (Figure 2, pink circle) and crossed the bioimpedance sensors. In both experiments, potentiometry measurements between the WE and the RE were performed with and without impedance measurements.

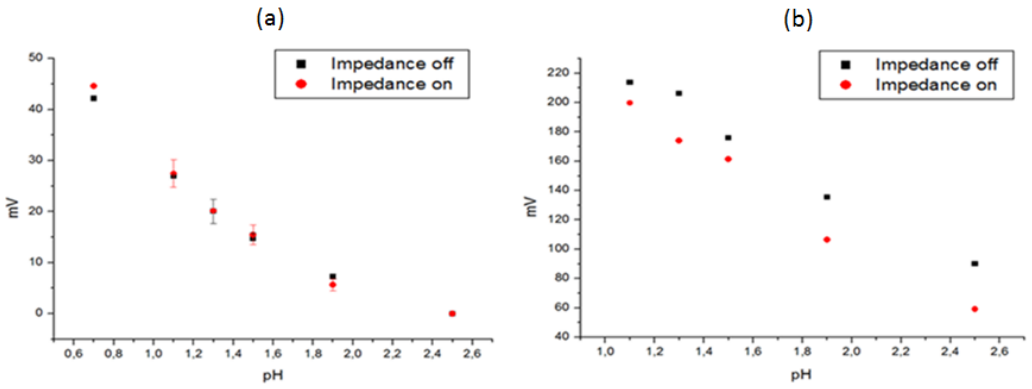

Figure 3. Interference of impedance sensor on all-solid-state pH sensor, when WE and RE of the sensor are on the same side (a) and opposite side (b)

The results proved that electric field generated from the impedance sensor was affecting potentiometry measurement, but just in the case that connected WE and RE electrodes had bioimpedance sensor in between (figure 3b). When the all solid-state ISE sensor connects its WE and RE closer without having the bioimpedance sensor in between, they were not affected by the generated electric field (figure 3a).

Thus, the distribution shown in figure 2 prevents any impedance electric field effect on potentiometry measurement.

4.2.3. Tissue-array contact test

The final application of the developed array is the in vivo detection inside the stomach by means endoscopic tools. The movement of the array inside the stomach will be performed with the rotational arm of the gastroendoscope and all the movements will be monitored thanks to a camera connected on the top of it. However, the 2D vision of the camera does not allow having a deep vision, thus we cannot have the real perspective of the tissue contact with the sensors. In order to overcome this problem, potentiometric sensors were used for this purpose. Based on the fact that the measured voltage is completely different if the electrodes are in contact with air or with the tissue, we developed some test to check the viability of potentiometric sensor usage for assuring the contact of the array with the tissue. For mimicking the situation inside the gastric juice of the stomach, a piece of chicken breast was wetted with HCl solution at pH 1,9 to have a real perspective of the contact of the tissue and the sensors. The impedance of the sensor array was tested in total contact and non-contact with this tissue.

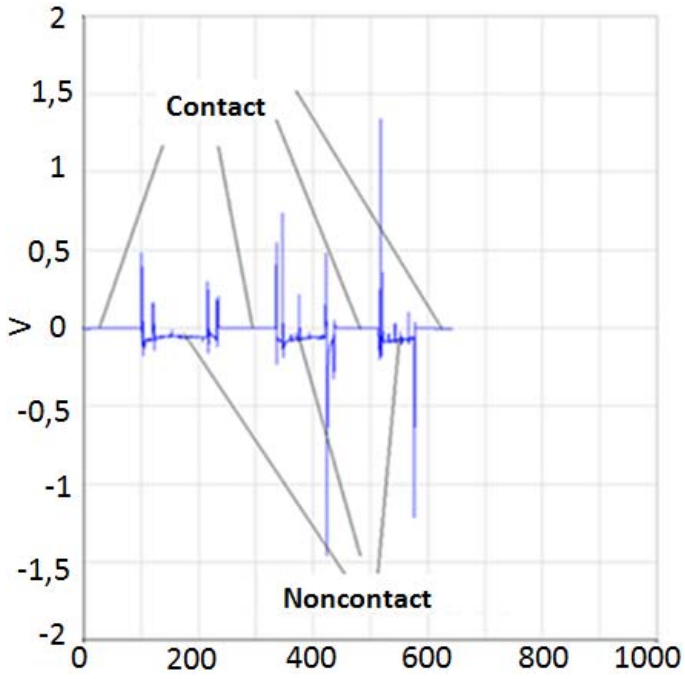

Figure 4. Potentiometric results of contact and non-contact of the array with the tissue.

A clear difference is observed with the array connected to the tissue and in contact with air (figure 4). When the array was not in contact a negative noise voltage is observed, while when it was in contact a stable zero voltage was recorded.

4.2.4. Stable contact between sensor and tissue

4.2.4.1. Effect of pressure on impedance sensor performance

Based on the experiments performed in the previous section, we realized that the voltage and the impedance response from the sensors in the array were affected by the contact on the tissue but also by the pressure that was done with the array to the tissue.

For testing the effect of pressure on the sensor performance, a platform was needed to sense pressure and impedance simultaneously. Thus, the sensor array was fixed to a pressure sensor and a controlled pressure is applied on the tissue with a strain gauge based pressure sensor (figure 5). At the same time, the impedance response in the array was monitored, being correlated the pressure applied on the sensor with the impedance response.

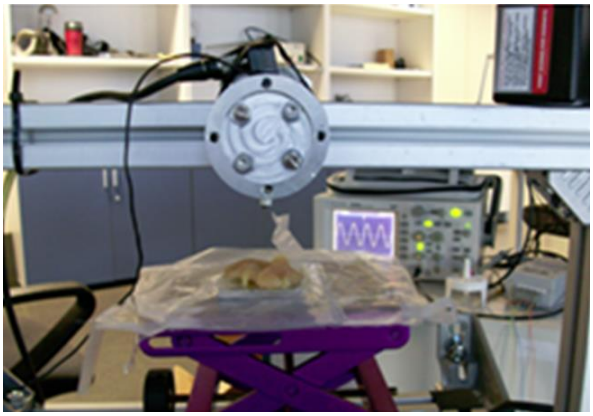

Figure 5. Pressure sensor to control the squeeze of the tissue with the sensor

The results obtained with the strain gauge pressure sensor are shown in figure 6. At low pressures, impedance signal starts to increase until a pressure of 78 kPa, where the impedance signal keeps stable. However, after 1220 kPa the impedance signal starts to get affected again by pressure, increasing exponentially.

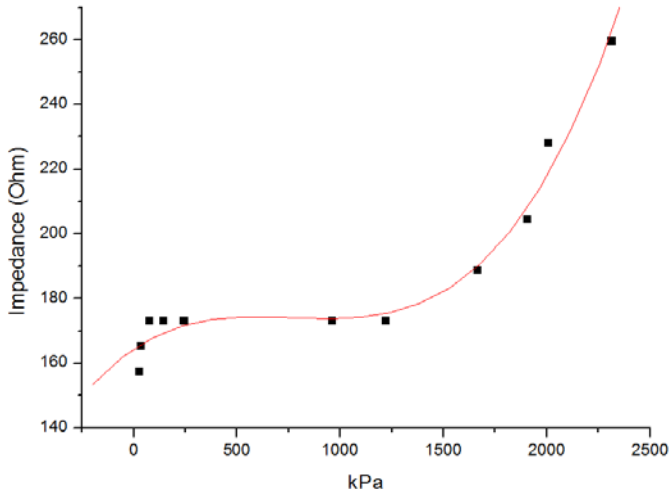

Figure 6. The effect of pressure on impedance signal for strained chicken breast

Thus, the working range of the impedance sensor is between 78 KPa to 1220 kPa, which is a useful range for the designed application, since pressure lower than 78 kPa were not strong enough to keep stable the sensors and at high pressures the electrodes could damage the tissue.

These results also open the window to other applications of this impedance sensor. For a certain ranges of pressure, this low cost and miniaturized electrochemical sensors could be a very useful and sensitive pressure sensor.

4.2.4.2. Tissue untouched stable contact with the sensor

In order to assure a reliable response of the sensors and stable pressure between 78 to 1220 kPa need to be guaranteed. This pressure contact needs to be applied without any manual contact with the sensor, since it will be introduced with the endoscope inside the stomach with the gastroendoscope. For providing a stable contact between the sensor array and the organ tissue during in-vivo experiments, the array was supported by means of magnetic field. For this purpose ring magnets were coupled around the sensors and an external magnet was used to create the magnetic field that maintained the array in a stable contact (figure 7).

Figure 7. Picture of the fabricated array with the magnet rings around (a). Scheme of the endoscopic insertion and stabilization of the array inside the stomach (b).

The attachment of the array with the tissue by means of the magnets was first tested in vitro with chicken breast and with an ablated pig stomach (Figure 8).

Figure 8 Magnetic field tests for a stable contact of the sensor on the tissue with chicken breast (a) and ablated stomach (b)

An easy insertion of the array was observed and strong attachment between the stomach wall and sensor array was achieved. The pressure exercised with the adapted ring magnets around the sensors and with the external magnet through the tissue was measured.

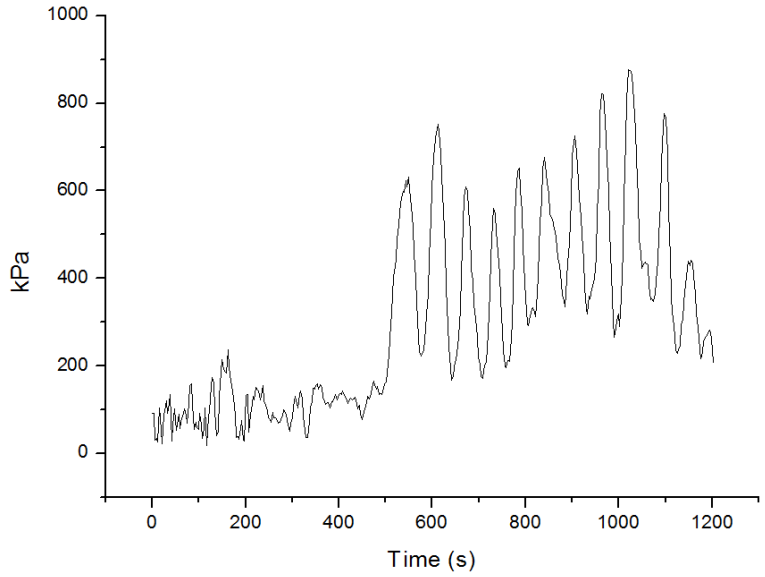

Figure 9. Pressure sensor responses under magnetic field generated with an external magnet and the ring magnets around the sensor by changing distance between both magnets.

According to figure 9, the applied pressure changes between 431 and 872 kPa. Each pressure peak corresponds to the manual approaching and getting away of the external magnet to the tissue in contact with the sensor array, being always inside the pressure working range where the impedance response is stable.

4.3. In vivo detection of ischemia

4.3.1. Preparations of animals for the surgery

The sensor prototypes were tested in vivo with animal model in domestic pigs (female, 80 and 125 kg). Animal experiments were carried out in accordance with German animal protection laws and within a government approved animal research program.

The procedures were conducted under general anesthesia in supine position of the animal. The experiments were performed in the Steinbeis University, thanks to the help of IHCI Institute and Novineon Company.

4.3.2. Detection of induced ischemia on the small intestine

Ischemia was sensed on small intestine tissue by opening the abdominal part of the pig body and getting the sensor array in contact with the small intestine tissue. Once, the constant contact of the sensor with the small intestine tissue and a stable and reliable signal from the sensors, discarding mechanical motion due to the pig respiration, were achieved, the perfusion of the respective area of the small intestine was interrupted by mesenteric artery crossclamping with tourniquets and scissors. For tissue reperfusion, the crossclamping was removed and the tourniquets opened (Figure 10).

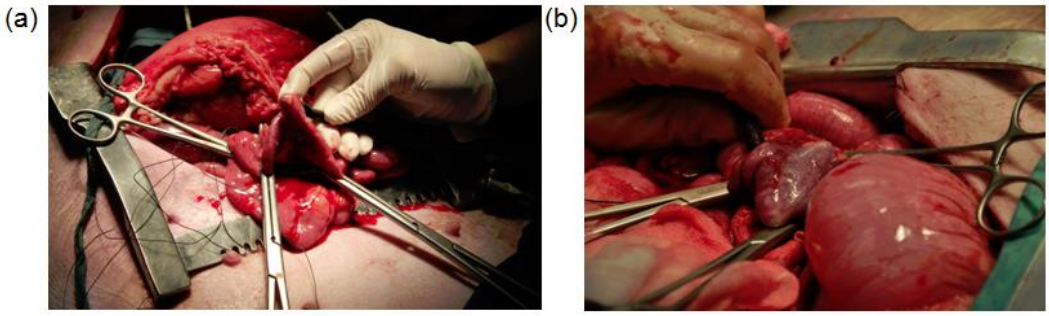

Figure 10. Crossclamping system for production of ischemia in the small intestine.

As was previously introduced, continuous and stable pressure should be applied with the array on the tissue to achieve stable impedance signal. This can be achieved easily in this in vivo detection, since the sensor had an external access and the surgery assistant or mechanical holders can hold in stable pressure the sensor on the area of interest (Figure 11).

Figure 11. Surgery assistant holding the array on the small intestine tissue.

Small intestine detection was performed with 3 different pigs and with a total of 5 pH and 4 potassium sensors. For each experiment, the initial equilibrium values were recorded for 100 s and then the arteries were clamped for blocking the blood flow and induce ischemic conditions for 200 s. Afterwards, the arteries were released for perfusing the tissue for 300 s (Figure 12).

A clear change on the signal after blocking the blood flow on the tissue was observed in both sensors, as well as a fast time response. The speed to achieve an ischemic equilibrium from the starting point of ischemia for pH sensor is faster; -0,00135 pH/s than potassium sensor; 0,034 mM/s.

Baseline pH sensed with our all-solid-state pH sensors was between 7,52 and 7,54, while the detected equilibrium potassium concentrations were between 1,79 and 2,38 mM. These values are agreeing with the literature results, being the values for potassium and pH for a normal small intestine respectively; 1,5 mM and 7,3 pH (Gonullu *et al.,* 2007).

After 200 s of ischemia, there were a saturation of the potassium and pH sensors to an nearly equilibrium point of 8,6 mM of potassium and 7,23 of pH. Thus, the potassium concentration and pH changes after ischemia were respectively; 6,5 mM and -0,3 pH. These pH and potassium changes are comparable to the ones reported on the literature, where Gonullu *et al* showed an increase of potassium concentration of 4,11 mM on small intestine. Previous reported in vivo detections of pH for ischemia on small intestine also coincided with our results obtaining a pH decrease of 0,29 (Gonullu *et al.,* 2007).

Once, we observed a stable ischemic response, the blood was left to flow again to the tissue. Both sensors require longer time for reaching an equilibrium point for reperfusion (300 s) than for ischemia (200s), being the pH sensor faster than potassium. The reason can be found in the fact that ischemia damage the tissue, so that it takes longer time to recover the initial stage.

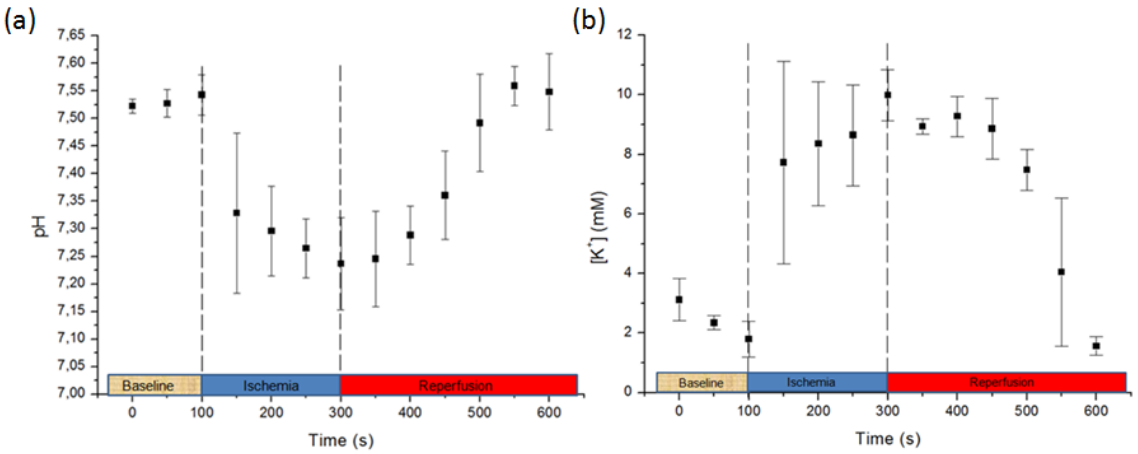

Figure 12. pH (a) and potassium (b) response of the developed array for ischemic and perfused intestine tissue

Also, impedance and phase results proved that ischemia and reperfusion can be sensed with our integrated array (figure 13). After 200 s of ischemia, there were a saturation of impedance module to an nearly equilibrium point of 1,3. Thus, the impedance module change after ischemia was 0.3. This impedance module change is comparable to the ones reported on the literature, where Ivorra *et al* showed an increase of impedance module of 0,15 on kidney.

Also, the results show that after reperfusion, the phase results are not returning to their respective baselines, while impedance, potassium and pH sensors were returning back to its initial signal. This irreversible process was observed by Ivorra et al., who interpreted as tissue damage, and explained these differences due to the different information collected by phase (intracellular changes) and ISE sensors (extracellular evolution) (Ivorra et al., 2003) (figure 12).

We should highlight that high standard deviations of impedance and phase results were observed, which decreases the reliability of this sensor compared to ISE sensors, which bring an excellent reproducibility. However, impedance sensors showed good reproducibility under in vitro conditions. Thus, it may be the fact that impedance is getting the intracellular information, makes these sensors more sensitive to the difference of the experimental conditions; clamping strength and differences of the pigs' nature.

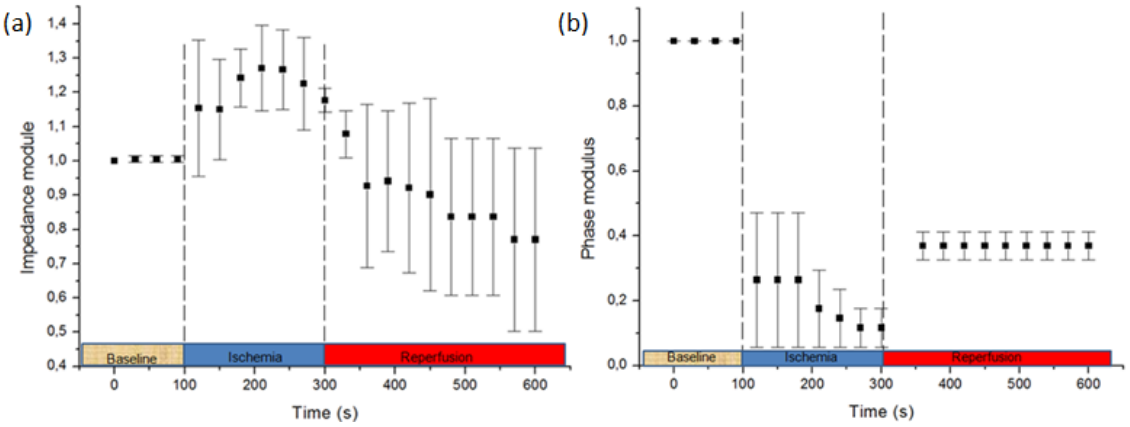

Figure 13. Impedance and phase results of the developed array for ischemic and perfused intestine tissue

4.3.3. Detection of induced ischemia on the stomach internal tissue

For the detection of ischemia inside the stomach was used a scarless access by means of endoscopic intra-gastric access. Also direct surgical access to the gastric tissue was performed for allowing the access to the surgery for ligate the gastric blood and release it for perfusion of stomach tissue.

Intra-gastric access was achieved by means of flexible endoscopy, with the sensor pre-mounted in a standard gastroscope before its introduction into the pig. The cables array with 2 mm diameter were inserted through the 2,5 mm working channel of the scope and the sensor device itself was fixed to the tip of the scope in a way providing sufficient endoscopic visualization. Helped by the camera and light contained in the endoscope the sensor, in a scarless way, was inserted from the mouth of the pig through the esophagus until the stomach. The position of the sensor array in the esophagus and stomach was controlled by the surgeon with the help of light, camera and position controller of the endoscope (figure 14).

Figure 14. Insertion of the gastroencospe with the array inside the pig mouth (a). Inserted array inside the stomach, shown through the abdominal cut of the pig (b)

The ischemia sensor was brought into direct contact with the tissue for baseline measurements. Sensor array was surrounded by ring magnets, which were strongly attached by the magnetic field generated from an external magnet. Figure 15 shows the external magnet handle by the surgeon assistant for attracting and stabilizing the position of the array on the tissue. For demonstration, the abdominal part of the pig was cut (Figure 14).

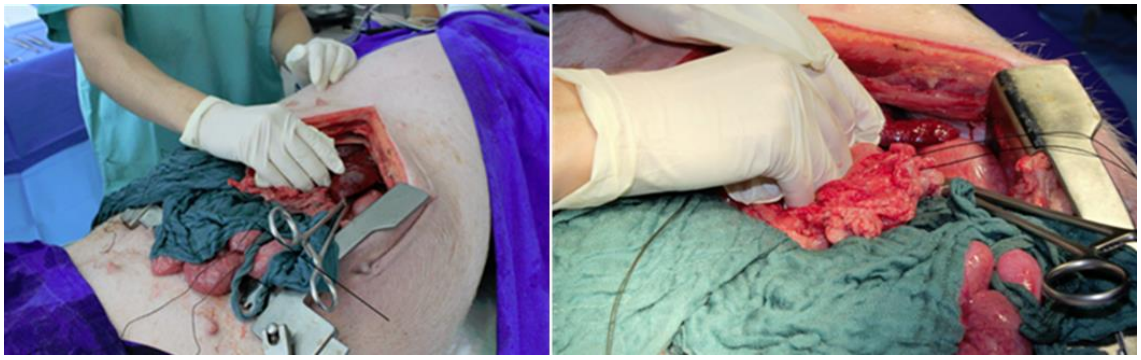

Figure 15. Sensor array inside the stomach of the pig was sandwiched between the outer and inner magnets

Once in the stomach, the constant contact of the sensor with the stomach tissue, by means of the sandwich magnets, brought a stable and reliable signal from the sensors, discarding mechanical motion due to the pig respiration.

The perfusion of the respective area of the stomach was interrupted by ligating or crossclamping vessels the organ wall. The stomach arteries were ligated and a tourniquet was placed for occluding and re-opening the vessels. The left and right gastric arteries were dissected a few centimeters away from the lesser curvature of the stomach. The left and right gastroepiploic arteries were ligated as proximally as possible from the sensor position and the perfusion from the spleen was crossclamped. In order to achieve maximal restriction of the perfusion taking into account that the stomach was fed by many arteries, the antrum of the stomach was also crossclamped to avoid perfusion from gastroduaodenal artery branches. For re-perfusion, the crossclamping was removed and the tourniquets were opened.

The experimental protocol relied on a gastric ischemia produced by total occlusion of the arteries of the stomach in two anesthetized pigs assigned to two different ischemia-reperfusion samples. Two measurement modalities (sample 1 and 2) were studied. In sample 1, the perfusion was clamped far from the probe placement area, so that the evolution of the ischemic state inside the tissue was slow. In sample 2, the tissue was clamped near to the detection area, so that the hypoxic damage to the tissue was more severe and the tissue taking longer time to recover after re-perfusion. For each experiment, two potassium and two pH sensors on an array was used to measure the

reproducibility of the measurement. The initial equilibrium values were recorded for 200 s and then the arteries were clamped for blocking the blood flow and induce ischemic conditions for 450 s. Afterwards, the arteries were released for perfusing the tissue during 200 s (figure 16).

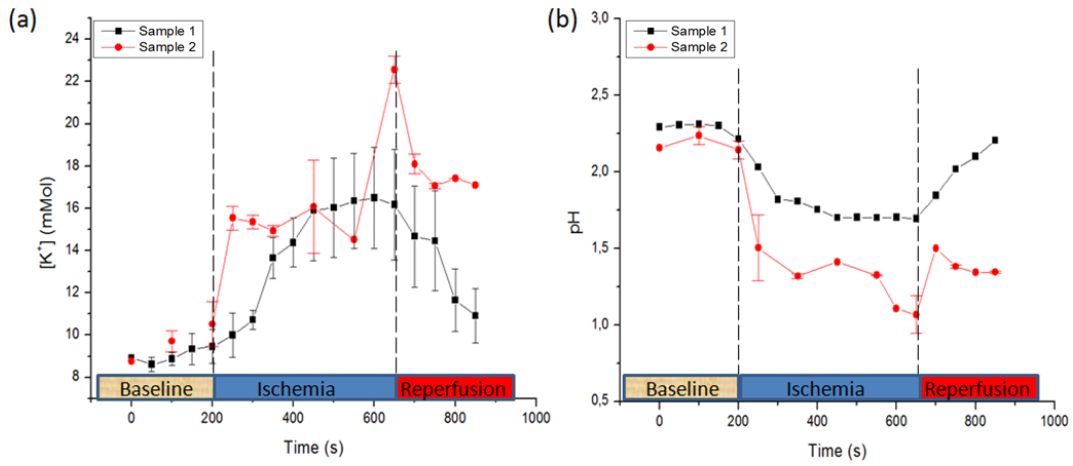

Figure 16. Potassium concentrations (a) and pH (b) under ischemia and reperfusion conditions on the stomach tissue of two pigs.

Potassium and pH sensors show a clear change on the signal after blocking the blood flow on the tissue. Both sensors require low time for responding, being the pH sensor faster than potassium, as was already observed in the ischemia intestine detection. The speed to achieve an ischemic equilibrium from the starting point of ischemia for pH sensor was -0,00195 pH/s and for potassium sensor was 0,03261 mM/s.

Baseline pH sensed with our all-solid-state pH sensors was between 2,15 and 2,3, while the detected equilibrium potassium concentrations was between 8,76 and 8,92 mM. These values are agreeing with the literature results, being the values for a normal stomach of around 10 mM and 2 of pH (Ivorra et al., 2003; Cosofret et al., 1995; Marzouk et al., 2002).

After 200 s of ischemia, sample 1 shown a saturation of the potassium and pH sensors to nearly equilibrium point of 18 mM of potassium and 1,7 of pH. Thus, the potassium concentration and pH changes after ischemia were 9,2 mM and 0,5 pH respectively. These pH and potassium changes were comparable to the ones reported on the literature, where Cosofret et al shows an increase of potassium concentration of 7,9 mM on ischemic heart obtaining similar results Ivorra et al on kidney. In vivo detections of pH for ischemia on kidney and on heart also coincided with our results obtaining a pH decrease of 0,7 on heart and 0,6 on kidney (Ivorra et al., 2003; Cosofret et al., 1995; Marzouk et al., 2002).

Once, we observed a stable ischemic response, the blood was left to flow again to the tissue. When the tissue is reperfused, we observed a different behavior for sample 1 and sample 2. Sample 1 was coming back to the baseline value in both sensors; while in sample 2, potassium concentration and pH did not return to their respective initial signal. The reason behind these results was the way of producing ischemia. In sample 2, the ischemia was produced closer to the sensing area and while in both samples, the clamped area was damaged, sample 2 was sensed closer to the damaged tissue and did not permit the perfusion on the sensing area, being observed in our results. These results show that not only ischemic and reperfusion states were detected with our integrated sensor, also tissue damage can be analyzed.

In addition, reperfusion speed from ischemic equilibrium to baseline for pH sensor was 0,00255 pH/s and for potassium sensor 0,03435 mM/s, being faster the recovery of the pH signal.

Ischemia and reperfusion steps were repeated one more time to see, if ischemia and reperfusion stages can be sensed continuously. As shows figure 17, the pH sensor under the second ischemia state was able to recover the same values observed after the first clamp of the blood flow, being possible to use the sensor for subsequent detections. On the other hand, potassium sensor did not show the same behavior being not appreciable the same signal change after the second clamping. The reason can be found in the fact that pH was related directly with the tissue blood flow as explained in the introduction part. However, potassium concentration is related to the ion channels of the cells and the reaction of the ions pumping, which was not so directly detectable as the blood flow.

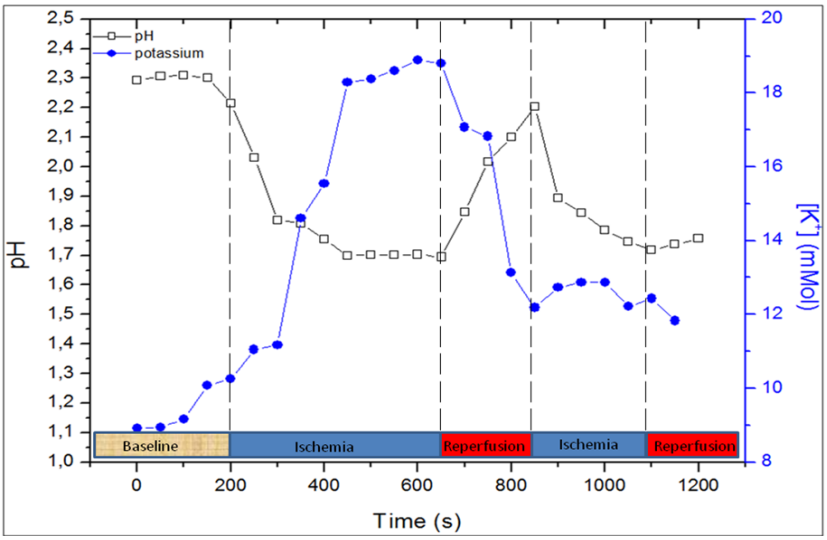

Figure 17. In vivo detection of potassium and pH of the second ischemia and reperfusion steps in the stomach tissue

References

A. Ivorra, R. Gómez, N. Noguera, R. Villa, A. Sola, L. Palacios, G. Hotter, J. Aguiló Biosensors and Bioelectronics., (2003), 391

A. Kisiel, H. Marcisz, A. Michalska, K. Maksymiuk Analyst, 130 (2005), 1655

A. Sayed, M. Marzouk, R. P. Buck, L. A. Dunlap, T. A. Johnson, W. E. Cascio Analytical Biochemistry., 308 (2002), 52

A. Simonis, H. Lüth, J. Wang, M.J. Schöning Sensors and Actuators B, 103 (2004), 429

Ammann, E. Pretsch, W. Simon, Analytical Chemistry., 58 (1986), 2285

A.W. Hassel, K. Fushimi, M. Seo Electrochemistry Communications, 1 (1999), 180

A.W.J. Cranny, J.K. Atkinson Measurement Science and Technology, 9 (1998), 1557

C. A. Gonzalez, C. Villanueva, S. Othman, R. Narvaez, E. Sacristan Physiol. Meas., 24 (2003), 277–289

C. D. Mathers, E. T. Vos, C. E. Stevenson, S. J. Begg Bulletin of the World Health Organization, 11 (2001), 79

D. A. Benaron, I. H. Parachikov, S. Friedland, R. Soetikno, J. Brock-Utne, P. J. A. van der Starre, C. Nezhat, M. K. Terris, P. G. Maxim, J. J. L. Carson, M. K. Razavi, H. B. Gladstone, E. F. Fincher, C. P. Hsu, F. L. Clark, W. Cheong, J. L. Duckworth, D. K. Stevenson Anesthesiology., 100 (2004) 1469

D. Ammann, P. Anker, E. Metzger, U. Oesch, W. Simon, 1985. Ion Measurements in Physiology and Medicine, in: Kessler, M., Harrison, D.K., Höper, J. (Eds.), Springer-Verlag., Berlin, 102

D. C. Steinemann, M. Schiesser, P. Clavien, A. Nocito BMC Surgery., 11 (2011), 33

D. Déjardin , F. Sabench Pereferrer, M. Hernàndez Gonzàlez, S. Blanco, A. Cabrera Vilanova Surgery., 153 (2013), 431

D. Gonullu, Y. Yankol, F. Isiman, A.A. Igdem, O. Yucal, F.N. Koksoy Turkish Journal of Trauma and Emergency Surgery, 13 (2007), 261

D.J. Harrison, L.L. Cunningham, X. Li, A. Teclemariam, D. Permann Journal of the Electrochemical Society, 135 (1988), 2473

F.X. Rius-Ruiz, D. Bejarano-Nosas, P. Blondeau, J. Riu, F.X. Rius Analytical Chemistry, 83 (2011), 5783

G. Blackburn, J. Janata Journal of the Eletrochemical Society, 129 (1982), 2580

G. Kicska, M. S. Levine, S. E. Raper, N. N. Williams AJR., 189 (2007), 1469

H.J. Lee, U.S. Hong, D.K. Lee, J.H. Shin, H. Nam, G.S. Cha Analytical Chemistry, 70 (1998), 3377

H. Jafarzadeh, P. A. Rosenberg JOE., 35 (2009), 3

H. Suzuki, H. Shiroishi, S. Sasaki, I. Karube Analytical Chemistry, 71 (1999), 5069

I. B. Tahirbegi, M. Mir, J. Samitier, Biosensors and Bioelectronics., 40 (2013), 323

J. A. Tice, L. Karliner, J. Walsh, A. J. Petersen, M. D. Feldman, The American Journal of Medicine., 121 (2008), 885

J.A. Russell, Intensive Care Med., 23 (1997), 3

J. Songer, (2001). Thesis: Tissue Ischemia Monitoring Using Impedance Spectroscopy: Clinical Evaluation

M. Borum, D. Graham, The American Journal of Gostroenterology., 104 (2009), 225

M. Mir, I. B. Tahirbegi, J. J. Valle-Delgado, X. Fernàndez-Busquets, J. Samitier Nanomedicine., 8 (2012), 974

M. Piao, J. Yoon, G. Jeon, Y. Shim Sensors, 3 (2003), 192

N. Abramova, A. Bratov Sensors, 9 (2009), 7097

N. Kwon, K. Lee, M. Won, Y. Shim, Analyst, 132 (2007), 906

P. A. Stewart,(2003) How to understand acid-base A quantitative acid-base primer for biology and medicine Brown University, Rhode Island 1981 Elsevier North Holland publication

P.C. Hauser, D.W.L. Chiang, G.A. Wright, Analytica Chimica Acta., 302 (1995), 241

R.S. Chung, D.C. Hitch, D.N. Armstrong, Surgery., 104 (1988), 824

S. A. Seidel, L. A. Bradshaw, J. K. Ladipo, J. P. Wikswo, W. O. Richards, Journal of vascular surgery., 30 (1999), 309

S. Friedland, R. Soetikno, D. Benaron, Gastrointest Endoscopy Clin., 14 (2004), 539

S. J. Watson, R.H. Smallwood, B. H. Brown, P. Cherian, K.D. Bardhan, Physiological Measurement., 17 (1996), 21

S. M. Hameed, S.M. Cohn, Chest., 123 (2003), 475

T. Blaz, J. Migdalski, A. Lewenstam Analyst, 130 (2005), 637

T Marchbank, R Boulton, H Hansen, R J Playford, Gut., 51 (2002), 787

U. Oesch, Z. Brzozka, X. Aiping, B. Rusterholz, G. Suter, P. Viet, D. Welti, D.

V. Cosofret, M. Erdosy, T.A. Johnson, R.P. Buck Analytical Chemistry, 67 (1995), 1647

Chapter 5

Array commercialization

5.1. Developed device cost

5.1.1. Sensor array fabrication

For the commercialization of a product, is compulsory to know the companies commercializing similar product and the cost of its in order to know if we can compete with the market available products. The first step is to know what the approximate cost of our equipment is. The cost will be calculated take into account that it is a prototype with higher cost that the final equipment produced on an assembly line, where the cost will decrease with scale buying.

The cost of the sensor array was calculated in the bases of the prices of providers (Table1) and considering the amount of each reagent used and the volume used for each sensor.

Electrodes preparation	Cost (Euro)
Silver conductive paste (Dupont) 1kg	200
Carbon conductive paste (Dupont) 500 g	50
Epotek 301-2 226 g	367
ISE membrane	
Hydrogen ionophore IV 50 mg	128
KTClPB 5g	316,5

Poly (vinyl chloride) (PVC) 50g	125,5
Nitrophenyl octyl ether 100ml	440
THF (Tetrahydrafurane) 2,5l	154,86
Valinomycin 100 mg	448,5
BBPA 25ml	224,5
RE membrane	
Nafion 500 ml	819

Table 1. Prices of compounds used to fabricate the sensor array

For the calculation of array fabrication costs, we considered the price of the mounted beryllium copper alloy pins, the amount of epoxy used for each array insulation and the covering of the polished pin surface with carbon and Ag/AgCl ink. Considering all, the cost for the electrodes preparation per array is 17,5 €. After this fabrication the electrodes of the array are ready as well as the bioimpedance sensor.

Once the electrodes where covered with the Ag/AgCl ink, for the fabrication of the sensor is just need it the covering of the RE with Nafion, this has a cost per array of 0,003 €.

The cost for pH and potassium membranes were calculated considering the volumes of each reagent used in the mixture of the membrane (see chapter 2, material and methods for details) and the volume required of this mixture for each array, taking into account that there are 3 pH and 2 potassium sensors in the array. Considering these calculations, the cost of the ISE membranes per array is 0,018 €.

Thus, total cost for this integrated array is 17,521 €.

5.1.2. Transductor fabrication

Initially, potentiometric measurements were performed with a commercial portable potentiostat from PalmSense. This device is a multipotentiostat with 5 WE channels, it does not allows a simultaneous measurements of the 5 channels, but a sequential measurement every 10 s. So, each channel has a delay of 40 s between measurements.

A custom made impedance system developed by SIC-BIO at University of Barcelona was used for the impedance measurements as explained in chapter 3. With the first

developed impedance device, it was required and external current generator and an analogical oscilloscope to monitor the signal response. These systems did not permit computing recording of the results (Figure 1a).

In order to have a more convenient device integrating potentiometry and impedance measurements and a continuous recording of the results, a new custom made system was developed by SIC-BIO. This portable equipment permits an autonomous use of the array for any kind of applications (Figure 1b).

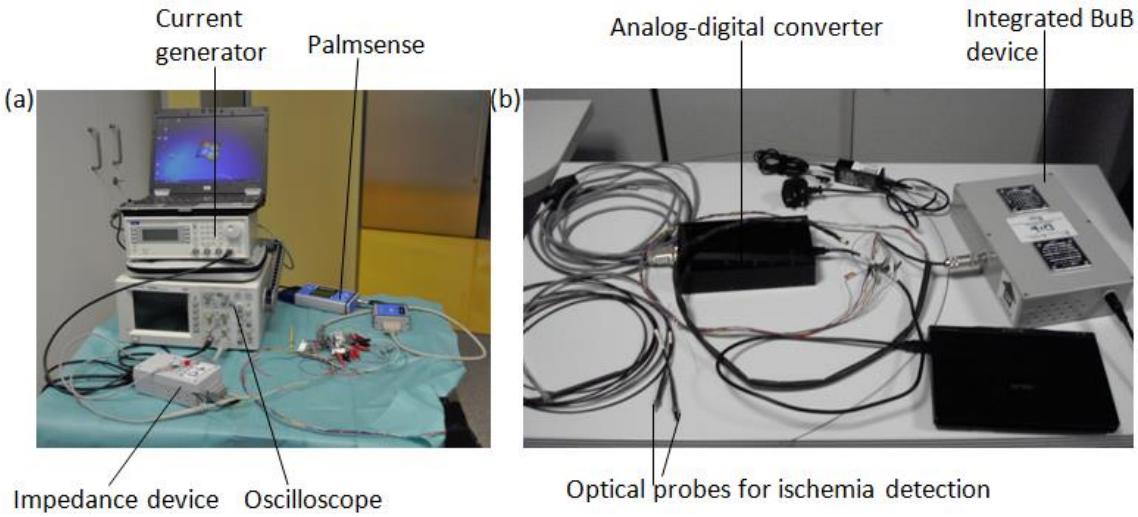

Figure 1. Initial impedance and potentiometry devices (a). Potentiometry and impedance integrated device developed by SICBIO (b)

The estimation of the total cost of manufacture for each of the components is;

- **Sensor array:** 17 € per unit (disposable)
- **Connector:** 16,5 € per unit (reusable)
- **Potentiostate:** 7830 € per unit (reusable)

Being the total cost of the electrochemical sensor device; 7863,5 €. As we already commented, this cost is calculated for a prototype, since the cost for an industry assembled device will be much lower. However, this cost calculation is not considered as the manufacturing cost.

5.1.3. Integration of the developed analytical system with ARAKNES robot

The goal of the ARAKNES project was to integrate the technologies of laparoscopic surgery to the endoluminal surgical approach for achieving minimally invasive surgical procedures by reducing the operative trauma. The robotic arms are inserted by means gastroendoscope or single port umbilical access to the stomach. The surgeon teleoperates the surgery by controlling the robot arms remotely by the incorporation of joysticks remote controllers and 3D vision, by means of advanced micro-nano technologies and information, communication technology (ICT) (Figure 2).

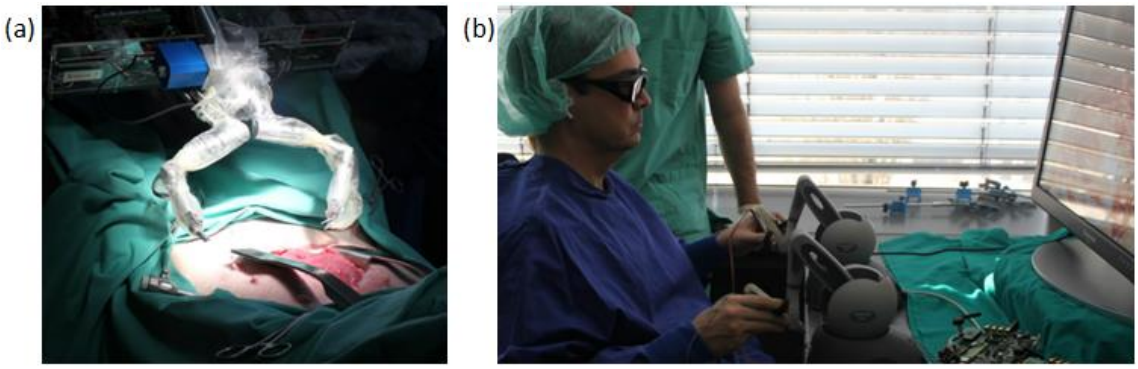

Figure 2. Remote control of the surgeon operating from the ARAKNES console

With help of robotic arms, our sensor array was brought to any specific place on the tissue to make measurements in the desired surgery area (Figure 3).

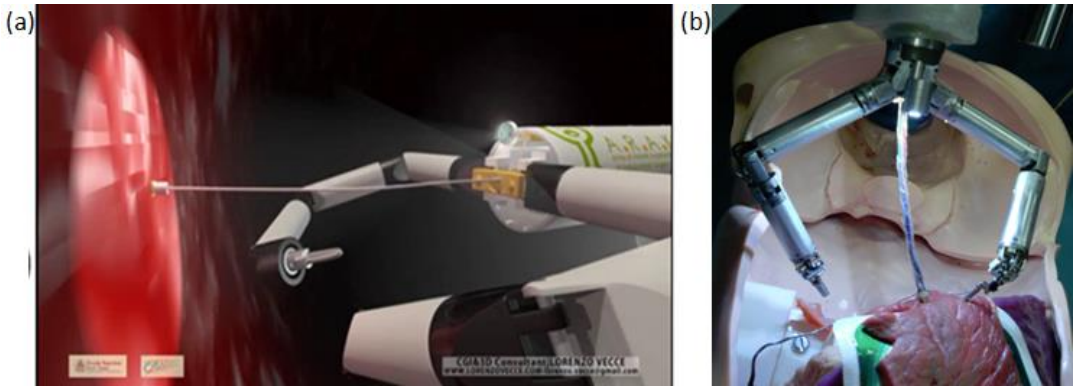

Figure 3. Robotic arms place the sensor array to the desired measuring area

The readout electrochemical array was integrated in the surgeon control consol. The interface of this equipment with the console was performed through an analog-digital

converter developed by University of St. Andrews (USTAN). Thus, optical and electrochemical sensors developed under the ARAKNES project were integrated and a final compact device was developed to sense ischemia optically and electrochemically (Figure 1 b)

5.2. Market research

There are few commercial products to sense ischemia, they are mostly from US. The products were in general sold with the name of tissue oxymeter and the detection method is based on optical readouts. There is also one company, which sense ischemia magnetically in the body (Table 2).

		FEATURES				
		Detection method	Dimensions of sensor	Detection area	**Price**	**Brand**
On the market (main competitor)	Spectros	Optical	1,5mm(Diameter)	All the body	Console: $35,000 Disposable sensor: $499	T-STAT VLS Tissue Oximeter
On the market	Tristan Technologies, Inc.	Magnetic	5cm (Diameter)	Intestine	No	GutSQUID
On the market	ViOptix	Optical	5*5mm	All the body	Console: $20,000 Disposable sensor: $500	T.Ox Tissue Oximeter
On the market	HyperMed	Optical	No	Just outside skin	No	OxyVu

Table 2. Competitor analysis of commercial ischemia sensors

From these companies, the device of hypermed can just be used to sense ischemia on skin, by means of spectral characteristics of the reflectance of light from the tissue. However, it is not applicable for endoscopic applications and it does not does not have property for multiple sensing.

Tristan Technologies Company measures ischemia on intestine by measuring the magnetic field according to the BER of the organ. It is not applicable for endoscopic

applications and does not have the property for multiple sensing. Tristan equipment is not portable and has detection constrains during surgery because of its big size. This equipment is based on SQUID, making very expensive each measurement, which requires to be cooled down each time before usage (Seidel *et al.,* 1999).

The companies of Vioptic and Spectros are sensing ischemia optically, by means of spectral characteristics of the reflectance of light, detecting the oxygen content of the tissue (Friedland et al., 2004; Jafarzadeh and Rosenberg, 2009; Benaron et al., 2004). The stronger company is Spectros with the product T-Stat, which have approved by Food and Drug administration (FDA) its equipment to sense ischemia. In clinical use, T-Stat can provide monitoring in real-time absolute, non-invasive, and continuous tissue analysis. Also, because of the 1,5 mm diameter of the sensor, it is useful for endoscopic applications. The main drawback of this equipment is the high cost; 35000 $ the equipment and 499 $ the sensor and it has not the property for multiple sensing.

The sensor developed in this project has similar testing abilities than T-Stat but permits multisensing, but the most important is that it cost 4 times less the equipment and 25 times less the sensors, which in fact is the part that could bring more benefits since it is disposable and need to be bought more often.

5.3. Risk analysis

A risk analysis of each device component was analyzed taking into account if the sensing device can harm the patient, depending on three criteria; severity (S), probability of occurrence (O) and probability of detection (D). Each criterion has its own 4 level of grading. Severity has the levels such as mistake can cause serious and/or life-threatening injury (4), mistake can cause injury, which needs medical care (3), mistake can cause injury, with no need of medical care (2) and mistake can cause discomfort or temporary pain (1). Each component of the sensor gets a point by level of grading multiplied by the three criteria called risk point (RP). If the points achieved are between 1 and 16, it can be concluded that the risk is minor; a low risk will be evaluated between 17 and 32, the risk is crucial between 33 and 48, and is a serious risk if the punctuation is between 49 and 64.

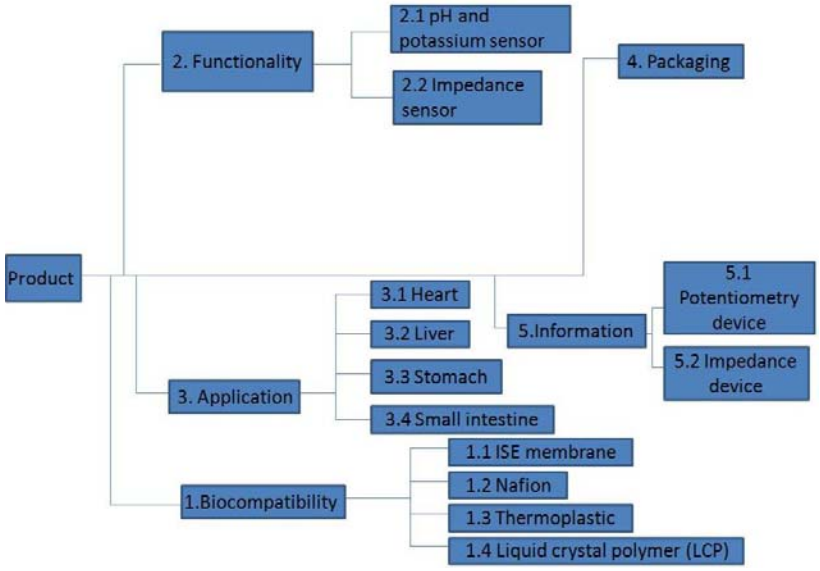

Figure 4. Risk analysis scheme of each component

Nr	Function	S	O	D	RP	Nr.	Function	S	O	D	RP
1	**Biocompatibility**					**2**	**Functionality**				
1.1		1	1	4	4	2.1		4	1	4	16
1.2		1	1	4	4	2.2		4	1	2	8
1.3		2	1	4	8						
1.4		1	1	4	4						
Nr.	Function	S	O	D	RP	Nr	Function	S	O	D	RP
3	**Application**					**4**	**Packaging**				
3.1		4	1	2	8	1.1		1	1	1	1
3.2		3	1	2	6	**5**	**Information**				
3.3		3	1	2	6	5.1		4	1	4	16
3.4		3	1	2	6	5.2		4	1	2	8

Table 3. Risk analysis of each component

All the components of the sensor array were evaluated according to the risk analysis criteria, which show that all the components have minor risk for the patient. For reducing the risk for the device application, all the parts of the sensor, which are in touch with the organ, was chosen biocompatible such as; PVC membrane and insulation resin. Also, very low current was applied to the tissues by impedance device, thus it cannot be harmful to the organs.

5.4. SWOT analysis

The SWOT analysis is a useful tool to identify the internal and external factors that are favorable and unfavorable to achieve the commercialization of the developed device. This analysis structure a planning method for evaluating the Strengths, Weaknesses, Opportunities and Threats. The SWOT analysis was conducted from the point of view of the customer (Table 4) and from the point of view of the producer of the developed sensor (Table 5).

	INTERNAL ANALYSIS/FACTORS	
EXTERNAL ANALYSIS/FACTORS	**Strengths**	**Weaknesses**
	– **Cheaper than competitors** – **Fast response** – **Accurate because of direct measurement on the tissue and multiple pH, potassium and impedance sensors on the same array** – **Integrated to an endoscope (Scarless surgery)** – **Easy to use**	– **In contact with the tissue**
	Threats	**Opportunities**
	– **New procedures for cleaning, sterilization, set-up, to be defined**	– **The use of new technologies brings publications chances.** – **New surgical procedures and diagnosis can arise** – **Collect new incomes (new patients coming to the hospital)** – **Hospital /surgeons participating to leading edge research projects** – **Improve healthcare delivery**

Table 4. Customer point of view (Surgeons/hospital/patient in the case of surgical devices)

	INTERNAL ANALYSIS/FACTORS	
EXTERNAL ANALYSIS/FACTORS	**Strengths**	**Weaknesses**
	– Cheaper than competitors – Easy for mass-production – Easy to use – More accurate than competitors – Multisensing abilities – Small size	– Polymer membrane is delicate – Short life time of potassium sensors – Clean and sterilize protocol needs to be developed – No knowledge in business, mass production and commercialisation
	Threats	**Opportunities**
	– Big competitors with long experience in this market	– Huge market – Few competitor with our advantages – Easy to apply to many other diagnosis, which could open many other fields of application

Table 5. Swot Analysis - Producing company point of view

5.5. Conclusions

We can concluded that our sensor array has important advantages over its competitors such as lower price; around 4 times less in the equipment and 25 times less in the disposable array comparing with the main competitor, easy mass production, multisensing abilities and small size, that makes this equipment portable and applicable to endoscopic systems. In the market, it can find possibilities as bioimpedance sensor and potentiometric all-solid-state ISE approaches for pH and potassium detection integrated in an array for monitoring ischemia, but also for a lot of other applications,

such as cancer monitoring directly on the tissue by free biopsy detection. The developed pH sensors permit low pH sensing from 0.7-2.5, which is the only example in the literature that allows so low pH detection, and thus, it makes this sensor a unique device for stomach sensing.

References

A. Ivorra, R. Gómez, N. Noguera, R. Villa, A. Sola, L. Palacios, G. Hotter, J. Aguiló Biosensors and Bioelectronics., (2003), 391

A. Sayed, M. Marzouk, R. P. Buck, L. A. Dunlap, T. A. Johnson, W. E. Cascio Analytical Biochemistry., 308 (2002), 52

A. Simonis, H. Lüth, J. Wang, M.J. Schöning Sensors and Actuators B, 103 (2004), 429

Ammann, E. Pretsch, W. Simon, Analytical Chemistry., 58 (1986), 2285

A.W. Hassel, K. Fushimi, M. Seo Electrochemistry Communications, 1 (1999), 180

A.W.J. Cranny, J.K. Atkinson Measurement Science and Technology, 9 (1998), 1557

A. Kisiel, H. Marcisz, A. Michalska, K. Maksymiuk Analyst, 130 (2005), 1655

C. D. Mathers, E. T. Vos, C. E. Stevenson, S. J. Begg Bulletin of the World Health Organization, 11 (2001), 79

C. A. Gonzalez, C. Villanueva, S. Othman, R. Narvaez, E. Sacristan Physiol. Meas., 24 (2003), 277–289

D. A. Benaron, I. H. Parachikov, S. Friedland, R. Soetikno, J. Brock-Utne, P. J. A. van der Starre, C. Nezhat, M. K. Terris, P. G. Maxim, J. J. L. Carson, M. K. Razavi, H. B. Gladstone, E. F. Fincher, C. P. Hsu, F. L. Clark, W. Cheong, J. L. Duckworth, D. K. Stevenson Anesthesiology., 100 (2004) 1469

D. Déjardin , F. Sabench Pereferrer, M. Hernàndez Gonzàlez, S. Blanco, A. Cabrera Vilanova Surgery., 153 (2013), 431

D. C. Steinemann, M. Schiesser, P. Clavien, A. Nocito BMC Surgery., 11 (2011), 33

D. Ammann, P. Anker, E. Metzger, U. Oesch, W. Simon, 1985. Ion Measurements in Physiology and Medicine, in: Kessler, M., Harrison, D.K., Höper, J. (Eds.), Springer-Verlag., Berlin, 102.

D.J. Harrison, L.L. Cunningham, X. Li, A. Teclemariam, D. Permann Journal of the Electrochemical Society, 135 (1988), 2473

D. Gonullu, Y. Yankol, F. Isiman, A.A. Igdem, O. Yucal, F.N. Koksoy Turkish Journal of Trauma and Emergency Surgery, 13 (2007), 261

D. A. Benaron, I. H. Parachikov, S. Friedland, R. Soetikno, J. Brock-Utne, P. J. A. van der Starre, C. Nezhat, M. K. Terris, P. G. Maxim, J. J. L. Carson, M. K. Razavi, H. B.

Gladstone, E. F. Fincher, C. P. Hsu, F. L. Clark, W. Cheong, J. L. Duckworth, D. K. Stevenson Anesthesiology., 100 (2004) 1469

F.X. Rius-Ruiz, D. Bejarano-Nosas, P. Blondeau, J. Riu, F.X. Rius Analytical Chemistry, 83 (2011), 5783

G. Kicska, M. S. Levine, S. E. Raper, N. N. Williams AJR., 189 (2007), 1469

G. Blackburn, J. Janata Journal of the Eletrochemical Society, 129 (1982), 2580

H. Suzuki, H. Shiroishi, S. Sasaki, I. Karube Analytical Chemistry, 71 (1999), 5069

H.J. Lee, U.S. Hong, D.K. Lee, J.H. Shin, H. Nam, G.S. Cha Analytical Chemistry, 70 (1998), 3377

H. Jafarzadeh, P. A. Rosenberg JOE., 35 (2009), 3

I. B. Tahirbegi, M. Mir, J. Samitier, Biosensors and Bioelectronics., 40 (2013), 323

J. A. Tice, L. Karliner, J. Walsh, A. J. Petersen, M. D. Feldman, The American Journal of Medicine., 121 (2008), 885

J.A. Russell, Intensive Care Med., 23 (1997), 3

M. Mir, I. B. Tahirbegi, J. J. Valle-Delgado, X. Fernàndez-Busquets, J. Samitier Nanomedicine., 8 (2012), 974

M. Borum, D. Graham, The American Journal of Gostroenterology., 104 (2009), 225

M. Piao, J. Yoon, G. Jeon, Y. Shim Sensors, 3 (2003), 192

N. Kwon, K. Lee, M. Won, Y. Shim, Analyst, 132 (2007), 906

N. Abramova, A. Bratov Sensors, 9 (2009), 7097

P. A. Stewart,(2003) How to understand acid-base A quantitative acid-base primer for biology and medicine Brown University, Rhode Island 1981 Elsevier North Holland publication

P.C. Hauser, D.W.L. Chiang, G.A. Wright, Analytica Chimica Acta., 302 (1995), 241

R.S. Chung, D.C. Hitch, D.N. Armstrong, Surgery., 104 (1988), 824

Songer J., (2001). Thesis: Tissue Ischemia Monitoring Using Impedance Spectroscopy: Clinical Evaluation

S. M. Hameed, S.M. Cohn, Chest., 123 (2003), 475

S. J. Watson, R.H. Smallwood, B. H. Brown, P. Cherian, K.D. Bardhan, Physiological Measurement., 17 (1996), 21

S. A. Seidel, L. A. Bradshaw, J. K. Ladipo, J. P. Wikswo, W. O. Richards, Journal of vascular surgery., 30 (1999), 309

S. Friedland, R. Soetikno, D. Benaron, Gastrointest Endoscopy Clin., 14 (2004), 539

T. Blaz, J. Migdalski, A. Lewenstam Analyst, 130 (2005), 637

T Marchbank, R Boulton, H Hansen, R J Playford, Gut., 51 (2002), 787

U. Oesch, Z. Brzozka, X. Aiping, B. Rusterholz, G. Suter, P. Viet, D. Welti, D.

V. Cosofret, M. Erdosy, T.A. Johnson, R.P. Buck Analytical Chemistry, 67 (1995), 1647

Chapter 6

Other applications of the developed pH ISE sensor

6.1. Introduction

Currently, in food industry, there is a need of fast methods for pathogen (Barreiros dos Santos et al, 2013), toxins (Prieto-Simón et al., 2012) and antibiotics detection (Pikkemaat, 2009). Detecting residues of veterinary medicines in foods, particularly antibiotics and sulfonamides, is very crucial, because of their consequences for Public Health as well as some technological processes such as fermentations.

Antibiotics and sulfonamides are frequently used in veterinary medicine both for therapeutic value and to enhance growth and food efficiency. Consequently, these practices might lead to a possible presence of residues in foods, even at concentrations above maximum limits of residues. Thus, the procedures for using antibiotics should be strictly controlled to prevent contaminated food reaching the consumer. Because of these reasons, the concentration of antibiotics residues in food was limited by the European legislation.

Milk products are one of the foods affected by this kind of contamination. Milk is examined for antibiotics residues since may cause allergies and development of bacterial resistance to the consumers. Also, the milk industry is affected in the production with subsequent financial losses, because antibiotic contamination inhibits the starter cultures of bacteria to produce fermented milk products. According to European legislation (Council Regulation 2377/90) has regulated the maximum levels (ML) of antibiotic residues in milk.

High Performance Liquid Chromatography (HPLC) (Senyuva et al., 2000) and gas chromatography (Okerman et al., 2003) are analytical techniques used for the detection of antibiotic residues. However, this method requires expensive equipment not affordable for the majority of small quality laboratories in food industry. Also, these systems are very sophisticated and highly specific. Because of that, there are some alternative techniques to detect antibiotic residues. One of the most traditional ways of detection is the bioassays. The most common bioassay method is four plate test. It is a microbial technique based on agar diffusion, where the samples are placed on the surface of plates seeded with *Bacillus subtilis* or *Kocuria rhizophila*. If the samples

contain antimicrobial compounds, they will diffuse through the media causing the appearance of microbial growth inhibition zones around the samples (Okerman et al., 1998). However, limit of detection (LOD) of this system is sometimes higher than ML and also, the identity of the bacteria and the concentration can affect the results, so that even high residue levels may not be detected or no conclusions can be determined. Thus, alternative techniques were necessary (Okerman et al., 2003). Eclipse farm from the Zeu Inmunotech SL Company is an alternative to these systems. This kit is based on the growth inhibition of *Geobacillus stearothrmophilus*, the spores germinate and grow depending on the presence of antibiotics, producing changes on the pH and, due to an indicator, in the medium color (Le et al., 2005). Based on this fact, also pH detection may be a good indicator of antibiotic residues. A common property of these two kits is that just bring qualitative detection of the antibiotic.

In this chapter, the pH sensor developed in this thesis (see chapter 2) was utilized in the quantitative detection of antibiotics (penicillin G) concentration inside milk solutions. For this purpose, the growth inhibition of *Geobacillus stearothrmophilus* and the change of pH produced by the bacteria was detected with the developed pH sensor.

6.2. Experimental methods

Tubes containing agar medium spread with bacteria of *Geobacillus stearothermophilus* and redox indicator (Sierra et al., 2009) were filled with 100 µl milk solution containing different penicillin concentrations (0 µg/L, 5 µg/L, 50µg/L, 250µg/L, 500µg/L, 1000µg/L, 2500µg/L, 5000µg/L, 10000µg/L, 25000µg/L) were incubated at 65^{o}C (Figure 1), optimal temperature for the bacteria growth. The growth medium controls the pH of the culture, because the pH of the medium is dependent on the balance of dissolved carbon dioxide (CO_2) and bicarbonate (HCO_3^-), changes in the atmospheric CO_2 according to the Henderson- Hasselbalch equation (Hameed et al., 2003);

$$pH = 6.1 + \log\left(\frac{[HCO_3^-]}{0.03 \times pCO_2}\right)$$

$CO_2 + H_2O \rightarrow HCO_3^- + H^+$ (Russel *et al.,* 1997)

When the bacteria germinates, it produced changes of the pH medium and the redox indicator in the tube, initially blue, turns to green as the medium gets reduced by the bacteria. By increasing amount of penicillin, fewer amounts of bacteria can grow. Thus, the change in the medium pH is lower. The samples containing antibiotic concentrations above the limit of detection inhibit germination and microbial growth, so that the color of the agar remains blue.

Figure 1. Tubes containing milk and different concentrations of antibiotics heated up to 65°C

The tubes were hold inside the incubator until the negative control sample has turned yellow for 2 hours and 30 minutes (Figure 2). A yellow color (negative) indicates the absence of penicillin. A blue color shows that the sample contains high amount of penicillin. A green-blue color demonstrates the presence of penicillin in low concentration.

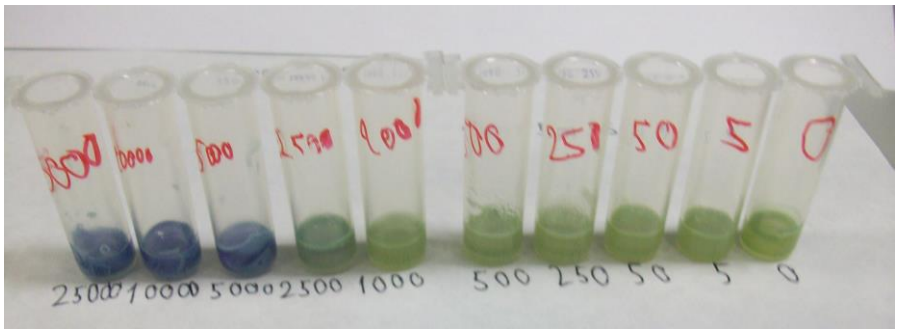

Figure 2. Colorimetric calibration tubes of milk solution containing different concentrations of penicillin

The incubated tubes were tested with the fabricated pH ISE sensors proving the feasibility of using the sensor developed in this thesis for the detection of antibiotics residues in milk (Figure 3).

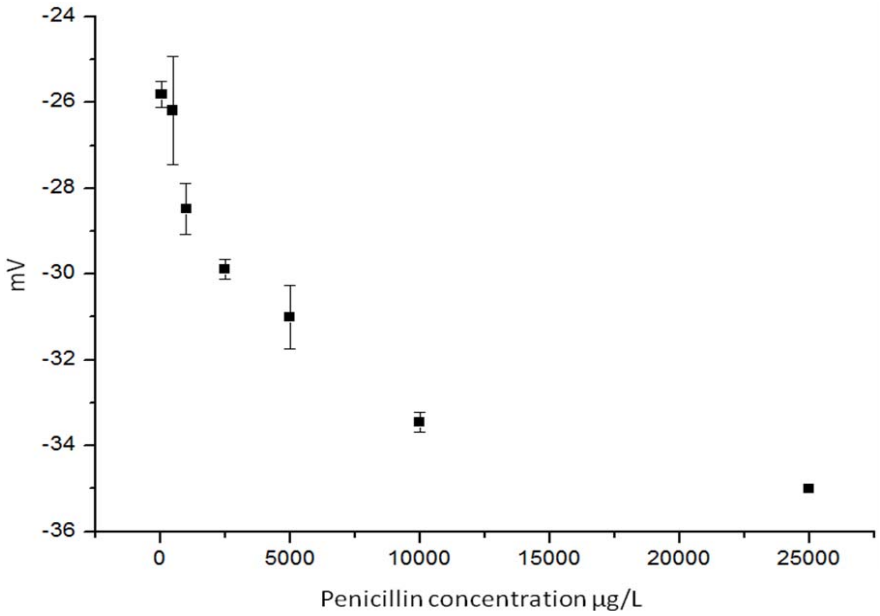

Figure 3. Potential response obtained with the ISE pH sensors in milk samples with different penicillin concentration (n=2)

Moreover, the pH ISE sensors previously calibrated with standard pH solutions, allows the translation of mV results to pH values, corresponding to the penicillin concentrations (Figure 4).

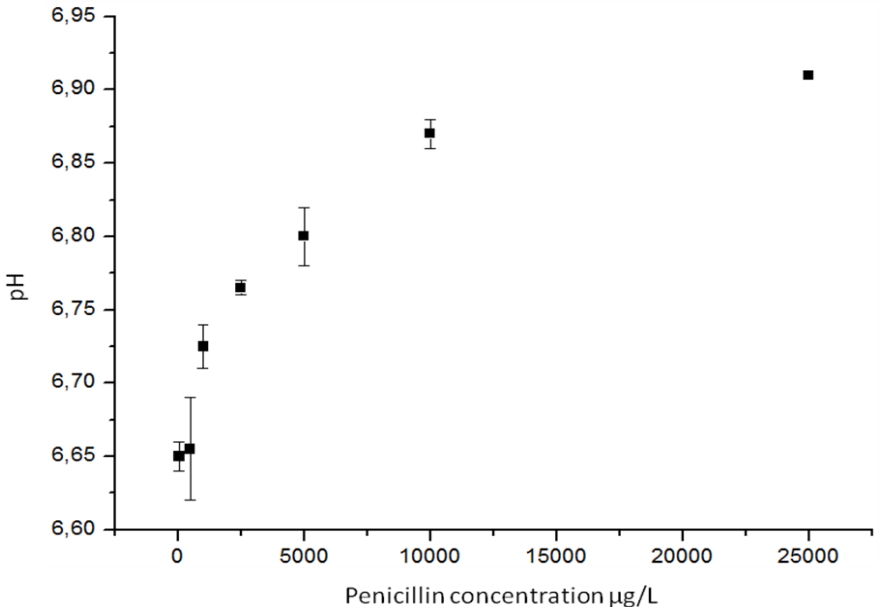

Figure 4. Penicillin concentration *vs* measured pH with all-solid-state pH sensor (n=2)

For this experiment, different arrays were used for pH sensing of each sample at different concentration of penicillin, in order to test the reproducibility response of different fabricated pH sensors. The repeatability of the sensor was tested with 3 repetitions, measuring the same concentrations of penicillin with the same sensor. The small error bars, except at low penicillin concentration, show good repeatability in the fabrication and detection of the developed all-solid-state pH sensors (Figure 5).

The measured pH samples with the developed all-solid-state pH sensor were also tested, using much higher volume, with commercial available pH meters for proving the correctness of the milk pH.

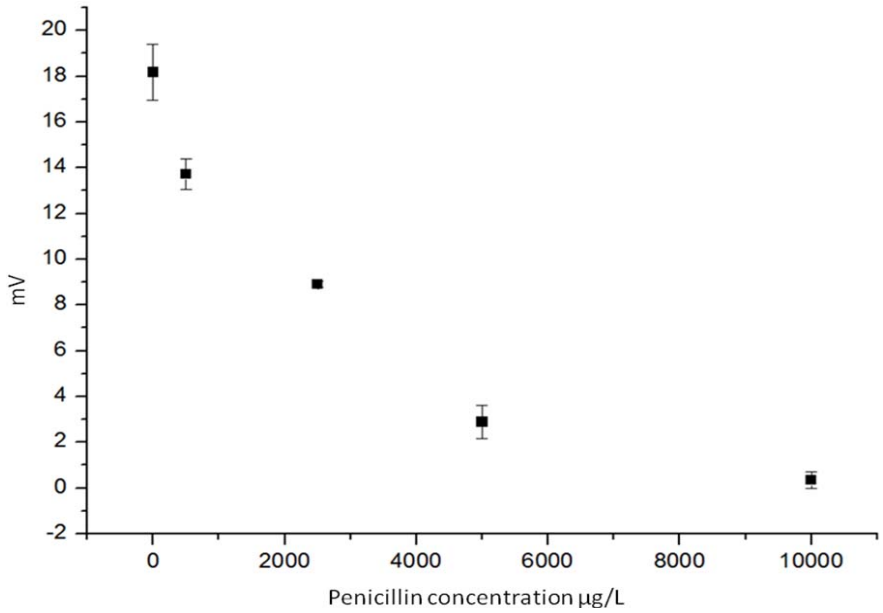

Figure 5. Potential response obtained with the ISE pH sensors in milk samples with different penicillin concentration for the same sensor (n=3).

The working range of the sensor is between 500 and 10000 µg/L of penicillin, being the signal saturated up to this concentration. The minimum level of detection measured with the all-solid-state pH sensor was 500 µg/L.

6.3. Conclusions

In this chapter, developed all-solid state pH sensor was compared with Eclipse farm kit, for the detection of penicillin in milk samples. The results proved that the developed sensor can quantitatively sense the concentrations of antibiotics inside milk solution.

This prototype has shown the ability for quantification of the presence of penicillin in milk samples. However, this sensor requires further optimizations in order to achieve lower LOD, since the ML published for penicillin by the Council Regulation is 4 µg/L.

The main difficulty encountered in the detection of this agar medium, which directly affects the detectability of the pH, was the high viscosity of the sample, and at this part of the project the company involved, Zeu Inmunotech SL, was not interested in introducing changes on its reagents.

References

B. Prieto-Simón, I. Karube, H. Saiki, Food Chemistry., 135 (2012), 1323

D. Sierra, A. Contreras, A. Sánchez, C. Luengo, J.C. Corrales, C.T. Morales, C. de la Fe, I. Guirao, C. Gonzalo, Journal of Dairy Science., 92 (2009), 4200

H. Senyuva, T. Ozden, D. Y. Sarica, Turk J Chem., 24 (2000), 395 .

http://www.zeulab.com/producto/eclipse-farm-3g

L Okerman, K. de wasch, J. van hoof J AOAC Int., 86 (2003), 236

L. Okerman, J. van Hoof, W. Debeuckelaere, J AOAC Int., 81 (1998), 51.

M. Barreiros dos Santos, J.P. Agusil, B. Prieto-Simón, C. Sporer, V. Teixeira, J. Samitier, Biosensors and Bioelectronics., 45 (2013), 174

M. G. Pikkemaat, Anal Bioanal Chem., 395 (2009), 893

R. N. Le, A. L. Hicks, J. Dodge, Applied Biosafety., 10 (2005), 248

Chapter 7

General conclusions

In this thesis, pH and potassium all-solid-state ISE based on potentiometry and bioimpedance sensors were designed, fabricated and integrated in a miniaturized array for its application in endoscopic surgery for in vivo ischemia detection inside the stomach. To achieve this goal, the developed array withstood the low pH and corrosive condition in the gastric juice of the stomach, being the developed sensors stable and reliable. Beside this application, the array was used for the ischemia detection on the small intestine tissue at physiological pH.

The array was designed for its main purpose that is the sensing of ischemia in a reliable and low cost way inside body organs by means of endoscopic scarless entrance of the sensor. For this reason, the shape and size of the sensor array were designed for being adapted to the commercially available gastroendoscopes. Round shaped cylinder of 7 mm diameter was fabricated with 12 electrodes pin of 600 μm diamiter, containing 3 RE, 3 pH and 2 potassium all-solid-state sensors and 4 electrodes in a row for impedance measurements.

These sensors have to demonstrate stability, but also high sensitivity, and selectivity. For this purpose, different ionophores specific to a single ion were tested. Octadecyl isonicotinate was the one that shown better results as pH ionophore and valinomycin, bis [(benzo-15-crown-4)-4-ylmethyl] pimelate for potassium detection. All these ionophores were embedded in PVC polymer membrane containing also plasticizers such as 2-nitrophenyl octyl ether, bis (1-butylpentyl) adipate (BBPA) and liphophilic anionic additives such as potassium tetrakis (4-chlorophenyl) borate (KTpClPB). The specific compositions of membranes to detect potassium or pH were optimized for the better performance of the sensors.

Ag/AgCl surface with pH ISE membrane shows a nernstian behavior (-54,38 mV/pH) at low pH and a nearly nernstian behavior at physiological pH (-34,899 mV/pH). The sub-nernstian behavior of all-solid-state pH sensor was fixed by the enhancement of KTpClPB concentration in ISE membrane. However, the increase in sensitivity is affected by mechanical instabilities and worse interference of cations, which reduces the selectivity of the sensor. Apart of cation interference, anion interference at low pH was

solved by array integration of all-solid-state ISE WE and internal RE fabricated on the same substrate. In this way, the ion interference that affected RE and ISE WE in the same tendency was canceled by the differential potentiometric measurement.

Reproducibility of different pH sensors on different arrays was tested, showing good reproducible response (−13.065 ± 0.4 mV/pH). Also, potassium sensors shown a good reproducibility in the measurement; 17,8 ± 0,62 mV/log[K^+]. The working range of pH sensors was between 0.7 and 2.5 and 6 and 8, while the working range of potassium sensor was between 10^{-5} and 10^{-1} M.

Bioimpedance sensor was tested and optimized in vitro with different solutions of ions concentration to mimic ischemia detection and with different kinds of tissues from different nature. For this purpose, chicken fat and breast tissues were taken as a model for mimicking non-ischemic and ischemic states respectively. The effect of electrodes insulation as well as the pressure applied on the tissue was studied. The dependence of the impedance response with different pressure applied to the sensor was overcome by applying magnetic field attachment. The sensor array was modified with ring magnets which were attracted by an external magnet, giving stable and reliable signal discarding mechanical motion.

pH, potassium and bioimpedance sensors were integrated on the designed array. The effect of impedance sensor on all-solid-state pH and potassium sensors was tested, and was observed the effect of the current applied in impedance measurement on the differential voltage measured in the ISE sensors. For preventing this effect; ISE sensors and impedance sensors were distributed on the array in separated places.

The sensor array was successfully integrated in commercial endoscope and inserted inside the pig stomach. The blood flow of certain area of the stomach was interrupted by ligating or crossclamping vessels and organ wall. Ischemia and reperfusion steps were sensed successfully with potassium and pH sensors. These results also indicate that information about hypoxic tissue damage can be collected with this array.

Ischemia was also sensed on small intestine tissue by opening the abdominal part of the body and getting the sensor array in contact with the intestine. By crossclamping of mesenteric artery by tourniquets and scissors, ischemic and reperfusion states were controlled. Results proved that ischemia and reperfusion can be monitored by our integrated sensor array.

Moreover, the pH ISE sensor was successfully used for the detection of antibiotics (penicillin G) residues inside milk, by the detection of the pH medium change in the inhibition growth of the bacteria; *Geobacillus stearothrmophilus.*

We can conclude that, a novel all-solid-state potentiometric, miniaturized, low cost and mass producible pH, potassium all-solid-state ISE and impedance sensors integrated in an array was successfully fabricated for detecting ischemia inside the stomach by means of endoscopic techniques and also on small intestine. This array was tested in vitro and

vivo giving reproducible and reliable results. A market study performed for the developed array conclude that this sensor array has important advantages over its competitors such as lower price; around 4 times less in the equipment and 25 times less in the disposable array comparing with the main competitor, easy mass production, multisensing abilities and small size, that makes this equipment portable and applicable to endoscopic systems. The developed all-solid-state pH sensors permit low pH sensing from 0.7-2.5, which is the only example in the literature that allows so low pH detection, and it makes this sensor a unique device for stomach detection.

Resumen

El diagnóstico médico es uno de los campos que más se ha beneficiado de la capacidad analítica de los sensores basados en electrodos selectivos de iones (ESI) para la detección de un amplio abanico de iones. Existen diferentes enfermedades, como cáncer, diabetes, desordenes neurolóicos, isquemia entre otros, en las que los cambios en la concentración de los iones, están directamente relacionados.

Isquemia es una disminución del suministro de sangre a un órgano y se requiere una detección rápida y precisa, ya que puede dañar irreversiblemente los órganos afectados. Los métodos de detección de isquemia *in situ* en el tejido de los órganos requieren una detección rápida y fiable y el estómago es uno de los órganos más importantes en la detección de isquemia . Sin embargo, el bajo pH del jugo gástrico del estómago hace difícil la fabricación de sensores ESI estables y funcionales, principalmente debido a la interferencia de aniones y a la falta de adhesión entre la membrana ESI y la superficie del electrodo.

En esta tesis, se han diseñado, fabricado y optimizado sensores basados en ESI de estado sólido para la detección de iones de pH y potasio. Estos sensores se complementaros con sensores de bioimpedancia, los cuales se integraron con los anteriores en un microarray, miniaturizado para su aplicación en la cirugía endoscópica para la detección de isquemia in vivo en el interior del estómago.

Para lograr este objetivo, el array desarrollado debe resistir el pH bajo y las condiciones corrosivas del jugo gástrico del estómago. Este objetivo se logró mediante el estudio de los materiales utilizados para la fabricación de los sensores. La superficie utilizada para los electrodos de los sensores se modificó con pasta conductora de Ag/AgCl. Esta pasta estaba fabricada con un polímero que contenía tanto grupos hidrófilos como hidrófobos, con lo que no se veía tan afectada por la alta concentraciones de protones de la matriz a analizar.

Estos sensores tienen que mostrar además de buena estabilidad, una alta sensibilidad, y selectividad. Para este fin, se probaron diferentes ionóforos específicos a los iones de interés. Octadecil isonicotinato fue el que mostró mejores resultados como ionóforo de pH y la valinomicina, y el bis [(benzo-15-corona-4)-4-ilmetil] pimelato fue el seleccionado para la detección de potasio. Estos ionóforos se añadieron a la membrana de polímero de cloruro de polivinilo (PVC) que contiene también plastificantes tales como 2-nitrofenil octil éter (NPOE), bis (1-butilpentil) adipato (BBPA) y aditivos aniónicos liphofilicos como el tetraquis (4-clorofenil) borato (KTpClPB). La composición específicas de las membranas para la detección de potasio y de pH fueron optimizados para un mejor comportamiento de los sensores.

El sensor ISE de pH muestra un comportamiento Nernstiano (-54,38 mV / pH), y por lo tanto una alta sensibilidad, a pH bajo y un comportamiento casi Nernstiano a pH

fisiológico (-34,89 mV/pH). El comportamiento sub-Nernstiano del sensor ha sido resuelto con el aumento de la concentración de KTpClPB en la membrana. Sin embargo, el aumento de la sensibilidad se ve afectada por inestabilidad mecánicas de la membrana y una mayor interferencia de cationes, lo que reduce la selectividad del sensor. Además de la interferencia de cationes, la interferencia de aniones, debido a la alta concentración de cloruros a pH bajo, fue resuelta por la integración del electrodos de trabajo y del electrodos de referencia en el mismo sustrato. De esta manera, la interferencia de iones afecta a los electrodos de referencia y de trabajo en el ISE en la misma proporción, con lo que es cancelada en la medición potenciométrica diferencial.

La reproducibilidad de los diferentes sensores de pH en diferentes arrays se puso a prueba, mostrando una buena repetibilidad (-13.07 ± 0,40 mV / pH), así como los sensores de potasio; 17,80 ± 0,62 mV / log [K +]. El rango de trabajo que se observó en los sensores de pH desarrollados está entre 0,7 y 2,5 y 6 y 8, mientras que el rango de trabajo del sensor de potasio está entre 10^{-5} y 10^{-1} M.

El sensor de bioimpedancia fue probado y optimizado *in vitro* con soluciones de diferente concentración de iones imitando las condiciones en el estómago.. Para simular la detección de isquemia en el tejido del estómago, se utilizaron diferentes tipos de tejidos. Para este propósito, pechuga y grasa de pollo se utilizaron como un modelo para imitar estados no isquémicos e isquémicos, respectivamente. Se estudió el efecto del aislamiento de electrodos, así como la relación entre la respuesta del sensor con la presión aplicada sobre el tejido. La dependencia de la respuesta de impedancia con la presión aplicada se eliminó mediante la aplicación de un campo magnético fijo, para mantener el array en un estable contacto con el tejido. El array de sensores se modificó con imanes que eran atraídos por un imán externo, dando una señal estable, fiable e independiente del movimiento del sensor.

El array de sensores fue diseñado para la detección de isquemia en el interior del estómago, sin generar cicatrices mediante la utilización de gastroendoscopio. Por esta razón, la forma y el tamaño del array de sensores se han adaptado a los endoscopios comerciales. El array se diseñó de forma cilíndrica de 7 mm diámetro, el cual contiene 12 electrodos de 600 μm de diámetro. Los electrodos se funcionalizaron con 3 electrodos de referencia, 3 electrodos de trabajo para detección de pH, 2 electrodos de trabajo para detección de potasio y 4 electrodos contiguos en fila para mediciones de impedancia.

El conjunto de sensores se integró con éxito en el array, el cual se adaptó satisfactoriamente a endoscopios comerciales y se insertó en el interior del estómago de un cerdo, para la monitorización *in vivo* de isquemia. El flujo de sangre de un área del estómago se interrumpió mediante el pinzamiento de los vasos sanguíneos y la pared del órgano. Los pasos de isquemia y reperfusión fueron detectados con éxito con los sensores de potasio y de pH. Estos resultados recogido con este array, también indican que se puede obtener información sobre el daño en el tejido hipóxico.

También se indujo y detectó isquemia en el tejido del intestino delgado, mediante la apertura de la parte abdominal del cuerpo del animal y el contacto del array de sensores con el intestino. Mediante el pinzamiento de la arteria mesentérica con torniquetes y tijeras, se controlaron los estados de isquemia y reperfusión. Los resultados demostraron que los estados de isquemia y reperfusión pueden ser monitorizados por nuestro conjunto de sensores integrados.

Por otra parte, el sensor ISE de pH se utilizó con éxito para la detección de residuos de antibióticos (penicilina G) en la leche, mediante la detección del cambio de pH del medio debido a la inhibición, por los antibióticos existentes en la leche, del crecimiento de la bacteria *Geobacillus stearothermophilus.*

Podemos concluir, que se ha fabricado con éxito un nuevo sensor de pH, potasio e impedancia integrados en un array electroquímico de bajo coste y producible en masa, así como miniaturizado para su utilización en técnicas endoscópicas para la detección de isquemia dentro del estómago, y en el intestino delgado. Este array de sensores se probó *in vitro* e *in vivo* dando resultados reproducibles y fiables. El estudio de mercado elaborado para el array concluye que, este sistema de sensores tiene importantes ventajas frente a sus competidores, tales como un precio menor, (alrededor de 4 veces menos en el equipo y 25 veces menor en el sensor, en comparación con el principal competidor). El array se diseñó para una fácil producción en masa, capacidad multisensórica y pequeño tamaño, lo que hace que este equipo sea portátil y aplicable a los sistemas endoscópicos comerciales. Los sensores de pH desarrollados permiten la detección bajos pH; de 0,7 a 2,5, que es el único ejemplo en la literatura para la detección de pHs tan bajos por lo que hace de este sensor un dispositivo único para la detección de isquemia en el estómago.